THE UNIVERSITY OF MICHIGAN
INDUSTRY PROGRAM OF THE COLLEGE OF ENGINEERING

EVAPORATION AND COMBUSTION OF SINGLE FUEL DROPLETS IN A HOT ATMOSPHERE

Michel A. Saad

This dissertation was submitted in partial fulfillment of the requirements for the degree of Doctor of Philosophy in the University of Michigan. The research was partially supported by the Power Plant Laboratory, Wright Air Development Center, through the Engineering Research Institute Projects 1988 and 2253-3.

January, 1956

IP-140

ACKNOWLEDGEMENT

We wish to express our appreciation to the author for permission to distribute this dissertation under the Industry Program of the College of Engineering.

ACKNOWLEDGMENTS

The writer wishes to express his gratitude for the help and advice of Professor J. A. Bolt, Chairman of the Doctoral Committee, under whose supervision this investigation was made. The writer also expresses his appreciation to the members of the Committee, Professor L. L. Carrick, Professor C. W. Good, Professor W. W. Hagerty, and Professor W. E. Lay, for their interest and guidance.

Acknowledgment is due to W. Mirsky and L. W. Wolf for their help on numerous occasions. The assistance of W. Salva in the construction of the experimental equipment is appreciated.

The financial assistance of the Power Plant Laboratory, Wright Air Development Center, in support of the Engineering Research Institute, Projects 1988 and 2253-3, is gratefully acknowledged. A grant from the Horace H. Rackham School of Graduate Studies is also appreciated.

TABLE OF CONTENTS

LIST OF TABLES

LIST OF ILLUSTRATIONS

ABSTRACT

This dissertation deals with a study of the combustion of falling fuel droplets in a hot atmosphere. This investigation was undertaken as a first step toward the understanding of the more general problem of combustion of a fuel spray. The fuel droplets fell in a furnace under gravity, buoyancy, and drag forces. They were burned in hot air while exposed to thermal radiation from the furnace walls. Reynolds number was not a controllable factor because the droplets changed in both diameters and velocities during their fall.

Kerosene and two pure hydrocarbon fuels, n-heptane and isooctane, were investigated at a furnace temperature of 1500°F. The range of droplet diameter was approximately 1150 μ to 300 μ.

The experimental procedure consisted in allowing single fuel droplets to fall freely in a vertical furnace. After leaving a fuel dropper, the droplets accelerated to about 87% of their terminal velocity by the time the first photographing stage was reached. Each droplet was photographed at several positions as it fell, and a record of droplet diameter and elapsed time was obtained. At every photographing stage, the droplet was detected by a multiplier phototube which actuated a high-speed photolight. The time intervals between successive photographs were determined by superimposing timing pips upon the traces obtained from a 60-cycle square-wave generator on an oscilloscope.

The combustion of the fuels investigated depended on the properties of the fuel, droplet size, and the relative velocity between the droplet and the furnace atmosphere, other factors such as ambient temperature and

furnace atmosphere being unchanged.

Preheating of the droplet was mainly by conduction and convection from the ambient atmosphere, since radiation from the furnace walls was found to have a comparatively small effect. The heat transfer to the interior of the droplet modified the rate of vaporization since an appreciable portion of the heat transferred was used for the internal heating of the droplet. During combustion, heat was transferred to the droplet from the local flame produced by the combustion of the vaporized fuel around and in the wake of the droplet.

The change of droplet size of the fuels investigated was represented by the equation

$$D^2 = D_o^2 - C\theta,$$

where D is the diameter of the droplet at time θ, D_o is the initial diameter of the droplet, and C is the coefficient of combustion. C was found to depend on the nature of the fuel and the velocity of the falling droplet. For n-heptane and isooctane C varied from 0.020 to 0.0255 cm^2/sec, while for kerosene C varied from 0.021 to 0.0222 cm^2/sec.

The experimental results show that the presence of the flame decreased the drag on the falling droplet.

I. INTRODUCTION

The combustion of single fuel droplets is a part of the overall problem of combustion of a spray of fuel. The combustion of sprays has not been thoroughly investigated as it involves so many variables and complicated processes, most of which occur simultaneously and are still incompletely understood. Accordingly, it was decided that observations of individual burning droplets in a hot atmosphere would provide a better starting point for the ultimate understanding of the phenomena of combustion of a liquid fuel spray.

The combustion of a fuel droplet can be considered as a combined problem of the physical processes of diffusion, heat transfer, evaporation, distillation, and the chemical process or reaction during which the main part of the thermal energy is released as heat of reaction. If the droplet is in motion relative to the surrounding atmosphere, more complexity is introduced into the problem, and the effect of Reynolds number on the combustion process must be accounted for. No analytical solution for the combustion rate of a single droplet in a moving gas stream has ever been obtained. Some solutions for stationary droplets are found in the literature but there is some doubt about the oversimplified physical assumptions involved in such solutions. The lack of mathematical analysis is dictated by the complexity associated with a theoretical approach and the difficulties encountered in experimental measurements.

Considerable work has been done on evaporation and burning of fuel droplets. A great portion of this work involved suspension of fuel droplets on supports, e.g., fine glass filaments or thermocouple wires. From

the practical point of view, it is more desirable to study freely falling droplets since the complete evaporation and burning of the droplet could be observed photographically while falling in a hot atmosphere. This also has the advantage of studying the evaporation and burning of very small droplets which are not conveniently studied by suspending them. On the other hand, a freely falling droplet of a given initial diameter restricts the value of Reynolds number at which it falls. The range of Reynolds numbers is usually low mainly because of the small sizes of the droplets and the relatively high kinematic viscosity of the ambient atmospheres.

The main purpose of the present investigation was to get fundamental data and to study the history of combustion of individual droplets in a hot atmosphere under controlled temperatures. It was desired to observe and photograph the burning droplets in free flight, continuously or at several positions during the burning process. The experimental setup was designed to fulfill this purpose. The experimental method consisted in allowing small fuel droplets to fall freely through a vertical furnace. Each droplet was photographed at several positions as it fell through a heated furnace, and a record of droplet diameter and elapsed time was obtained. This method is applicable only to volatile fuels, since the evaporation of residual fuels and heavy fuel oils is generally accompanied by swelling. Thus the diameter of the droplet does not give an adequate measure of the combustion process. Accordingly, the determination of the weight, rather than the size of the partially burned droplets, is preferred and is usually measured by a microbalance.

In the combustion of single fuel droplets there is no mutual interference which is the case in the combustion of a spray. Closer control could be maintained on a single falling droplet and its surroundings than

with a group of burning droplets. Many of the variables of interest in combustion could be controlled quite easily, with the exception of the relative air velocity, and a more fundamental understanding of the combustion process would follow.

Quantitative information on the rates of burning, the total burning time of fuel droplets, and the factors which influence them are of significant value in the design and performance of jet-engine combustors and internal-combustion engines.

II. SURVEY OF PAST WORK AND GENERAL CONSIDERATIONS

A. Survey of Past Work

Investigation of the literature indicates that little work has been done on the production and burning of single free droplets of liquid fuel. Most investigators prefer to study stationary droplets while others use pseudo-drops. In this way they simplify the problem by reducing the number of the variables which affect the combustion process.

Godsave[13,14,15] suspended single fuel droplets on a fine silica filament and measured with a cinematograph camera the rate of decrease in size during combustion in still air. He obtained data of the burning rates of various fuels and pure hydrocarbons, and found that the burning droplets decreased in size at a mass rate proportional to the first power of their diameters. The heat transfer was the dominant factor in determining the life of the fuel droplet and the rate of burning was a strong function of the total heat required to evaporate a unit mass of the fuel.

The conditions under which Godsave's experiments were performed were different from those encountered in a furnace. The burning of the fuel droplets took place at atmospheric conditions. The range of droplet sizes was from 1500 to 2000 microns in diameter, suspended on a silica filament 200 microns in diameter. Suspension of droplets on fine wires or glass filaments distorts the droplets' shape and makes it impossible to study the completion of the burning process or the burning of very small droplets. The filament causes heat transfer and affects the airflow pattern around the droplet. On the other hand, since the droplet is stationary, suspended droplets allow better and easier focusing and photography.

Godsave represented the combustion history of a droplet by the equation

$$D^2 = D_o^2 - \lambda\theta, \tag{2.1}$$

where D is the diameter of the droplet at time θ, D_o its diameter at $\theta = 0$, and λ the evaporation constant, having dimensions of length^2/time. If ρ_ℓ is the density of the liquid fuel, the above equation is equivalent to

$$\frac{dm}{d\theta} = -\frac{\rho_\ell \pi \lambda D}{4} \tag{2.2}$$

which states that the mass rate of vaporization of the droplet is proportional to its diameter. The life of a droplet θ_1 is also given by

$$\theta_1 = \frac{D_o^2}{\lambda} . \tag{2.3}$$

From a simplified picture of the combustion of a fuel droplet, Godsave developed an expression for the evaporation constant λ given by

$$\lambda = 8K_g \frac{\rho_g}{\rho_\ell} \frac{D_F}{D_F - D} \ln\left[1 + \frac{c_g(T_F - T_S)}{\lambda'}\right], \tag{2.4}$$

where

D_F = the diameter of the assumed spherical flame around the droplet,

T_F = the temperature of the flame,

T_S = the temperature at the surface of the droplet,

$K_g = \frac{k_g}{c_g \rho_g}$ = the thermal diffusivity of the gases between the droplet surface and the flame envelope,

k_g, c_g, and ρ_g = the thermal conductivity, specific heat, and density of these gases, respectively, and

λ' = the heat required to vaporize a unit mass of the fuel.

Godsave was also able to obtain experimental evidence that the rate of

combustion is chiefly dependent on the enthalpy of the liquid and the latent heat of vaporization.

Topps[38] obtained the rate of evaporation of fuel droplets from 300 to 500 microns in diameter falling at their terminal velocity in a vertical tubular furnace. Pure hydrocarbons and residual fuels were investigated at atmospheric and higher pressures. No attempt was made to observe the droplet during its fall and the results were based on the initial and final size measurements. The mass of the final residue was estimated by measuring the diameter of the residual droplet collected on solid carbon-dioxide snow. The furnace temperature varied between 400° and 1000°K.

Gohrbrandt[16] measured the evaporation of suspended camphor spheres in a hot-air stream at Reynolds numbers from 100 to 2000 and air temperatures from 30° to 500°C. The rate of change of size and shape of the spheres was recorded with a cinematograph camera. The results of his investigation showed that the evaporation rate of a sphere was approximately proportional to the product of the diameter and the square root of Reynolds number, viz.,

$$\frac{dm}{d\theta} \alpha D\sqrt{Re}. \qquad (2.5)$$

Chang[5] burned droplets of Bunker C fuel oil by dropping them through a vertical furnace and extinguishing them at the bottom of the furnace. The degree of combustion was measured by comparing the weights of the original and residual droplets. The residence time in the furnace was measured by knowing the falling velocity at different points along the droplet's path through the furnace. This was accomplished by intermittent flash photography. The furnace was constructed so that its effective length could be changed, and in this way it was possible to subject the droplets

to the high-temperature atmosphere for different lengths of time.

Simpson[31] used a spinning disc to atomize liquid fuel into droplets of diameters between 350 to 650 microns. He injected a stream of droplets into a heated furnace. The partially burned droplets were extinguished as they fell out of the furnace. The residence time in the furnace was recorded photoelectrically and the rate of burning of a droplet was obtained by comparing the weights before and after passage through the furnace. The droplets did not burn in an isothermal atmosphere and the relative velocity of the droplet in the furnace was not controllable and was unknown. Simpson obtained combustion data of six hydrocarbons and two residual fuels.

Ingebo[20] placed a wetted cork sphere 0.688 cm in diameter in a flowing air stream of constant mass flow rate and varying temperature. The tip of a hypodermic needle was located at the center of the cork sphere and fuel was forced through the pores of the sphere. Evaporation rates were determined by measuring the rate of feed of fuel into the cork sphere, so that the surface of the cork was kept wet. Ingebo determined evaporation rates of nine pure liquids in air streams having temperatures ranging from 80° to 1000°F. The Reynolds numbers ranged from 1200 to 5700. The following expression for the vaporization rate was derived:

$$-\frac{dm}{d\theta} = \frac{k_a \Delta t}{H_v} \pi D \left(\frac{k_a}{k_v}\right)^{0.5} \left[2 + 0.303(ReSc)^{0.6}\right], \qquad (2.6)$$

where

k_a and k_v = the thermal conductivities of the air and vapor,

H_v = the latent heat of vaporization,

Δt = the difference between air temperature and surface temperature of the droplet,

Re = the Reynolds number based on the diameter of the droplet,

Sc = the Schmidt number based on the mass diffusivity, and

D = the diameter of the droplet.

Equation (2.6) is of the same form as the Frössling equation where the rate of mass transfer is given by

$$-\frac{dm}{d\Theta} = 2\pi DD_f \frac{MP}{RT}\left[1 + 0.276\ Sc^{1/3}\ Re^{1/2}\right], \qquad (2.7)$$

and the Nusselt number for mass transfer is

$$\frac{hRTD}{D_f P} = 2\left[1 + 0.276\ Sc^{1/3}\ Re^{1/2}\right], \qquad (2.8)$$

where

D_f = the diffusion coefficient,

M = the molecular weight of the vapor,

P = the vapor pressure at droplet surface,

R = the universal gas constant,

T = the absolute temperature of the saturated vapor-air mixture at the droplet surface,

h = the heat transfer coefficient,

$Re = \frac{\rho VD}{\mu}$ = Reynolds number, and

$Sc = \frac{\mu}{\rho D_f}$ = Schmidt number.

Frössling evaluated the rates of evaporation of single suspended spherical particles of aniline, naphthalene, nitrobenzene, and water into moving air at atmospheric pressure. The range of Reynolds numbers was from 2 to 800.

As indicated by Perry[26], the similarity of heat and mass transfer can be readily shown from the Frössling equation if the Nusselt number for heat transfer $\frac{hD}{k_g}$ is substituted for $\frac{hRTD}{D_f P}$ and the Prandtl number $\frac{C_p \mu}{k}$ for $\frac{\mu}{\rho D_f}$.

Diederichsen and Hall[6], using a spinning-disc atomizer, projected fuel droplets upward in an electric furnace. The furnace had an observation quartz window in the side. The trajectories of the burning droplets were recorded continuously on a drum camera. The range of droplet size was from 150 to 600 microns and the furnace temperature was approximately 710°C. In their investigation no attempt was made to account for the variable velocity of the burning droplets.

Another phase of Diederichsen and Hall's investigation was to study the effect of pressure on the combustion of a fuel droplet. The droplet was suspended by a silica filament at the room temperature and in still air in a special chamber, the pressure of which could be raised to twenty atmospheres. The droplet was ignited by a spark and the combustion process was recorded on a drum camera. The droplet size range was from 200 to 1000 microns in diameter. It was concluded that the average distance between the flame and the droplet surface was independent of the droplet diameter and roughly inversely proportional to the square root of the total absolute pressure. The effect of pressure on the rate of burning was given by the following equation:

$$-\frac{dm}{d\theta} \alpha DP^{1/4}. \qquad (2.9)$$

Spalding [32-37], used five metal surfaces as fuel burners; a flat plate and four different sizes of spheres ranging from 1/2 to 1-1/2 inches in diameter. Fuel flowed up inside the burner, spilled over the top, and burned as it flowed down the outside surface. The excess fuel was collected and recycled and the rate of combustion was estimated from the rate at which make-up fuel was added.

Spalding found that the mass vaporization rate per unit area of fuel

surface could be expressed in terms of a dimensionless number B called the transfer number and is defined as

$$B = \frac{h_\infty - h_s}{\lambda'} , \tag{2.10}$$

where

h_∞ = the enthalpy of the main air stream per unit mass,

h_s = the enthalpy of the vaporized fuel at the surface temperature per unit mass, and

λ' = the heat required to vaporize unit mass of fuel.

For a sphere of diameter D in an infinite stagnant medium, Spalding gives the following equation:

$$\dot{m} D \frac{c_g}{k_g} = 2 \log_e (1 + B), \tag{2.11}$$

where

$\dot{m}$ = the mean mass transfer rate per unit area = $- 1/2 \rho_\ell \frac{dD}{dt}$, ρ_ℓ being the density of the fuel,

c_g = the specific heat, and

k_g = the thermal conductivity.

Substituting the value of $\dot{m}$ into equation (2.11), the following expression is obtained for the lifetime θ of a vaporizing droplet:

$$\theta = \frac{\rho_\ell D_o^2 c_g}{8 k_g \log_e (1 + B)} , \tag{2.12}$$

D_o being the initial droplet diameter.

Experiments were also performed to determine the combustion rate in natural and forced convection. In natural convection, over the range of transfer number from 0.25 to 3, the rate of mass transfer was expressed by the empirical formula

$$\frac{\dot{m}Dc_g}{k_g} = 0.45\, B^{3/4} \sqrt[4]{\frac{gx^3}{\alpha 2}}, \qquad (2.13)$$

where

g = the acceleration due to gravity,

x = a typical dimension, the plate height or the sphere diameter for the two burners, and

α = the thermal diffusivity.

The metal spheres were subjected to considerable free-convection effects which were difficult to predict. In forced convection, the Reynolds number was introduced and the following empirical formula was derived:

$$\frac{\dot{m}D}{\mu} = 0.53\, B^{3/5}\, Re^{1/2}, \qquad (2.14)$$

for $0.6 < B < 5$ and $800 < Re < 4000$. It is clear that equation (2.14) does not hold at low Reynolds numbers, which is characteristic of small fuel droplets.

It should be noted that Spalding treated the combustion of the fuel droplet in one dimension only and assumed the analytically derived expressions to apply for the spherical case of the fuel droplet. Spalding's experiments were performed at room temperature, which makes comparison with other investigators somewhat difficult.

B. Formation of Fuel Droplets

There are three types of atomizers used in practice: the pressure atomizer, the air atomizer, and the spinning-disc atomizer. Pressure atomization has a wide application in fuel-injection systems. In the air atomizer uniform droplets are produced by blowing off the tip of a capillary through which liquid is supplied. In this type, either constant or intermittent air pressure can be used. If an intermittent air jet is

used, the droplet size is a strong function of the frequency of intermittence. The third method of atomization consists of supplying liquid to the center of a spinning disc. The atomization produced from rotating devices is usually characterized by remarkable uniformity in droplet size as compared with the normal sprays produced either by pressure or air atomization.

In the present investigation, a concentric jet of air was used to push off droplets from the tip of a hypodermic needle. The droplets formed at the end of the tip were dragged off by the air stream. The size of the droplet was controlled mainly by the air pressure while the head of the fuel was kept constant.

If there is no air flow and the head of the fuel is small, the equilibrium equation at the time when a droplet begins to fall is

$$\rho\, g\, \frac{1}{6}\, \pi\, D^3 = T_n\, \pi\, d_o, \tag{2.15}$$

where

D = the diameter of the droplet,

d_o = outside diameter of the capillary tube,

T_n = the surface tension at needle tip, and

ρ = the density of fuel.

If there is an airflow of pressure p_a, the equilibrium equation becomes

$$\rho\, g\, .\frac{1}{6}\, \pi\, D^3 + p_a\, \frac{\pi}{4}(D^2 - d_o{}^2) = T_n\, \pi\, d_o. \tag{2.16}$$

In the case of small droplets, the influence of gravity is very small and can be neglected. The above equation then reduces to

$$D^2 - d_o{}^2 = \frac{4\, T_n\, d_o}{P_a}, \tag{2.17}$$

which indicates that the droplet diameter decreases as the air pressure increases.

At the instant when the droplet leaves the capillary tip, it is totally subjected to the pressure p_a. The surface tension in the surface of the droplet causes the pressure inside the droplet to be greater than the outside. The surface-tension pressure of a sphere is obtained by equating the surface tension and pressure forces

$$\pi D T_d = \frac{\pi}{4} D^2 p_t$$

or

$$p_t = \frac{4 T_d}{D}, \tag{2.18}$$

where

p_t = the pressure due to surface tension and

T_d = the liquid surface tension.

Equation (2.18) indicates that the surface-tension pressure of a droplet increases as the diameter decreases.

If we consider a droplet in a state of equilibrium, the internal pressure of the droplet, p_i, must be equal to the outer pressure, p_a, and the surface-tension pressure, p_t, or,

$$p_i = p_a + p_t = \text{constant for a certain droplet diameter.} \tag{2.19}$$

If p_a is increased, the droplet is deformed, reducing the value of p_t so that p_i is kept constant. By further increase of p_a, a further decrease in p_t will occur in certain points till the droplet collapses, splitting into smaller ones. The size of the smaller droplets is determined such that the surface-tension pressure, p_t, is large enough to ensure a constant value of p_i as indicated by equation (2.19). Substituting the above values for p_a and p_t in equation (2.19), then

$$P_i = \frac{4\ T_n\ d_o - 2/3\ \rho\ g\ D^3}{D^2 - d_o^2} + \frac{4T_d}{D} . \qquad (2.20)$$

If the weight of the droplet is negligible, then

$$P_i = \frac{4\ T_n\ d_o}{D^2 - d_o^2} + \frac{4T_d}{D} . \qquad (2.21)$$

Equation (2.21) is a cubic equation in D in which D, T_n, d_o, and t_d are related.

Chang[5] found out that if the droplet diameter is D and the air velocity is V, then DV = constant. This formula was derived by equating the air drag and the surface-tension force at the tip of the capillary. The derivation was as follows:

Neglecting the gravitational force, the surface-tension force, F_t, is given by

$$F_t = \text{the drag force} = \frac{\pi}{8} C_D\ \rho'\ D^2\ V^2, \qquad (2.22)$$

where

C_D = the drag coefficient,

ρ' = the density of the air, and

V = the velocity of the air.

F_t can be considered constant for a certain liquid and tip diameter.

For the range of Reynolds numbers of the air stream between 2 and 500, $C_D = \frac{18.5}{R^{0.6}}$ Substituting this value of C_D in equation (2.22) gives

$$(DV)^{1.4} = \text{constant}$$

or

$$DV = \text{constant}. \qquad (2.23)$$

The constant depends on the surface tension and the geometry of the tip of the capillary.

A small tail is formed at the part of the droplet attached to the tip, but due to the liquid surface tension the droplet takes the form of

a sphere as soon as it leaves the tip. The smaller the capillary, the smaller is the surface tension at the tip and the smaller is the tail of the droplet. If the air pressure is small, the droplet wets the outside wall of the needle and causes an increase in surface tension which results in the formation of large droplets.

Very small droplets (below 500 microns) were undesirable in the present investigation, as they were scattered when leaving the tip of the capillary. The convection currents also affected the vertical path of such droplets. Large droplets (above 1200 microns) were also undesirable as, first, they acquired only a small percentage of their terminal velocities when they reached the first photographing position and, second, from the practical point of view the data of burning big fuel droplets was well outside the range of practical interest.

C. The Motion of a Droplet in Air

The forces acting on a droplet falling freely in air are the gravity, buoyancy, and drag or frictional resistance. The buoyancy effect results from the displacement of the air by the droplet and the drag force from the relative motion between the droplet and the air.

Let us consider a droplet of diameter D and initial velocity $V_o = 0$, falling from the tip of a dropper in still air. When the droplet leaves the dropper tip, it accelerates rapidly, the main acting forces being the gravitational forces. As the droplet gains speed, the drag forces become appreciable and tend to lower the acceleration.

Stokes' law for the resistance to the motion of a sphere in a fluid does not hold above values of Reynolds number more than two. Above this value of Re, the air-resistance force is given over a wide range by

$$\text{drag force} = \frac{\pi}{8} D^2 C_D \rho' V^2 , \qquad (2.24)$$

where

D = the diameter of the droplet,

C_D = the coefficient of drag,

ρ' = the density of the medium into which the droplet falls, and

V = the velocity of the droplet.

The drag coefficient, C_D, is a function of Re and is represented by the Goldstein curve (C_D vs. Re). The relationship between C_D and Re depends on whether the flow is laminar, turbulent, or in the intermediate region between these two conditions. The plot could be conveniently represented to a fair degree of accuracy by the relations

$$\left.\begin{aligned} C_D &= \frac{24}{Re}, \text{ for } 0 < Re < 2 \quad \text{laminar} \\ C_D &= 0.4 + \frac{40}{Re}, \text{ for } 2 < Re < 500 \quad \text{semiturbulent} \\ C_D &= 0.44, \text{ for Re above } 500 \quad \text{turbulent.} \end{aligned}\right\} \qquad (2.25)$$

During the total motion of the droplets of the sizes used in this investigation, the flow could be considered laminar or semiturbulent. The exact value of C_D was obtained by the method explained in detail in Appendix B.

The equation of a freely falling droplet is

$$\frac{dV}{dt} = g\left(1 - \frac{\rho'}{\rho}\right) - \frac{3}{4} C_D \frac{\rho'}{\rho} \frac{V^2}{D} , \qquad (2.26)$$

ρ being the density of the liquid of the droplet and g the acceleration due to gravity.

If Re < 2,

$$C_D = \frac{24}{Re} = \frac{24\,\mu'}{\rho' V D} .$$

Hence,

$$\frac{dV}{dt} = g\left(1 - \frac{\rho'}{\rho}\right) - \frac{18V\mu'}{\rho D^2} .$$

Integrating this equation and assuming no evaporation to take place, we have

$$\int dt = \int \frac{dV}{g\left(1 - \frac{\rho'}{\rho}\right) - \frac{18V\mu'}{\rho D^2}}$$

$$t = - \frac{\rho D^2}{18 \mu'} \ln \left[g\left(1 - \frac{\rho'}{\rho}\right) - \frac{18V\mu'}{\rho D^2} \right] + C \qquad (2.27)$$

at $t = 0$ and $V = 0$.

Thus

$$C = \frac{\rho D^2}{18 \mu'} \ln g\left(1 - \frac{\rho'}{\rho}\right) ,$$

and, when substituted back, equation (2.27) becomes,

$$t = - \frac{\rho D^2}{18 \mu'} \ln \left[1 - \frac{18V\mu'}{D^2 g(\rho - \rho')} \right]. \qquad (2.28)$$

Hence,

$$V = \frac{D^2 g(\rho - \rho')}{18\mu'} \left[1 - e^{- \frac{18\mu' t}{\rho D^2}} \right] \qquad (2.29)$$

$$V_{max} = \frac{D^2 g(\rho - \rho')}{18 \mu'} \qquad (2.30)$$

$$V = V_{max} \left(1 - e^{- \frac{18\mu' t}{\rho D^2}}\right). \qquad (2.31)$$

The above equation shows that the variation of velocity with time is exponential.

The distance of fall is given by

$$s = \int_o^t V dt = \frac{D^2 g(\rho - \rho')}{18 \mu'} \left[t + \frac{\rho D^2}{18 \mu'} \left(e^{- \frac{18 \mu'}{\rho D^2} t} - 1\right) \right]. \qquad (2.32)$$

For Re > 2, the following equation is used to determine the elapsed time to reach a certain velocity:

$$t = \frac{4D^2\rho}{3\mu'} \int_0^V \frac{dRe}{(C_D\, Re_{max}^2) - (C_D\, Re^2)} , \qquad (2.33)$$

and the distance of fall is obviously $s = \int V\, dt$.

The derivation of equation (2.32) is given in Appendix B.

It was possible to integrate equation (2.33) graphically and obtain the time as a function of Re, as shown in Fig. 24 (Appendix B). From this plot the velocity of the droplet after a certain time was estimated. A graphical integration of a plot of velocity vs. time gives the position of the droplet after attaining a required velocity. Such a curve is shown in Fig. 25.

When the drag force is equal to the gravitational forces, the droplet falls at a constant maximum velocity which is usually called terminal velocity. The terminal velocity is given by

$$V_{max} = \sqrt{\frac{4(\rho - \rho')g\, D}{3\,\rho'\, C_D}} . \qquad (2.34)$$

Theoretically speaking, the terminal velocity of a freely falling droplet is attained after infinite time. This is readily seen from Fig. 25, as the curve is asymptotic to the terminal-velocity line and meets it in infinity.

In this investigation, droplets of 1000 microns or less reached the first photographing stage at a velocity at least equal to 87% of their terminal velocity. The determination of the elevation of the fuel dropper above the first photographing stage is given in Appendix B.

In actual fuel injection, the droplets generally move at velocities

higher than their terminal velocities. The high initial velocity with which fuel is discharged from the atomizer increases the air resistance on the fuel droplet to an extent that the gravity force can be neglected. This is particularly true during the first part of the droplet travel. Furthermore, the period allowed for spray dispersion is short and no time is allowed for the droplet to slow down to its terminal velocity. When the droplet decelerates, its kinetic energy is dissipated mostly in overcoming air resistance.

D. Mechanism of Vaporization and Combustion of a Single Droplet

The combustion process consists of a succession of diverse and complicated reactions. During the heating and evaporation of a fuel droplet, partial decomposition and oxidation are likely to take place. This is followed by chemical reactions between the fuel and oxygen during which the main energy of the fuel is released. The chemical reactions affect the temperature distribution around the droplet and, hence, the rate of heat transfer to the droplet. The combustion of a fuel droplet thus can be considered a combination of heat transfer, evaporation, diffusion, and chemical reaction. The basic principles of the combustion of liquid fuels can be investigated by considering in detail the mechanism of combustion of an individual fuel droplet in a hot atmosphere.

Preheating of the Droplet

As the droplet enters the furnace, it is suddenly subjected to an atmosphere of greatly higher temperature. The droplet is first heated by conduction and convection from the ambient atmosphere and by radiation from the furnace walls till vaporization and ignition of the gaseous fuel takes place. The time necessary to heat up the liquid of a fuel droplet

before any evaporation occurs is an important item in determining the total rate of combustion of the droplet. This time is calculated by equating the heat received by the droplet to its rate of heating up:

$$\pi D_o^2 h(t_a - t_s) + \pi D_o^2 \sigma \alpha_d \epsilon T_w^4 = \frac{\pi}{6} D_o^3 \rho C_p \frac{dt_\ell}{d\theta}, \qquad (2.35)$$

where

D_o = the diameter of the droplet,

h = the coefficient of heat transfer of the air,

t_a = the temperature of the air,

t_ℓ = the mean temperature of the liquid of the droplet,

t_s = the temperature of the droplet surface,

T_w = the absolute temperature of the furnace walls,

σ = the Stefan-Boltzmann constant,

α_d = the absorptivity of the droplet,

ϵ = the emissivity of the furnace walls,

ρ = the density of the droplet, and

C_p = the specific heat at constant pressure of the droplet.

In the radiation term of the above equation, the temperature of the droplet surface was neglected, compared to the wall temperature, as they are raised to the fourth power.

Integrating between the limits $\theta = 0$, θ and $t_\ell = t_{\ell_o}$, t_ℓ, the heating time is given by

$$\theta = \frac{1}{6} \rho C_p D_o \int_{t_{\ell_o}}^{t_\ell} \frac{dt_\ell}{h(t_a - t_s) + \sigma \alpha_d \epsilon T_w^4}, \qquad (2.36)$$

where t_{ℓ_o} is the mean initial droplet temperature and t_ℓ is the mean droplet temperature just before evaporation starts. To complete the integration of equation (2.36), the variation of t_s with respect to t_ℓ must be

known. If it is assumed that the thermal conductivity of the fuel is high, the temperature can be considered uniform throughout the droplet at all times.[9] The internal circulation in the droplet increases the conductivity of the liquid. With this assumption, equation (2.36) is integrated to give

$$\theta = \frac{1}{6} \rho C_p D_o \frac{1}{h} \log_e \frac{h(t_a - t_{\ell_o}) + \sigma \epsilon \alpha_d T_w^4}{h(t_a - t_\ell) + \sigma \epsilon \alpha_d T_w^4} \qquad (2.37)$$

Vaporization of the Droplet

When evaporation starts, the heat received by the droplet is used in heating the liquid of the droplet and in supplying the latent heat required for vaporization till an inflammable mixture is formed which is able to maintain the flame front.

The quantity of sensible heat generally exceeds the amount of latent heat of vaporization till the steady state of temperature is approached, and then the major portion of the heat used is latent. It is reasonable to assume that the surface temperature of the droplet is close to the boiling point before any flame is produced. The higher the boiling point and the latent heat of the fuel, the greater the tendency for the surface temperature to be less than the boiling point.

After the flame has been established, the droplet vaporizes, receiving heat mainly by conduction and convection from the surrounding flame. The heat transfer by radiation due to the luminous flame is small (see page69). As shown in Fig. 1, the combustion surface is formed at a certain distance from the droplet and the vapor from the droplet surface feeds the combustion surface. The reaction or combustion surface is actually a reaction zone with a definite thickness and is usually defined as the surface where both the vapor and oxygen pressures are zero.

The heat developed at the combustion surface is dissipated in two opposite directions, the first toward the droplet to supply the sensible heat, the latent heat of vaporization, and to raise the temperature of the vapor, and the second away from the droplet into the surrounding atmosphere. Heating of the droplet may continue during combustion and sensible heat is transferred by conduction and convection from the surface of the droplet to the interior.

As the liquid of the droplet diffuses, heat is carried with the diffusing vapor toward the combustion surface, thus reducing the net heat transfer toward the liquid from the combustion surface. The heat transfer to the droplet is thus occurring in the presence of mass transfer of the vapor. The temperature of the vapor increases with distance from the droplet to the combustion surface while its partial pressure decreases. It should be noted that to maintain the combustion around the droplet, air has to move toward the combustion surface, replacing the products of combustion which move in the opposite direction. A schematic diagram of a burning fuel droplet is shown in Fig. 1.

In the following section, the equations governing the vaporization and burning of a fuel droplet are discussed.

The heat-balance equation for a vaporizing droplet in an air atmosphere is

$$-\frac{dm}{d\theta} = \frac{hA}{H_v} (t_a - t_s) , \qquad (2.38)$$

where

$\frac{dm}{d\theta}$ = the vaporization rate, mass/sec,

h = the heat transfer coefficient evaluated at the vapor-air interface,

A = the area of the droplet,

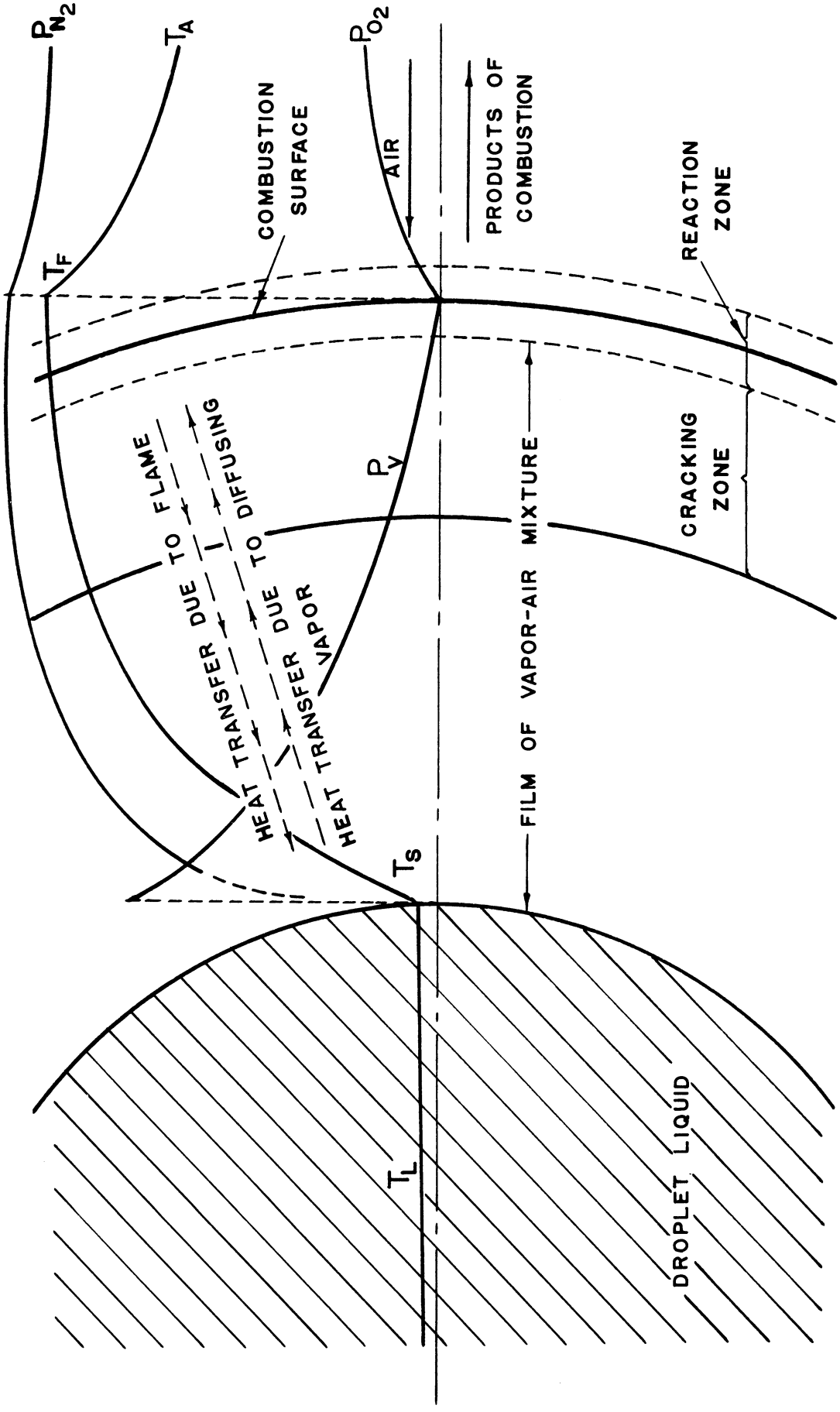

FIG. 1 SCHEMATIC DIAGRAM OF A BURNING FUEL DROPLET.

H_v = the latent heat of vaporization, and

$t_a - t_s$ = the difference between the air temperature and the surface of the droplet.

If there is a difference in the temperature between the surface and the bulk of the droplet, heat is transferred from the surface to the interior, and the above equation becomes

$$-\frac{dm}{d\Theta} = \frac{hA}{H_v + C_{p_\ell}(t_s - t_\ell)} (t_a - t_s), \tag{2.39}$$

where t_ℓ and C_{p_ℓ} are the temperature and the specific heat of the liquid of the droplet, respectively.

If the thermal conductivity of the liquid is high, the heat penetrates rapidly into the droplet and the term $C_{p_\ell} (t_s - t_\ell)$ is small.

If the surrounding atmosphere is at a temperature lower than the boiling point of the droplet, the rate of evaporation is controlled by the increase of vapor pressure and the process is mainly considered as a diffusion process. At high surrounding temperatures, heat transfer is the main controlling factor. The diffusion of the droplet depends on the temperature and on the vapor concentration around the droplet, the latter being a function of temperature, pressure, and turbulence. The turbulence affects the thickness of the boundary layer around the droplet, which is inversely proportional to the rate of diffusion.

The heat transfer coefficient, h, is represented by the equation for the Nusselt number for heat transfer. In natural convection the Nusselt number is a function of Prandtl and Grashof numbers and is given by the following correlations:

$$Nu = 2 + k_1 (Pr)^{1/3} (Gr)^{1/4} \tag{2.40}$$

$$Nu' = 2 + k_2 (Pr)^{1/3} (Gr)^{1/4}, \tag{2.41}$$

where

Nu = the Nusselt number for heat transfer,

Nu' = the Nusselt number for mass transfer,

$Pr = \frac{c_{pm}\mu_m}{k_m}$ = Prandtl number,

$Gr = \frac{D^3 \rho_m^2 g \beta \Delta T}{\mu^2}$ = Grashof number,

k_1 and k_2 = constants, and

β = the expansion ratio of the vapor-air mixture.

In forced convection the motion of the fluid medium past the droplet increases the Nusselt number. In this case the Nusselt number for heat transfer is a function of Prandtl and Reynolds numbers, while for mass transfer it is a function of Schmidt and Reynolds numbers. Most of the data available for Nu or Nu' are at high Reynolds numbers, and for the range of Re of this investigation the writer finds the Ranz and Marshall equation the most suitable. Ranz and Marshall[27] determined evaporation rates of suspended droplets at Reynolds numbers ranging from 0 to 200. The droplet diameters varied from 600 to 1100 microns and the air temperature from 60° to 400°F. Ranz and Marshall gave the following equations:

$$Nu = \frac{hD}{k_g} = 2 + 0.6(Pr)^{1/3} (Re)^{1/2} \qquad (2.42)$$

$$Nu' = M \frac{D p_a K_g}{D_f \rho_m} = 2 + 0.6(Sc)^{1/3} (Re)^{1/2}, \qquad (2.43)$$

where

M = the average molecular weight,

D = the droplet diameter,

p_a = the partial pressure of the air in the film surrounding the droplet,

K_g = the coefficient of mass transfer in film,

Sc = the Schmidt number $\frac{\mu m}{\rho_m D_f}$, and

Re = the Reynolds number $\frac{\rho_m V D}{\mu}$.

It is clear from equations (2.42) and (2.43) that the theoretical minimum for either Nu or Nu' is 2.0. This is nearly true when the droplet diameter is extremely small and the Reynolds number approaches zero. For a stationary droplet evaporating radially in an infinite atmosphere, the Nu equals 2.0. The variation of Nu and Nu' with Re is shown in Fig. 2, where Pr and Sc are taken to be 0.71. Introducing the Nusselt number $Nu = hD/k_g$, k_g being the thermal conductivity of the surrounding atmosphere, equation (2.38) is written

$$-\frac{dm}{d\theta} = \frac{k_g}{H_v} \pi D \, Nu \Delta t, \tag{2.44}$$

but

$$m = \rho_\ell \frac{1}{6} \pi D^3.$$

Then

$$-3D^2 \frac{dD}{d\theta} \frac{1}{6} \pi \rho_\ell = \frac{k_g}{H_v} \pi D \, Nu \Delta t$$

or

$$-D \frac{dD}{d\theta} = \frac{k_g}{H_v} \frac{2 Nu \Delta t}{\rho_\ell} = \frac{\lambda}{2}, \tag{2.45}$$

where

$$\lambda = \frac{4 k_g Nu \Delta t}{H_v \rho_\ell}. \tag{2.46}$$

It is seen from equation (2.45) that λ is directly proportional to Nu.

Equation (2.45) can be rewritten as

$$-\frac{d(D^2)}{d\theta} = \frac{4k_g}{H_v} \frac{Nu \Delta t}{\rho_\ell} = \lambda.$$

Integrating the above equation and assuming that at $\theta = 0$, $D = D_o$, we have,

$$D^2 = -\lambda\theta + D_o^2, \tag{2.47}$$

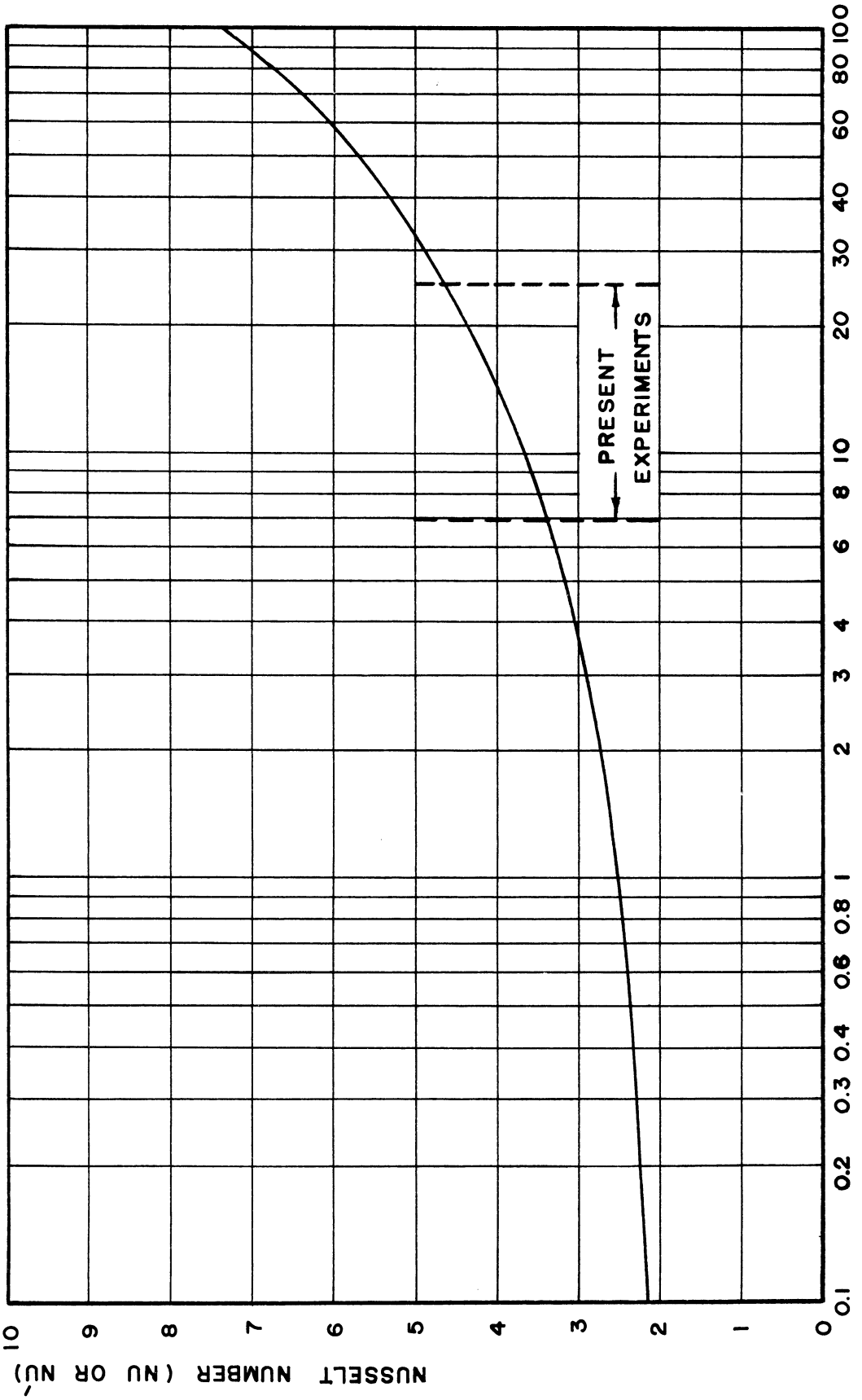

FIG. 2 NUSSELT NUMBER FOR HEAT AND MASS TRANSFER FOR SPHERES MOVING AT LOW REYNOLDS NUMBER (RANZ)

and the total time for complete evaporation is given by

$$\theta = \frac{D_o^2}{\lambda}, \tag{2.48}$$

also

$$-\frac{dm}{d\theta} = \frac{\pi}{4}\rho_\ell \lambda D, \tag{2.49}$$

or the rate of change of mass of a stationary evaporating droplet is proportional to the first power of its diameter.

If equation (2.38) is written as a conduction equation for a stationary droplet in an infinite medium, then

$$-\frac{dm}{d\theta} = \frac{k_g A}{H_v}\frac{dt}{dr}, \tag{2.50}$$

which, upon integration from $t = t_s$ and t_a and $r = r$ and ∞, gives

$$-3D^2\frac{dD}{d\theta}\frac{1}{6}\pi\rho_\ell = \frac{4k_g\pi r}{H_v}\Delta t$$

or

$$-\frac{dD^2}{d\theta} = \frac{8k_g\Delta t}{\rho_\ell H_v} = \lambda. \tag{2.51}$$

Comparing equation (2.46) and equation (2.51), we see that Nu = 2.0 for a stationary droplet evaporating in an infinite quantity of medium.

If there is other heat exchange, equation (2.44) becomes

$$-\frac{dm}{d\theta} = \frac{k_g\Delta t}{H_v}\pi D\ Nu \pm \frac{Q}{H_v}, \tag{2.52}$$

where Q is the amount of heat exchanged and the positive and negative signs mean heat addition and subtraction, respectively. Thus, in the case of heat addition by radiation from the surrounding gas,

$$Q = \sigma F' A(T_g^4 - T_\ell^4), \tag{2.53}$$

where

σ = the Stefan-Boltzmann constant,

F = a factor to allow for interchange between the droplet and the radiating medium,

A = the surface area, πD^2,

T_g = the absolute gas temperature, and

T_ℓ = the absolute liquid temperature.

By putting

$$h_r = \frac{\sigma F (T_g^4 - T_\ell^4)}{T_g - T_\ell}, \tag{2.54}$$

and since only a fraction of the incident radiation is absorbed by the droplet, then $Nu_r = \alpha_d \frac{h_r D}{k_g}$ = Nusselt number for the absorbed radiation, where α_d is the absorptivity of the droplet. Equation (2.52) becomes

$$-\frac{dm}{d\theta} = \frac{k_g \Delta t}{H_v} \pi D(Nu + Nu_r). \tag{2.55}$$

Up to this point, nothing has been said regarding the heating of the vapor leaving the droplet surface. In this case, if the sensible heat is small, the heat-balance equation is

$$\frac{dm}{d\theta}\left[H_v + c_{p_v}(t - t_s)\right] = -Ak_g\frac{dt}{dr}, \tag{2.56}$$

where

c_{p_v} = the average specific heat of the vapor,

t = the temperature of the vapor,

k_g = the average thermal conductivity of the surrounding atmosphere, and the other terms are as defined before.

Integrating equation (2.56) between the limits $t = t_s$ and t_a and $r = r$ and ∞, we have

$$-\frac{dm}{d\theta} = \frac{2\pi k_g D}{c_{p_v}} \ln\left[1 + c_{p_v}\frac{t_a - t_s}{H_v}\right]. \tag{2.57}$$

Putting the value of m in terms of D, equation (2.57) reduces to

$$-\frac{dD^2}{d\theta} = \frac{8k_g}{\rho_\ell \, c_{p_v}} \ln\left[1 + c_{p_v}\frac{t_a - t_s}{H_v}\right] \tag{2.58}$$

$$\lambda = \frac{8k_g}{\rho_\ell \, c_{p_v}} \ln\left[1 + c_{p_v}\frac{t_a - t_s}{H_v}\right]. \tag{2.59}$$

Then, integrating equation (2.58), we get

$$D^2 = D_o^2 - \lambda\theta. \tag{2.60}$$

In the same manner as before, if equation (2.56) is written as a convection equation, the expression for λ is

$$\lambda = \frac{4Nu\, k_g}{\rho_\ell \, c_{p_v}} \ln\left[1 + c_{p_v}\frac{t_a - t_s}{H_v}\right]. \tag{2.61}$$

Evaporation of a Droplet in a Gas Stream

In a gas stream, where there is relative velocity between the vaporizing droplet and the surrounding atmosphere, the rate of mass transfer is greater than when the droplet is at rest. Frössling gives the following equation for Nusselt number for mass transfer:

$$\frac{hRTD}{D_f P} = 2\left[1 + 0.276\, Re^{1/2}\, Sc^{1/3}\right]. \tag{2.62}$$

Nearly all work done on evaporating droplets in a gas stream has been based on Frössling's semi-empirical equation. Ingebo gives a similar equation for Nu for heat transfer:

$$Nu = \left(\frac{k_g}{k_v}\right)^{0.5}\left[2 + 0.303(Re\, Sc)^{0.6}\right], \tag{2.63}$$

where

$Re = \frac{\rho V D}{\mu}$, $Sc = \frac{\mu}{\rho D_f}$, D_f being the diffusion coefficient, R the gas constant, and T and P absolute temperature and pressure of vapor, respectively.

For a constant value of Δt, Sc can be considered a constant and the

above equation is written as

$$-\frac{1}{6}\pi\rho\, 3D^2\frac{dD}{d\theta} = \frac{k_a\Delta t}{H_v}\,\pi D\left(\frac{k_a}{k_v}\right)^{0.5}\left[2 + .303(Re\ Sc)^{0.6}\right]$$

or

$$-\frac{dD}{d\theta} = \frac{a}{D} + \frac{b}{D}R^{0.6} = \frac{a}{D}\left[1 + \frac{b}{a}\,R^{0.6}\right], \qquad (2.64)$$

where

$$a = \frac{4k_a\Delta t}{\rho\, H_v}\left(\frac{k_a}{k_v}\right)^{0.5}$$

and

$$b = \frac{.606\ k_a\Delta t(Sc)^{0.6}}{\rho\ H_v}\left(\frac{k_a}{k_v}\right)^{0.5}.$$

From equation (2.64) it is seen that the effect of the relative velocity is the introduction of the term $\left[1 + fR^{0.6}\right]$, where

$$f = \frac{b}{a} = 0.1515\ (Sc)^{0.6}. \qquad (2.65)$$

If the same procedure is applied to the Frössling equation, the mass evaporation rate in flowing air $\frac{dm}{d\theta}$ is given by

$$\frac{dm}{d\theta} = \frac{dm'}{d\theta}\ (1 + f'R^{0.5}), \qquad (2.66)$$

where $\frac{dm'}{d\theta}$ is the mass evaporation rate in still air, where

$$f' = 0.276(Sc)^{1/3}. \qquad (2.67)$$

From the Frössling equation it is readily seen that the mass transfer rate is twice the rate without relative motion when the Reynolds number is about 13, other factors remaining unchanged.

Heat Transfer From the Flame to the Droplet

When the flame is established around the droplet, the rate of burning becomes essentially a problem of heat transfer and the vapor pressure

has only a little effect in determining the rate of vaporization. The flame increases the thermal gradient close to the droplet surface and the amount of vaporization is governed by the temperature gradient, the surface temperature, and the latent heat of the fuel.

For a stationary droplet, the flame forms a complete envelope around the fuel surface, but for a moving droplet the flame may either form a complete envelope or only be attached to the wake of the droplet, depending on the relative velocity between the droplet and the surrounding air.

Mathematically speaking, combustion is the same as evaporation since the droplet is only affected by the amount of heat it receives. If it is assumed that the surface temperature of the droplet is near its boiling point, the value $\Delta t = t_F - t_\ell$, where t_F is the flame temperature and t_ℓ is the boiling point of the liquid, remains fairly constant during the combustion process. Thus the burning droplet can be considered as an evaporating droplet, taking into consideration the higher thermal gradient. The vapor leaving the droplet maintains the diffusion flame, and the rate of vaporization is the same as the rate of burning.

For a stationary droplet, heat is transferred to the droplet by both radiation and conduction from the flame, the latter being more important. The radiation absorbed by the droplet is given by

$$q_r = \sigma A \epsilon_F \alpha_d (T_F^4 - T_\ell^4) , \qquad (2.68)$$

where

q_r = the rate of heat transfer by radiation,

σ = the Stefan-Boltzmann constant,

A = the area of the droplet,

ϵ_F = the emissivity of the flame,

α_d = the absorptivity of the droplet,

T_F = the absolute flame temperature, and

T_ℓ = the absolute liquid temperature.

In the above equation, T_ℓ^4 is negligible when compared to T_F^4. The rate of combustion due to radiation from the flame is thus given by

$$\frac{dm}{d\theta} = \frac{\sigma A \epsilon_F \alpha_d T_F^4}{H_V + c_{p_\ell}(t_s - t_\ell)} , \tag{2.69}$$

where

H_V = the latent heat of the fuel,

c_{p_ℓ} = the specific heat of the liquid of the droplet, and

t_s = the surface temperature of the droplet.

The heat conduction from the flame is estimated with the assumption that the vapor flow is radial and the flame is spherically symmetrical about the droplet. The heat transfer toward the surface of the droplet is given by

$$q_c = - k A \frac{dt}{dR} , \tag{2.70}$$

where

q_c = the rate of heat transfer by conduction,

k = the thermal conductivity of the vapor-air mixture,

A = any spherical area through which heat is conducted from the flame to the droplet = $4\pi R^2$, and

$\frac{dt}{dR}$ = the temperature gradient at radius R.

$$q_c = -k\, 4\pi R^2 \frac{dt}{dr} . \tag{2.71}$$

Separating the variables and integrating between the limits $t \leq t_F$, t_ℓ and $R = R_F$, R_ℓ where F and ℓ stand for flame and liquid,

$$q_c = k_m\, 4\pi \frac{t_F - t_\ell}{\frac{1}{R_F} - \frac{1}{R_\ell}} , \tag{2.72}$$

k_m is the mean value of k of the vapor-air mixture, q_c is used in supplying the latent heat to the fuel evaporated, in heating the droplet, and in raising the temperature of the vapor-air mixture, thus,

$$q_c = \frac{dm}{d\theta} \left[H_v + c_{p_\ell} (t_s - t_\ell) + \int c_{p_v} \, dt \right] , \qquad (2.73)$$

where c_{p_v} is the specific heat of the vapor-air mixture, and the other terms are as defined in equation (2.39).

If the surface of the droplet is assumed to be at the boiling point and $t_s = t_\ell$, then, if we assume a mean value of c_{p_v},

$$q_c = \frac{dm}{d\theta} \left(H_v + c_{p_{vm}} \int dt \right). \qquad (2.74)$$

Equating equations (2.72) and (2.74), the rate of combustion due to heat transfer by conduction is given by

$$\frac{dm}{d\theta} = 4\pi k_m \frac{t_F - t_\ell}{\frac{1}{R_F} - \frac{1}{R_\ell}} \frac{1}{H_v + c_{p_{vm}}(t_F - t_\ell)} . \qquad (2.75)$$

The total rate of combustion is obtained by adding equations (2.69) and (2.75).

It is clearly seen from equation (2.75) that the thermal conductivity of the vapor-air mixture is an important factor in determining the rate of heat transfer to the droplet and, consequently, the rate of combustion.

In considering heat transfer in the region between the droplet surface and the flame front, the mean properties of the substances present must be used in the calculations. Very little oxygen penetrates the flame front, and nitrogen, fuel vapor, and products of combustion are the main substances present in that region.

Godsave,[15] in order to simplify mathematical treatment, considered steady-state conditions to prevail for a burning droplet with no source

or sink of heat within the droplet. He further assumed spherical symmetry, fixed size of both the droplet and the flame, and radial heat and mass transfer. By equating the inward flow of heat at the droplet surface to the heat content of the vapor leaving the droplet, Godsave was able to deduce the following analytical expression for the burning rate in the presence of the evaporative flow from the droplet:

$$\frac{dm}{d\theta} = \frac{\ln\left[1 + \frac{c\,\Delta T}{(\Delta H - a)}\right]}{\frac{c}{4\pi k}\left(\frac{1}{R_\ell} - \frac{1}{R_F}\right)}, \tag{2.76}$$

where

c = mean heat capacity at constant pressure of the vapor between the droplet surface and the flame front,

ΔT = difference in temperature between the droplet surface and the flame front,

ΔH = amount of heat per unit mass necessary to raise the temperature and to evaporate the fuel,

a = amount of radiant heat absorbed per unit mass of fuel evaporated,

k = mean thermal conductivity of the vapor between the droplet surface and the flame front,

R_ℓ = radius of the droplet, and

R_F = radius of the spherical flame front.

He assumed that the solution given by equation (2.76) for a fixed-size droplet applies to a droplet decreasing in size when it reaches the diameter used in the steady-state solution.

Mathematical treatment of a burning fuel droplet moving relative to the surrounding atmosphere is quite complex. At present, all that can be said is that the relative motion increases the rate of burning of a drop-

let which can be estimated if equation (2.76) is multiplied by the factor $(1 + f''Re^{0.5})$ as in the case of evaporation, f" being a constant. With an increase in Re, the boundary-layer thickness will decrease and the flame moves toward the droplet, increasing the temperature gradient and, consequently, the evaporation rate.

III. EXPERIMENTAL METHOD AND PROCEDURE

The experimental technique consisted in photographing burning fuel droplets falling freely in a heated atmosphere. The two main measurements necessary to study the evaporation and burning rates of fuel were the changes in the droplet sizes or diameters and the time intervals between these changes. In this section a brief description of the experimental equipment and the difficulties encountered in its operation are described. The details of the design and construction of the equipment are given in Appendix A.

A. Description of Equipment

The main objective in the design of the furnace was to attain the required temperatures, to minimize convection currents, to have uniform temperature within the furnace, and to make possible the photographic observation of the falling droplets.

The furnace, as shown in Figs. 3 and 4, was in the form of a rectangular parallelepiped of dimensions 4 x 17-1/2 x 45 inches. It consisted of two main heating elements placed opposite to each other and one inch apart. The heating wire was embedded in two alundum (Al_2O_3) pieces of dimensions 1-1/4 x 4 x 45 inches, which constituted the heating sides of the furnace. The resistance wire was 16-gage Chromel A; it was made into a helix before being cast in the alundum. The total power of the furnace was 7.64 kw and the maximum temperature reached was 1700°F. The furnace was insulated on two sides only by firebrick and vermiculite contained within a sheet-metal steel shell. Two continuous and opposite glass windows provided easy observation and photographing of the fuel droplets as they fell through the furnace.

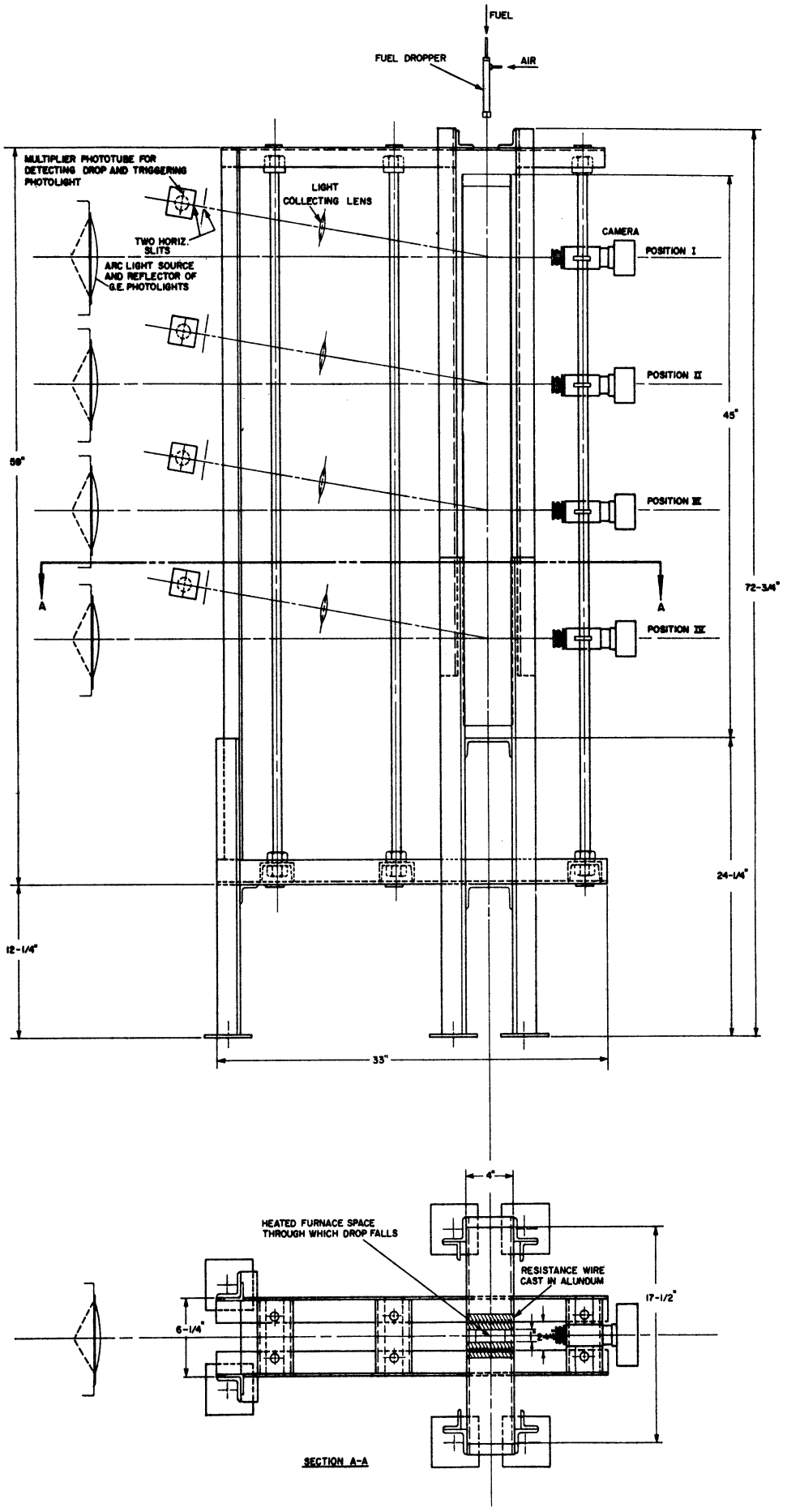

FIG. 3 ELEVATION AND CROSS-SECTION PLAN OF THE VERTICAL FURNACE

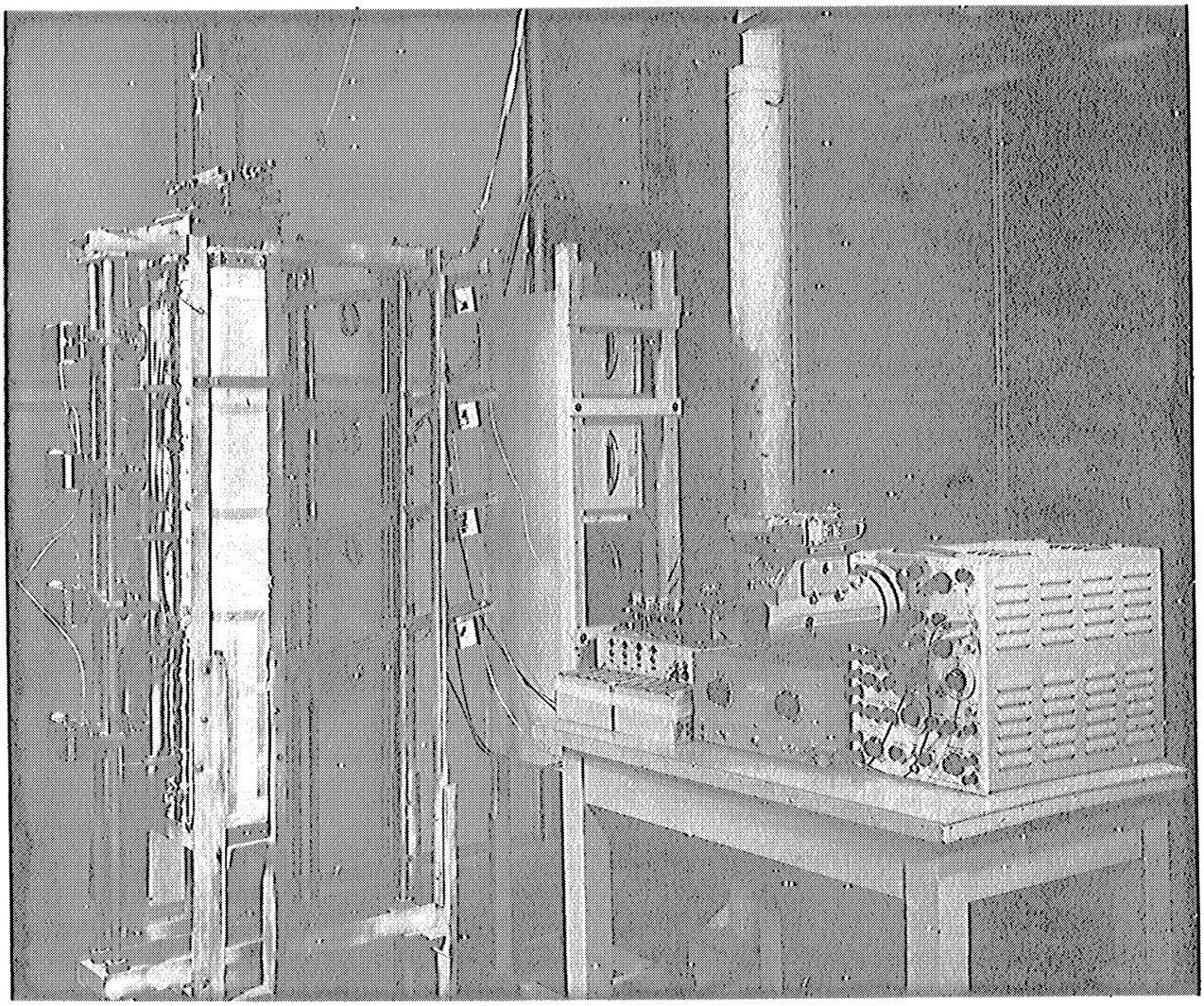

Fig. 4. Experimental equipment.

The temperature of the furnace was measured with three iron-constantan thermocouples. The potentials developed by the thermocouples were read by means of a Leeds and Northrup potentiometer.

The formation of fuel droplets was accomplished by a small-bore tube from which the droplets were thrown off by a concentric jet of air. It was difficult to form a droplet of a diameter less than that of the outside diameter of the capillary tube and still suitable for this investigation. Experience shows that the droplet size can be controlled by capillary bore size, pressure of the concentric air jet, head of the fuel, and the distance the capillary protrudes beyond the air nozzle.

The fuel dropper, shown in Fig. 5, consisted of a hypodermic needle of 0.0185-inch outside diameter, to which the fuel line was connected. The needle was centered into a 4-1/2-inch-long, 1/2-inch-outside-diameter brass tube. The tube was closed at one end, except for the fuel supply line, and had an orifice plate at the other end. The tip of the needle passed through the hole of the orifice plate. Compressed air supplied to the brass tube passed through the orifice, and small fuel droplets at the tip of the needle were thrown off by the concentric air jet.

Three of the four photographing positions were used to record the drop diameter as it fell through the furnace. The fourth position was not used, first, due to the unavailability of a fourth G. E. light, and, second, due to the fact that the bottom section of the furnace was slightly cooler than the rest of the furnace. On one side of the furnace the cameras were mounted in front of the window of the furnace, and on the other side three G. E. high-speed photolights were placed opposite the cameras, the main feature of the photolights being the extremely short duration of the illumination. This permitted the open-shutter technique during the

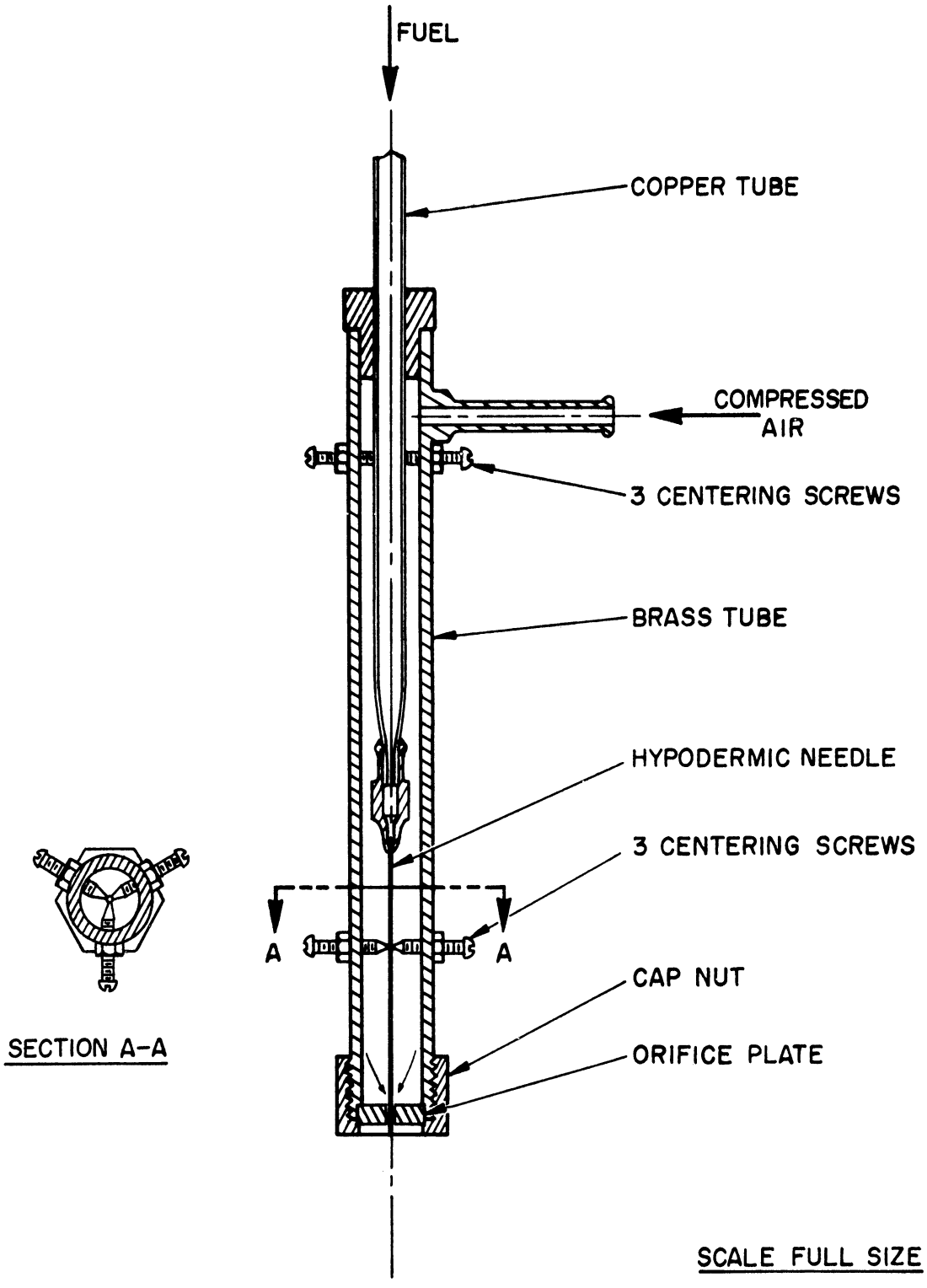

FIG. 5 FUEL DROPPER

fall of the droplets. Due to the high intensity of illumination supplied by the photolights, the droplet's silhouette, without the flame, appeared on the film.

The detection of the falling droplet was done by multiplier phototubes which, by means of thyratron tubes, trigger the high-speed photolights. The light of the burning droplet activated the multiplier phototubes. The detection and triggering circuit is shown in Fig. 6. The multiplier phototube amplified the pulse produced by the light emitted from the burning droplet high enough to drive the input of a 6SF5 amplifier tube. The output of this amplifier was capacitively coupled to the grid of the thyratron tube 2050. The sensitivity of the thyratron was controlled by the variable d-c grid bias effected through a 6-volt battery and a potentiometer. The thyratron breakdown current was self-controlled.

The timing pulses produced when the photolights flashed were recorded on the screen of a Tecktronix oscilloscope. At the same time, pulses from a 60-cycle square-wave generator were superimposed on the timing pulses of the photolights. These pulses were photographed for every falling droplet by means of a Polaroid camera mounted on the oscilloscope. Knowing the exact timing between the pulses produced by the square-wave generator, it was possible to know the time intervals between the flashes of the photolights. A typical photograph of the timing pulses is shown in Fig. 7, and the arrangement of the electrical equipment is shown in Fig. 8.

In the following section, some of the difficulties encountered in setting up the experimental equipment and the procedure of running a test are briefly outlined.

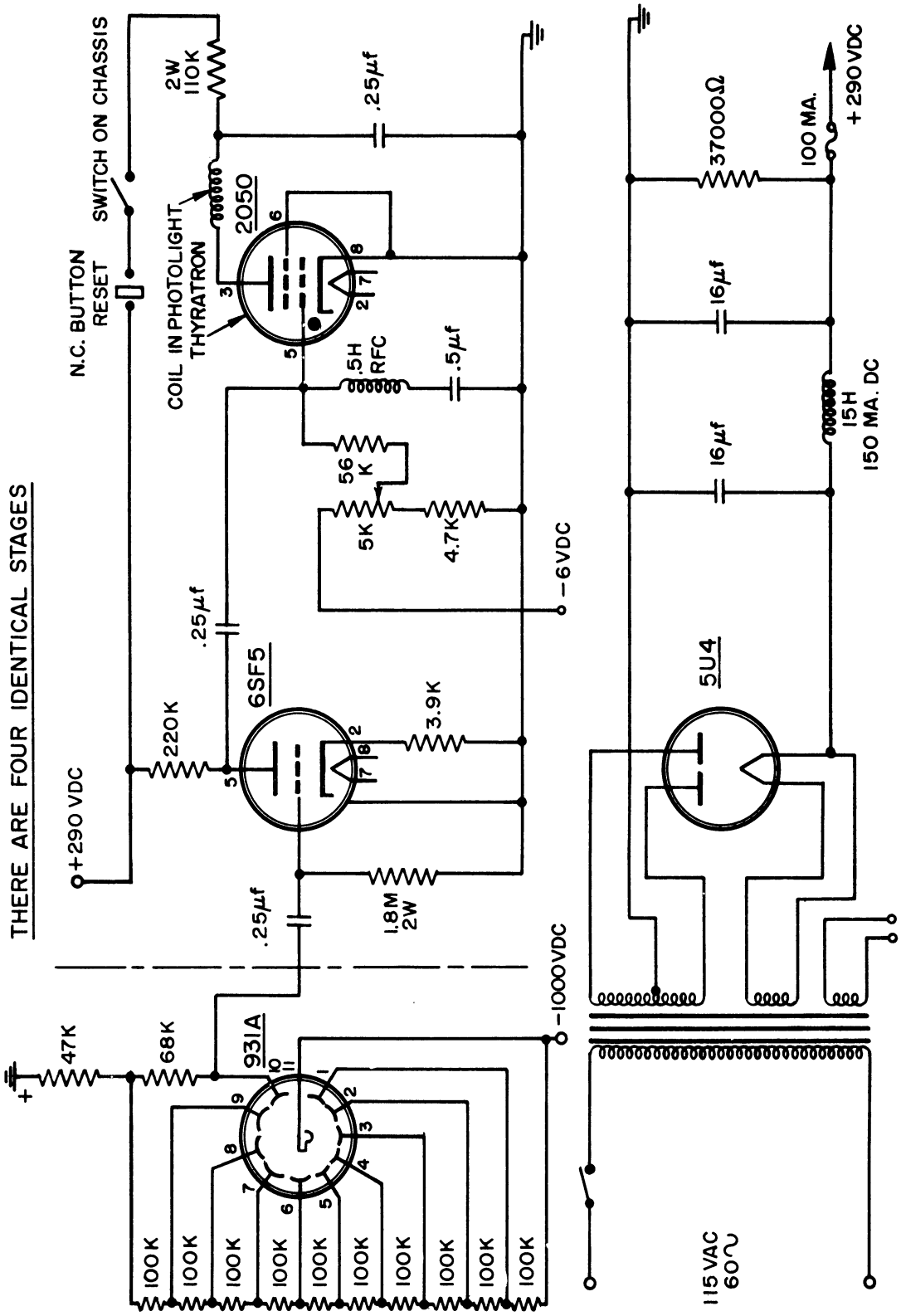

FIG. 6 DETECTION CIRCUIT DIAGRAM

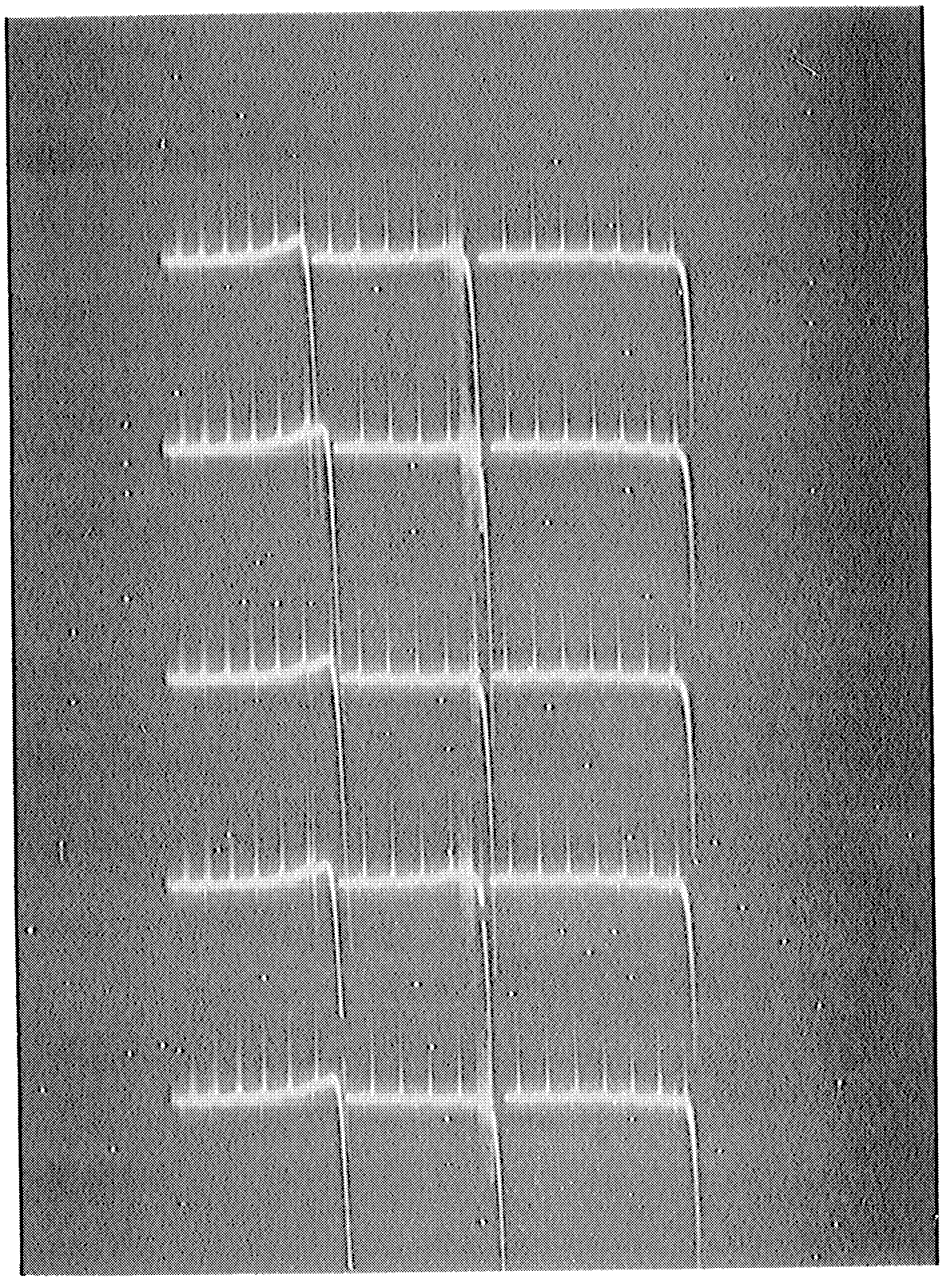

Fig. 7. A typical photograph of the timing pulses.

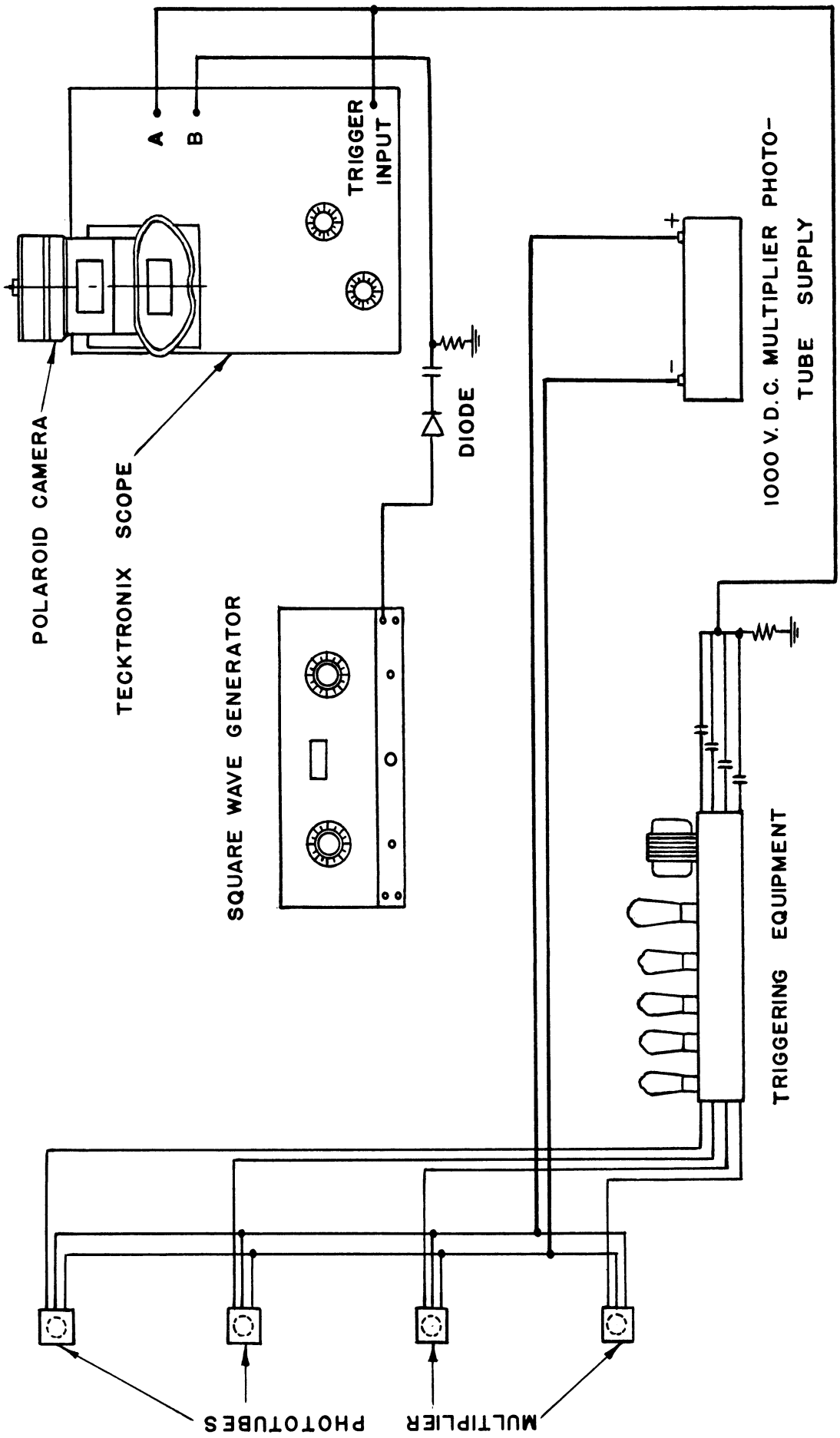

FIG. 8 ARRANGEMENT OF ELECTRICAL EQUIPMENT.

B. Operation of Equipment and Procedure

The work on combustion of falling droplets was carried out while using pure hydrocarbon fuels and kerosene at a furnace temperature of 1500°F. The fuel dropper was carefully aligned with the furnace center line and was placed 21 inches above the first photographing position. As indicated in Appendix B, approximately 87% of the terminal velocity of the falling droplet was reached before that position. The droplet entered the furnace through a small hole of 1/4-inch diameter at the top of the furnace and, although this was the only opening in the test action of the furnace, convection currents were appreciable. Although some air flow was desirable in the furnace to prevent accumulation of vapor and products of combustion, the velocity of air flow was kept down to a minimum. Trouble was experienced in confining the droplets to fall along a vertical line. Convection currents were practically inevitable and small droplets were disturbed by the eddies and currents at the furnace entrance.

The preliminary tests were done with droplets of relatively large size (above 1000 microns) so that the problems of vertical fall and detection of the droplets were minimized. As experience was gained, smaller drops within the desired range were used to obtain the experimental data. Practically all the initial work was done while using n-heptane as fuel.

The air necessary for the dropper was controlled by a needle valve and the change of the size of the droplets produced was very sensitive to any variation in the air pressure. By increasing the air pressure, very minute droplets could be obtained, but they were hard to see unless a light was concentrated on the tip of the capillary. These small droplets were unsuitable for this investigation as they were scattered after leaving the capillary.

Ignition of the droplets was accomplished by the hot atmosphere of the furnace, and at 1500°F the droplets started burning soon after they entered the furnace. By visual observation, burning started when the droplets were one inch or less inside the furnace. The light of the burning droplet was used as an actuation source for the multiplier phototubes.

The time delay between the detection of the falling droplet by the multiplier phototubes and the flashing of the photolights was desired to be a minimum. If the delays were long or variable, there was no guarantee that the falling droplets would be within the fields of view of the cameras. The variation of the delay could be due to the variation of the velocity of the droplets, which in turn depends on the size of the droplets, furnace temperature, furnace atmosphere, and the type of fuel used.

As a first attempt in designing the detection circuit, each thyratron tube was made to actuate the photolight by means of a relay. The relay was also made to actuate a solenoid mounted above the camera. The function of the solenoid was to open the camera shutter at the instant when the falling droplet was in the field of view of the camera. Checking the delay step by step by an electronic interval timer revealed that most of the delay occurred in the mechanical elements of the circuit, i.e., the relay and the solenoid. The total delay was variable and was about 0.08 sec, which was too large a value to permit photographing of the droplet at the proper instant. To overcome this difficulty, attention had been directed toward eliminating the mechanical units from the circuit, substituting electronic means for the flashing of the photolight. This was done by connecting the plate of the thyratron tube to the energizing coil in the photolight, and the thyratron tube was made to flash the light directly, thus eliminating the mechanical relay. To eliminate the solenoid which opened the shutter of the camera, advantage was taken of the very short

duration of the light when the photolight flashed. The duration of the light was approximately one microsecond, which permitted the open-shutter technique for the cameras.

Difficulty had been experienced with the triggering circuits, and the thyratron tubes all triggered simultaneously, when only one should have triggered. This was a result of radiation and pickup from one circuit to another and was remedied by shielding, shortening leads, and by means of minor circuit changes.

After overcoming these difficulties, the time delay was reduced to a very small duration which made possible the detection and the photographing of the droplet before it moved out of the 7/8-inch length covered by the camera. The time delay was in the microsecond range.

The magnification ratio was about 1:1. It was desirable to have a bigger magnification ratio, but this had the disadvantage of a smaller field of the camera and longer extension tube between the camera lens and the image. With the above-mentioned magnification ratio, the field of the camera was a circle of about 7/8-inch diameter. The distances shown in Fig. 9 were calculated from the following relations:

$$u = (m + 1) f$$

$$v = (1/m + 1) f ,$$

where

u = the object-lens distance,

v = the image-lens distance,

f = the focal length, and

m = the magnification.

For f = 75 mm and m = 1, u = v = 150 mm.

Actually, these distances differed slightly from the above values

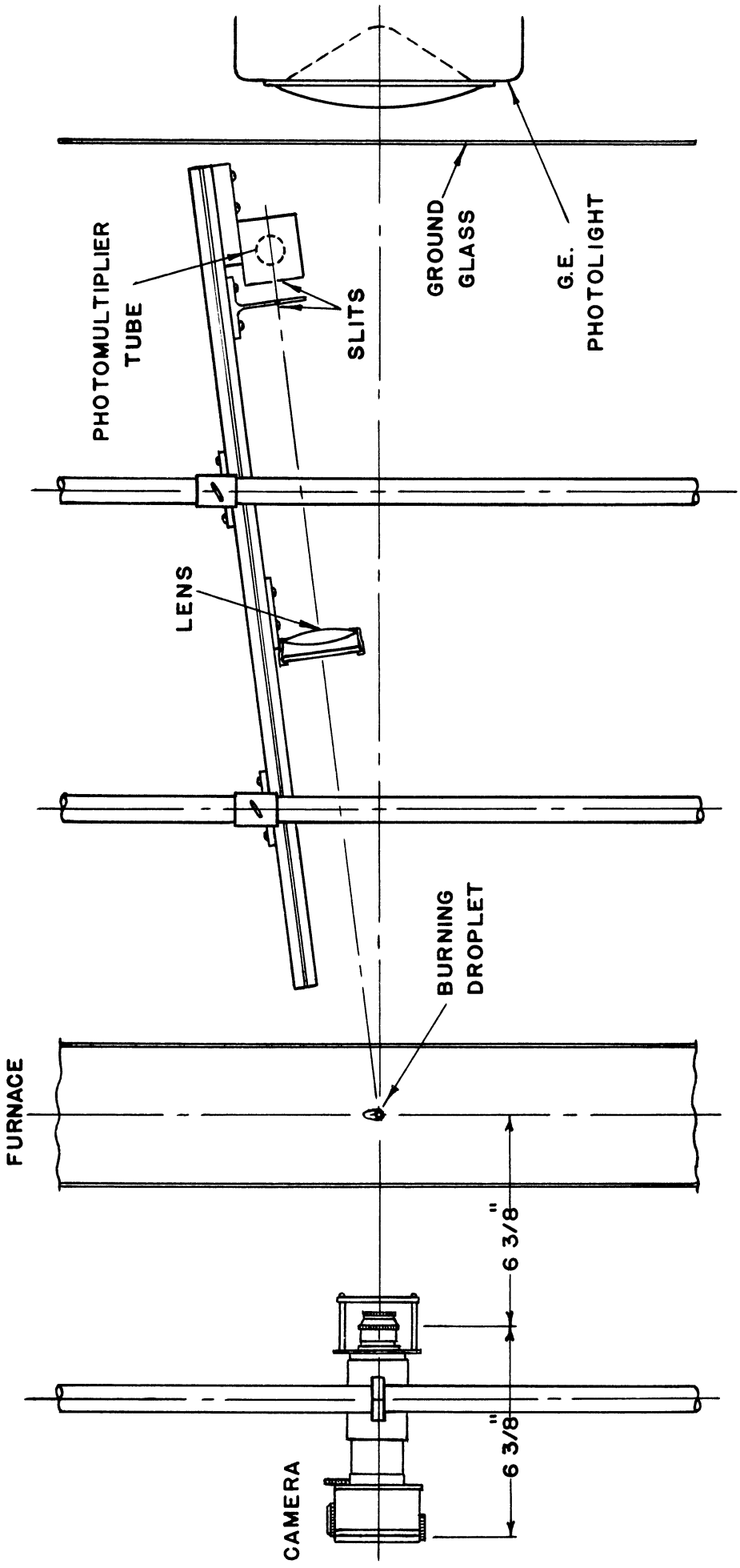

FIG. 9 TYPICAL DETECTOR AND CAMERA POSITION.

but were equal to 6-3/8 inches. The exact magnification ratio was obtained by photographing an accurately measured wire of diameter 0.08253 inch. The image of the wire was magnified twenty times before being measured. When the photographed droplet was in focus, the magnification ratio of image to object was 0.977. The photographs of the falling droplets had to be of sufficient clarity and sharpness to provide magnification up to about twenty times, suitable for accurate measurements.

The multiplier phototubes were carefully aligned with respect to the cameras. A typical detector and camera position is shown in Fig. 9. The best method of alignment consisted in hanging a small bulb in the furnace at the intersection of the furnace center line and the axis of the camera. The light from the bulb was checked to see if it fell on the slit of the box enclosing the photomultiplier tube.

The procedure of running a test was as follows. The hypodermic needle of the fuel dropper was checked to see if it was carefully centered in the middle of the air orifice. Careful centering of the needle was necessary to ensure a vertical path of the droplets leaving the tip. This was done by the two sets of the centering screws of the dropper. The dropper was then aligned with the furnace center line and placed 21 inches above the first photographing stage. If the dropper was placed at a higher elevation, it was difficult to confine small droplets to a vertical path.

The temperature of the furnace was brought to the desired value and was checked by the thermocouples. It took about 45 minutes to bring the furnace to 1500°F. Little advantage was obtained from the tapped winding and a mean value of the temperatures of the thermocouples was considered the sustaining value.

Fuel was introduced into the dropper and the air pressure was adjusted

to give the required size of droplets. The droplets fell intermittently through the small hole at the top of the furnace and were ignited by the heat of the furnace. It was possible to see the droplets falling through the furnace only if they were surrounded by a flame. Several minutes before the run was made, the electronic circuit, oscilloscope, and square-wave generator were turned on and allowed to warm up. The traces on the screen of the scope were checked through the eye shield and the viewing door of the Polaroid camera. The viewing door could be opened and closed by means of a lever knob.

At the instant before a droplet left the dropper, the camera shutters were opened by a master cable release to which the individual cable releases were connected. At the same time, the cable release of the Polaroid camera was pressed in order to photograph the timing pips. The flame attending the drop energized the multiplier phototubes, which in turn triggered the high-intensity photolights. The shutters were closed as soon as the photolights flashed. If this failed to happen, the pictures of the following droplet and its timing pips would be superimposed on the original picture. The films were then wound and the Polaroid camera was moved back to await the following picture. After every five exposures it was necessary to change and develop the frame in the Polaroid camera and, in the meantime, the furnace temperature was checked.

The examination of the films consisted of measuring the diameters of droplets and the timing intervals between the successive flashes. By means of a comparator, the droplet images were magnified about twenty times to permit accurate measurements of the diameters. Some droplets, especially large ones, were distorted and they were not included in the results. The diameters were measured in two perpendicular directions and the average

was taken, the result for any droplet with its greatest and least diameters differing by more than 5% being discarded. The timing intervals between the photolights' flashes were accurately measured by comparing the distance between these pulses and the equal distances between the pulses of the square-wave generator. The error in measuring the droplet images on the comparator and the timing intervals was estimated to be within $\pm$ 1%.

Curves of diameter vs time were plotted for the fuels investigated. By knowing three diameters and two timing intervals, it was possible to draw a curve between diameter vs time for every droplet. The curves shown in Figs. 10, 11, and 12 were obtained by superimposing the individual curves of the different sizes of droplets. In Figs. 13, 14, and 15, the square of the diameter is plotted vs the elapsed time.

IV. RESULTS

The combustion of two pure hydrocarbon fuels and kerosene was investigated at an ambient temperature of 1500°F. The range of the droplet diameters was approximately from 1150 to 300 microns.

The pure hydrocarbons investigated were n-heptane and isooctane bought from the Phillips Petroleum Company. They were classified as pure grades. Kerosene was bought from the Fisher Scientific Company. Detailed properties of the fuels are given in Appendix D. Figure 17 shows various sizes of burning n-heptane droplets and Fig. 18 shows a series of photographs of n-heptane, isooctane, and kerosene taken in sequence as they fell through the furnace.

The results of combustion studies are presented in Figs. 10, 11, and 12, where the diameters of the droplets at the photographing positions are plotted against time. In Figs. 13, 14, and 15, the square of the diameter was plotted against time.

It was difficult to obtain data for droplets below 300 microns with the present setup, but the curves could be extrapolated for smaller droplets.

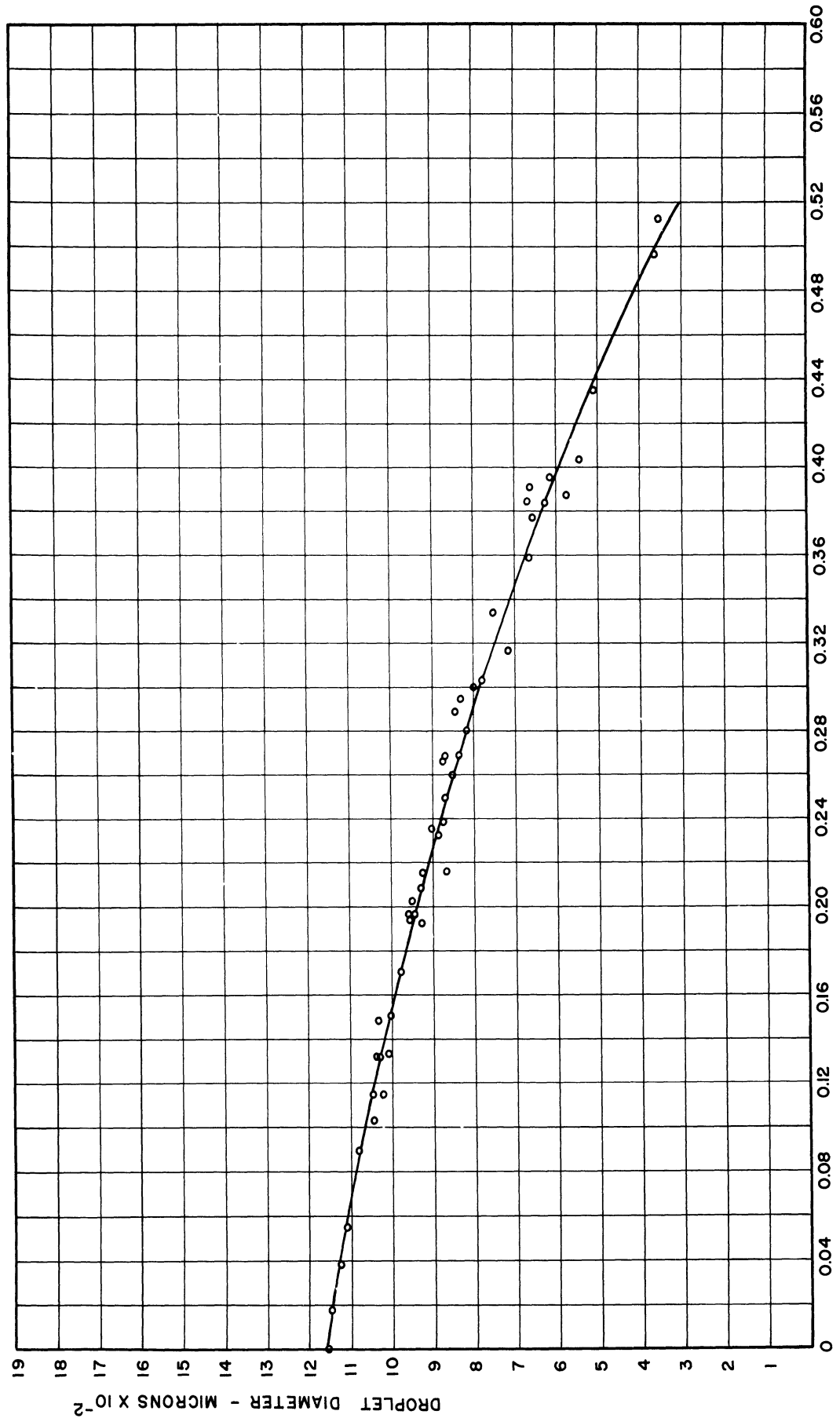

FIG. 10 COMBUSTION OF N-HEPTANE IN AIR AT 1500 °F

DIAMETER VS TIME

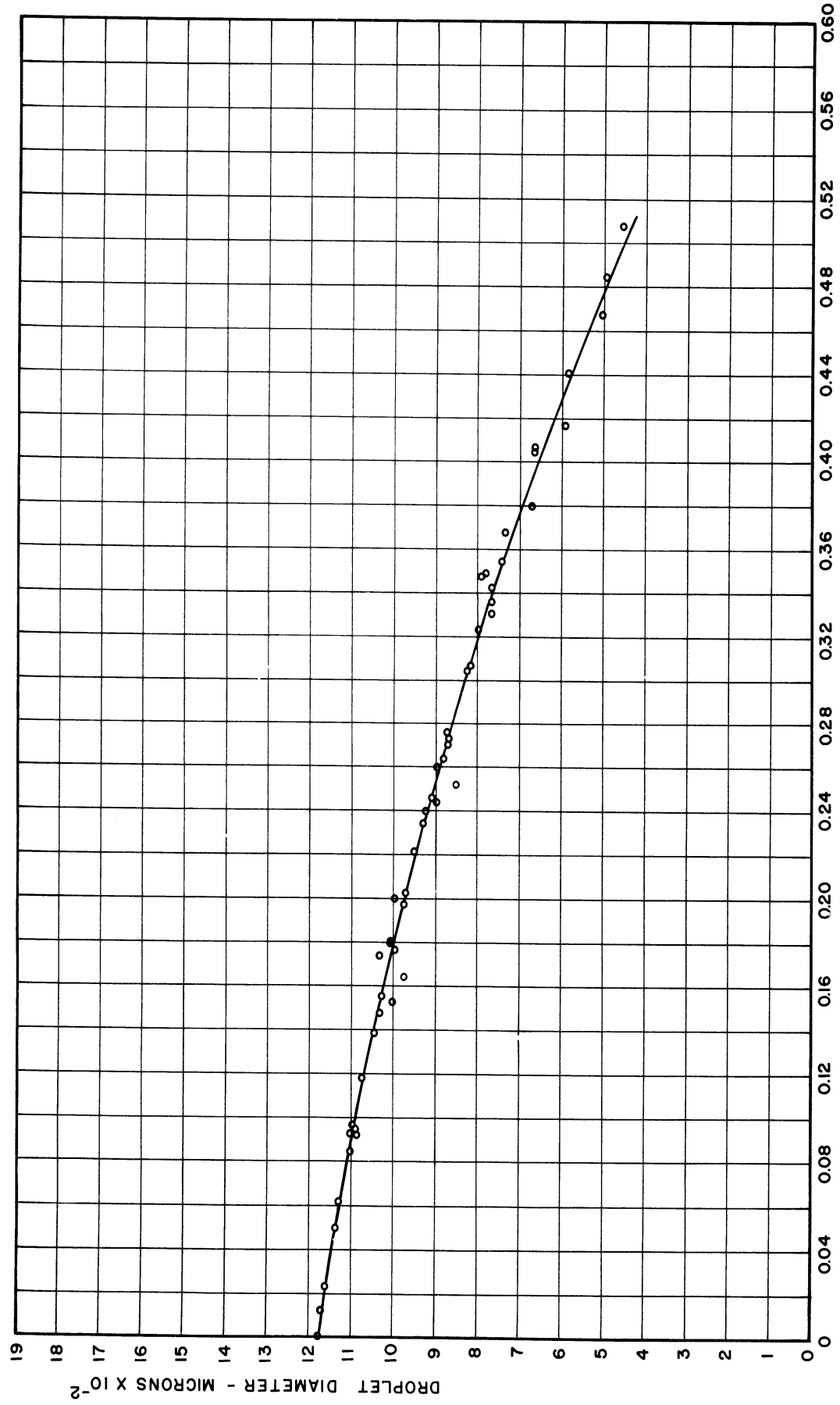

FIG. 11 COMBUSTION OF ISOOCTANE IN AIR AT 1500 °F

DIAMETER VS TIME

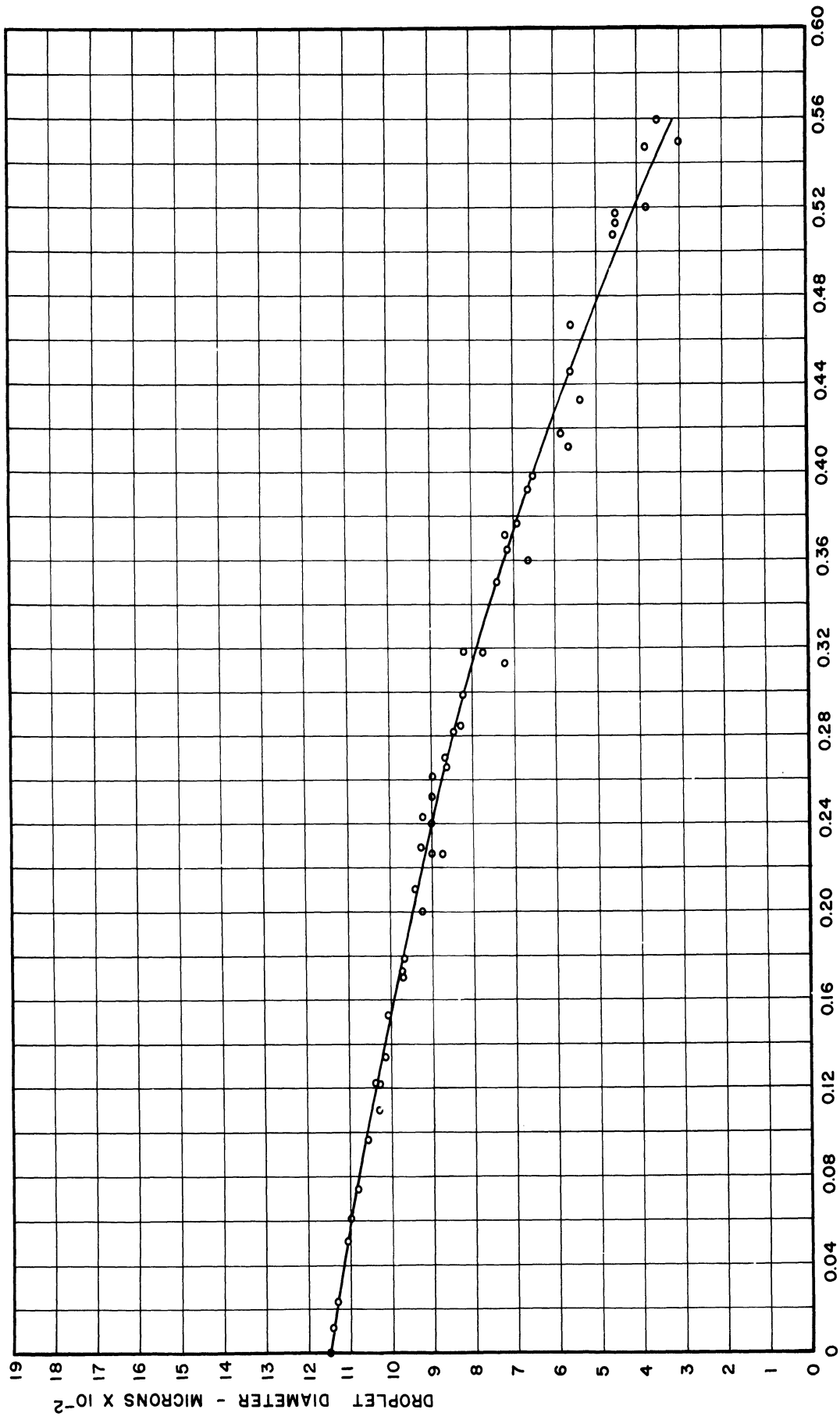

FIG. 12 COMBUSTION OF KEROSENE IN AIR AT 1500 °F
DIAMETER VS TIME

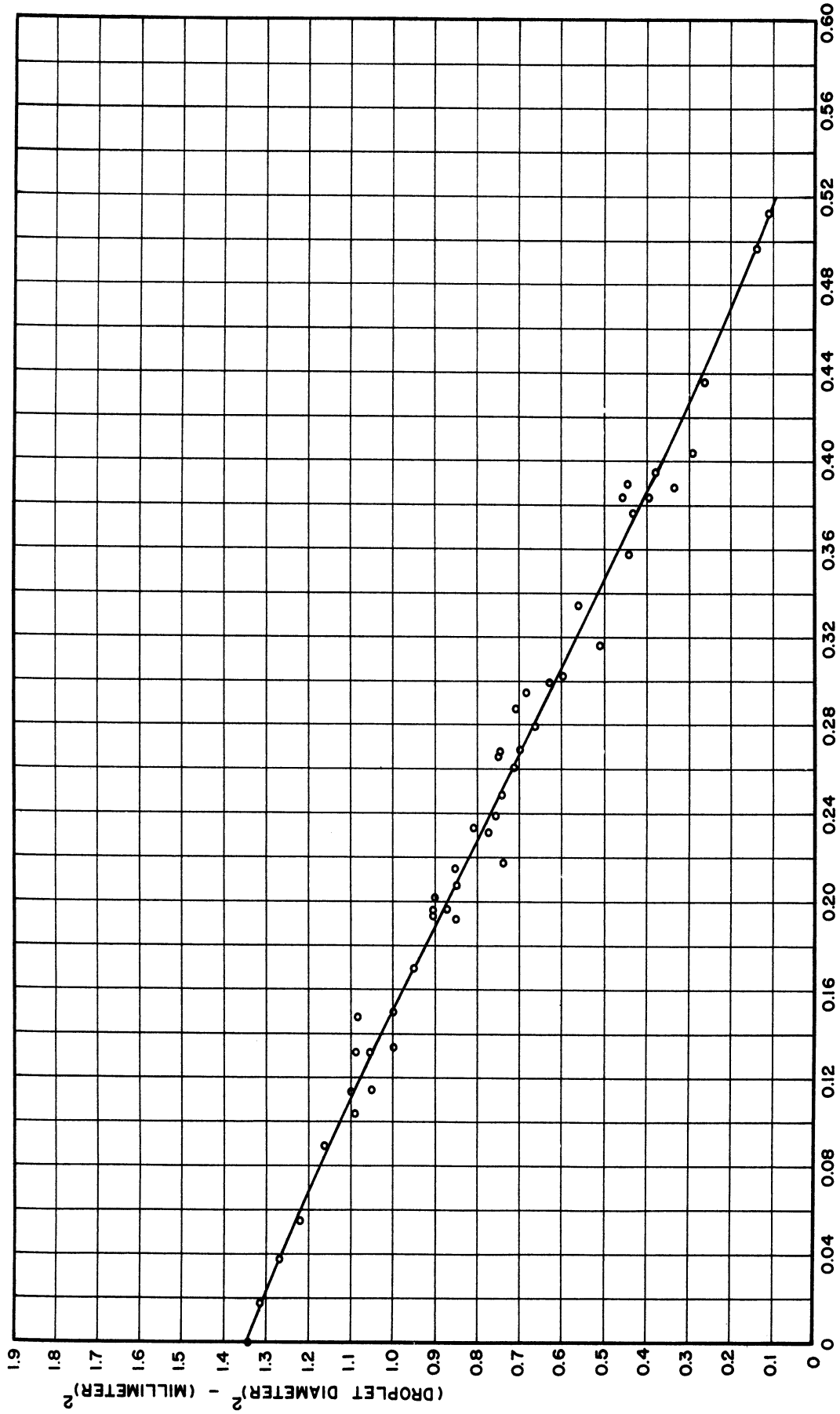

FIG. 13 COMBUSTION OF N-HEPTANE IN AIR AT 1500 °F
(DIAMETER)^2 VS TIME

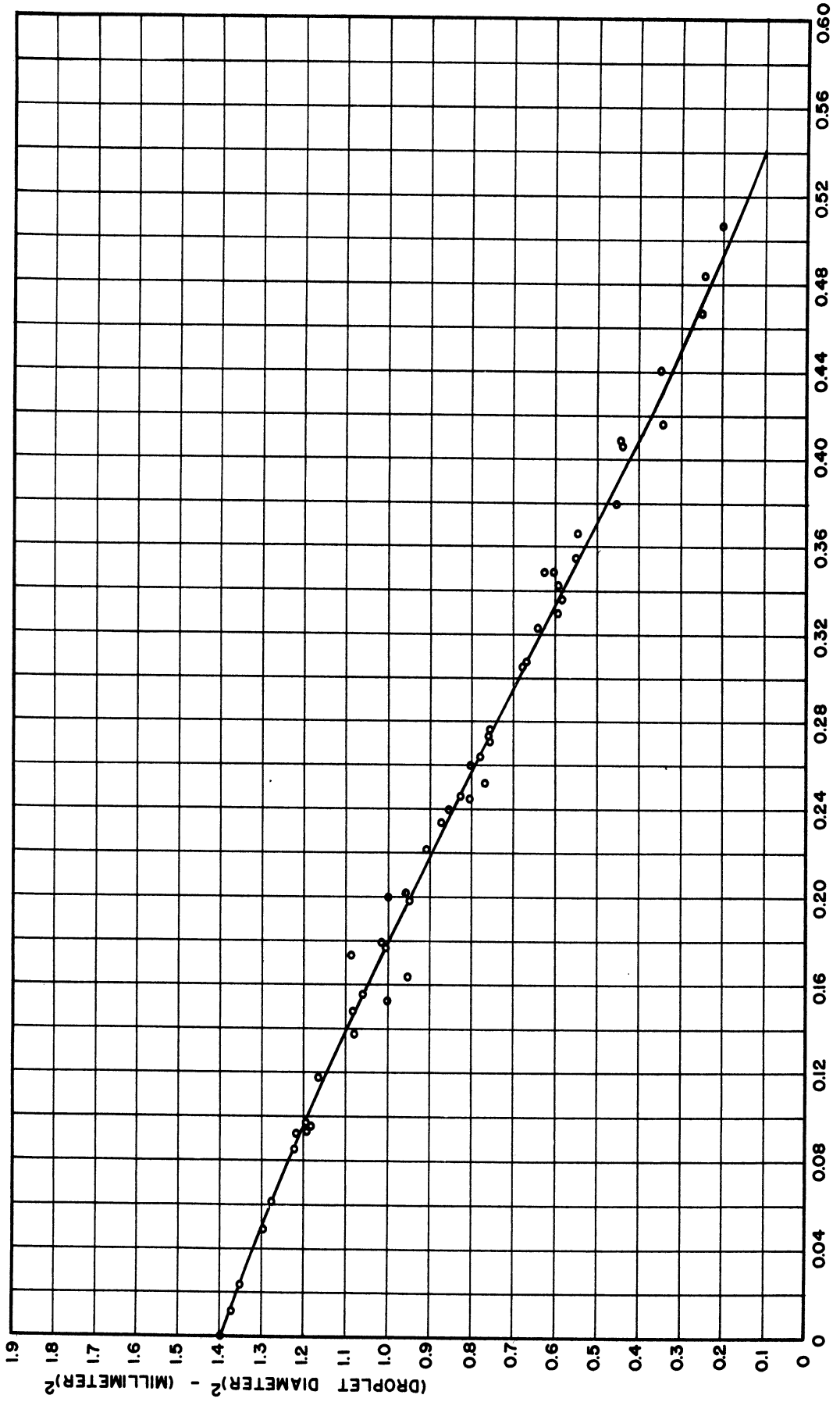

FIG. 14 COMBUSTION OF ISOOCTANE IN AIR AT 1500 °F
(DIAMETER)^2 VS. TIME

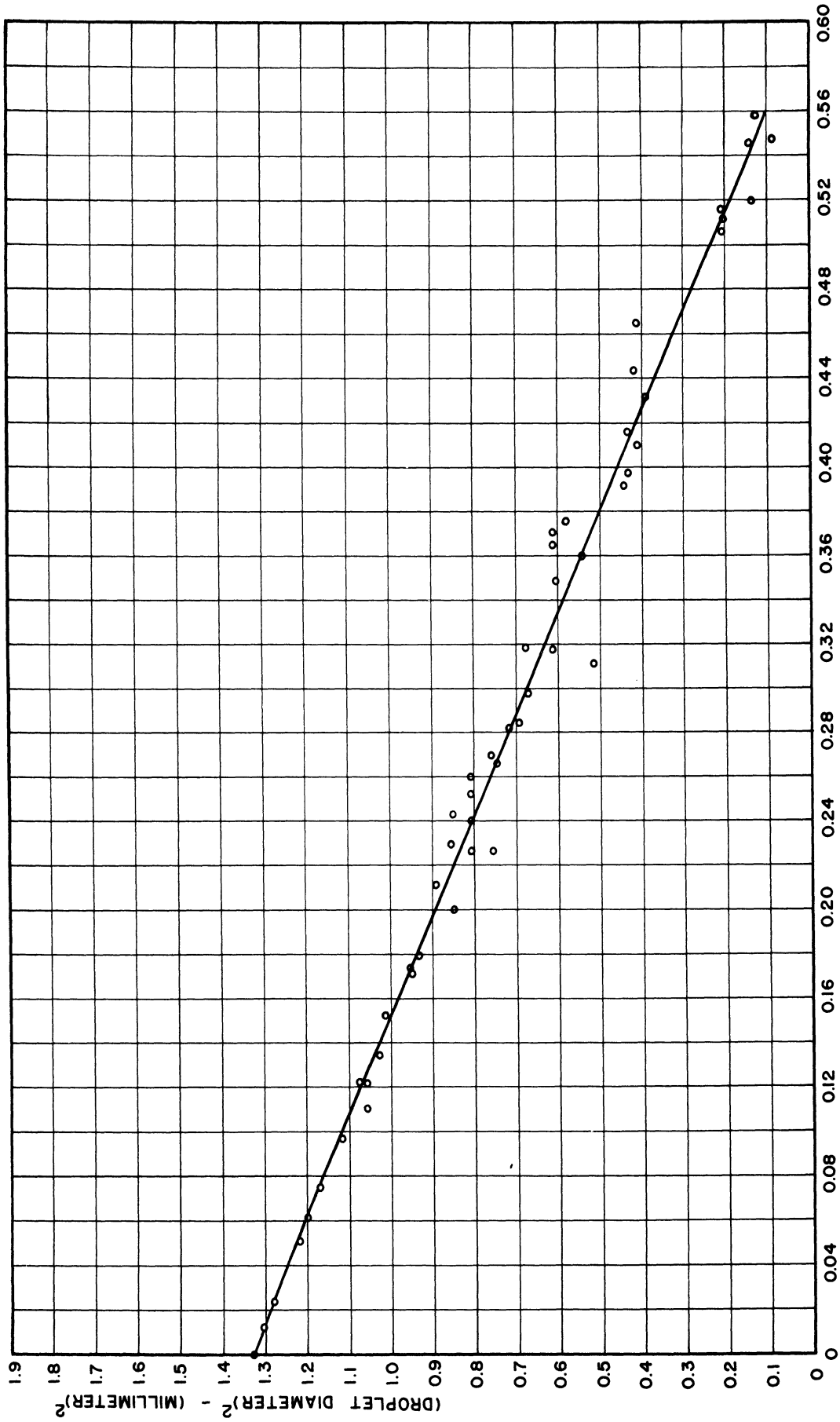

FIG. 15 COMBUSTION OF KEROSENE IN AIR AT 1500 °F
(DIAMETER)^2 VS TIME

V. DISCUSSION OF RESULTS

The discussion of results is divided into three sections: first, the effect of flame on drag, distortion of the falling droplets, and observations about the flame enveloping the droplet are outlined; second, the heat transfer to the droplet is discussed; third, the experimental curves are explained and an analytical expression for the rate of combustion is given.

Effect of Flame on Drag

The existence of the flame around and in the wake of the droplet tends to decrease the drag force. This fact is confirmed by Spalding.[36] It was found that the mean velocity of the falling droplets, between the second and third photographing stages, was much higher than the terminal velocities for solid spheres of the same size and under the same conditions of surrounding atmosphere. Although it is believed that the drag on liquid spheres is less than for solid ones, the big increase in velocity was more than could be accounted for by this fact alone. As an example, a 487-micron n-heptane droplet was falling, between the second and third photographing stages, at a mean velocity of 7.22 ft/sec. The corresponding value for a nonevaporating solid sphere falling at its terminal velocity is only 4.2 ft/sec. This increase in velocity was more noticeable in the case of small droplets.

The reduction of drag is explained by the fact that the flame increases the rate of mass transfer from the droplet and, consequently, the velocity of vapor leaving the droplet surface. The circulation of the liquid near the surface of the droplet and the vaporization of the fuel cause a reduction in the relative velocity of the gas close to the liquid surface.

The velocity of vapor leaving the droplet surface is evaluated as follows. The rate of the mass transfer of the vapor is given by

$$\frac{dm}{d\theta} = -\rho_v A v , \tag{5.1}$$

where

$\frac{dm}{d\theta}$ = the rate of mass transfer,

ρ_v = the density of the vapor,

A = the area of the droplet, and

v = the velocity of the vapor.

If ρ_ℓ is the mean density of the liquid of the droplet, then

$$m = \frac{1}{6} \pi D^3 \rho_\ell \tag{5.2}$$

$$\frac{dm}{d\theta} = \frac{1}{2} \pi \rho_\ell D^2 \frac{dD}{d\theta} . \tag{5.3}$$

Equating equations (5.1) and (5.3),

$$\begin{aligned} -\rho_v \pi D^2 v &= \frac{1}{2} \pi \rho_\ell D^2 \frac{dD}{d\theta} \\ \text{or } v &= -\frac{1}{2} \frac{\rho_\ell}{\rho_v} \frac{dD}{d\theta} = -\frac{1}{4} \frac{\rho_\ell}{\rho_v} \frac{1}{D} \frac{dD^2}{d\theta} . \end{aligned} \tag{5.4}$$

The vapor-air mixture is richest at the droplet surface and decreases away from it. The density of the vapor can be calculated from the characteristic gas equation:

$$\rho_v = \frac{P}{\mu R T} , \tag{5.5}$$

where

P = atmospheric pressure,

R = gas constant, and

T = absolute temperature.

The symbol μ is a dimensionless constant depending on the ratios of T/Tc and P/Pc, where T, P, Tc, and Pc are the temperature, pressure, critical temperature, and critical pressure of the vapor, respectively. The symbol μ is called the compressibility factor; values of μ are found in Maxwell's Data Book on Hydrocarbons.[24]

The value of $dD^2/d\theta$ is the slope of the combustion curves of D^2 vs θ at the corresponding diameter shown in Fig. 19. Thus, equation (5.4) can be written

$$v = \frac{1}{4}\frac{\rho_\ell}{\rho_v}\frac{1}{D} C , \qquad (5.6)$$

where C is the slope of the D^2-vs-θ curve.

As an example, for a 1000-μ n-heptane droplet, C = -0.0251 cm^2/sec. At boiling point and at atmospheric pressure T/Tc = 0.4075, P/Pc = 0.0373, giving

$$\rho_v = \frac{14.7 \times 144 \times 100}{0.935 \times 1544\ (460 + 209)} = 0.219\ lb/ft^3$$

$$v = \frac{1}{4}\frac{38.6}{0.219}\ \frac{1}{\left(\frac{0.1}{2.54 \times 12}\right)}\ \times\ \frac{0.0251}{(2.54 \times 12)^2} = 0.362\ ft/sec .$$

For a 300-μ droplet, C = -0.0195 cm^2/sec, which gives v = 0.938 ft/sec.

It has been pointed out that the velocity of the vapor leaving the surface of the droplet increases as the diameter decreases. For a small droplet, the falling velocity is small and at the same time its vapor velocity is high, resulting in an appreciable reduction of the relative velocity between the droplet and the surrounding atmosphere. Consequently, the drag force on the droplet is reduced.

Further work is necessary on this point, and the determination of the exact velocity history of the droplet rather than average velocities is recommended.

Distortion of the Falling Droplets

While falling in the furnace, the droplets were subjected to certain deformations due to the external drag force of the surrounding air. This drag was counteracted by the forces caused by the surface tension and viscosity. Fuels having high values of surface tension or viscosity are less subject to distortion.

Any distortion or change of the spherical contours of the droplet as it fell through the furnace had an effect on the drag coefficient since the latter is a function of the shape of the moving particle. As the outside area of the droplet changed, the rate of heat and mass transfer were affected accordingly.

It was observed that if a small droplet of fuel were deformed as it left the tip of the dropper, it would come back to spherical shape very quickly. This fact was more observable with small droplets since the pressure due to surface tension is higher for small droplets than for large ones. More distortion was to be expected at the bottom side than at the top side of the droplet.

Hughes and Gilliland[19] found out that for a given distortion, Reynolds number, and surface-tension group defined as $(\sigma\ D\ \rho_g/\mu_g^2)$ a distortion coefficient can be represented by the equation

$$\psi\ h = \frac{Re^{2.35}}{\left(\frac{\sigma\ D\ \rho_g}{\mu^2 g}\right)}\ , \qquad (5.7)$$

where

ψ = the distortion coefficient tabulated by Hughes and Gilliland,

h = the ratio of the major to the minor axis of the droplet,

Re = the Reynolds number of the droplet,

σ = the liquid surface tension,

D = the diameter of the droplet,

ρ_g = the density of the surrounding atmosphere, and

μ_g = the viscosity of the surrounding atmosphere.

If σ = 13.6 dynes/cm, $\rho_g = 3.26 \times 10^{-4}$ g/cc, μ_g = 0.00044 poises, and D = 0.1 cm, the surface-tension group $\sigma D \rho_g/\mu_g^2$ = 2290. The Re for a 1000-μ droplet falling at its terminal velocity in an air atmosphere at 1500°F is 23.5; then,

$$\psi \quad h = \frac{(23.5)^{2.35}}{2290} = 0.73,$$

from which h = 0.997, i.e., distortion is 0.3%, which is a small value and can be neglected in the present experiments.

Actually, distortion was more than the above value because of the initial distortion due to the attachment of the droplet to the tip of the dropper and also due to the presence of the flame around the droplet. The effect of the flame on distortion was unknown, but it certainly was not symmetrical around the droplet in either shape or temperature. This caused uneven rates of evaporation from the surface of the droplet. It was found that droplets above 1000 microns were liable to slight distortion and were not included in the results if the major and minor diameters differed by more than 5%.

Observations About the Flame Enveloping the Droplet

A diffusion flame was formed very shortly after the droplet entered the furnace. At a furnace temperature of 1500°F, the flame was yellow. Visual observation indicated that the luminous region was at the wake of the droplet. Very little or no oxygen penetrates the flame front, and a

cracking zone is liable to form on the fuel side before the reaction zone. The luminosity of the flame was due to the presence of incandescent carbon particles which burned slowly, radiating the bright yellow color. At lower temperatures and in the absence of carbon particles, the hydrocarbon fuels burned with a blue flame which was characteristic of the reaction zone.

In the combustion of kerosene, more soot and carbon particles were formed, which increased the luminosity of the flame, than in the case of the pure hydrocarbon fuels.

Figure 16 shows a droplet in the middle of a white zone appearing on the film. This white zone was caused by the luminous flame when the burning droplets passed in front of the open-shutter cameras. The width of the zone is the lateral dimension of the flame. The other white areas in the figure are caused by the background illumination.

Due to the open-shutter technique, the vertical dimension of the flame could not be determined. The surrounding flame was from 1.9 to 2.1 times the diameter of the droplet in the lateral direction for large and small droplets, respectively. These figures were for the fuels investigated and under the conditions of the present experiments. These values are less than the values given by Godsave. This was due to the motion of the droplets in the present investigation, conditions differing from Godsave's experiments. Godsave[15] found that D_F/D, where D_F and D are the flame and droplet diameters, was approximately constant for suspended stationary droplets and ranged from 2.4 to 3.0, depending on the fuel investigated.

Preheating of the Droplet

As the droplet entered the furnace, it received heat by radiation from the furnace walls and by conduction and convection from the ambient

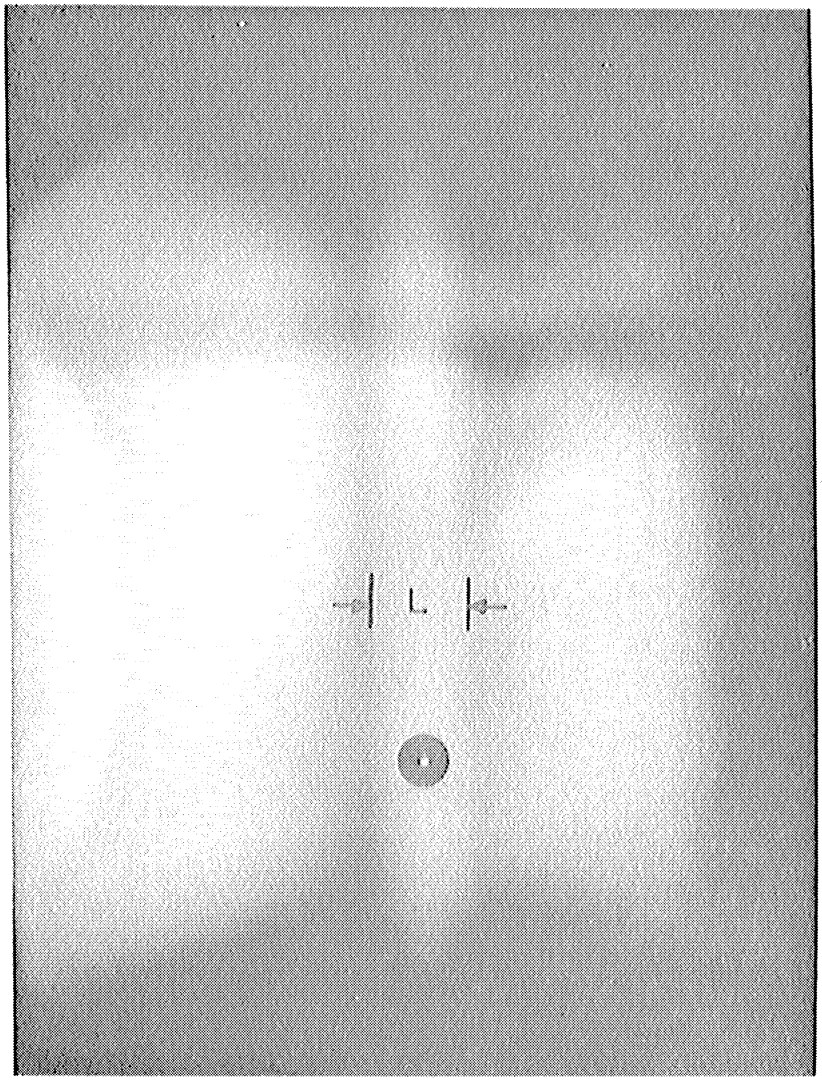

FIG. 16 LATERAL DIMENSION
OF THE FLAME SURROUNDING A FALLING DROPLET
(X ~ 6:1)

air. In what follows, the relative importance of the different kinds of heat transfer is considered.

The heat transfer by radiation is given by

$$q_r = h_r \pi D^2 (T_w - T_s) = \pi D^2 \sigma \epsilon T_w^4 \qquad (5.8)$$

and

$$h_r = \frac{\sigma \epsilon T_w^4}{(T_w - T_s)} , \qquad (5.9)$$

where

h_r = the radiation heat transfer coefficient,

σ = the Stefan-Boltzmann constant,

ϵ = emissivity of the furnace wall,

T_w = the absolute temperature of the furnace wall, and

T_s = the absolute temperature of the surface of the droplet.

The Nusselt number is used to determine the forced-convection heat transfer coefficient.

$$Nu = \frac{h_c D}{k_g} , \qquad (5.10)$$

where

h_c = the convection heat transfer coefficient,

D = the diameter of the droplet, and

k_g = the average thermal conductivity of the surrounding atmosphere.

The term k_g is estimated at an average temperature $1/2 (T_w + T_s)$. The ratio of the two heat transfer coefficients is given by

$$\frac{h_r}{h_c} = \frac{\sigma \epsilon D T_w^4}{k_g Nu (T_w - T_s)} . \qquad (5.11)$$

It is seen from equation (5.11) that h_r/h_c depends greatly on the diameter of the droplet, the wall temperature, and Nusselt number. The temperature

of the furnace wall was measured by a Leeds and Northrup optical pyrometer (potentiometer type) and was found to be 1630°F when the ambient-air temperature was 1500°F. Taking T_s as 200°F, k_g was estimated at (200 + 1630)/2 = 915°F, and was found to be .031 Btu/(hr)(ft^2)(°F/ft).

The emissivity of alundum was taken as 0.3 at 1630°F and $\sigma = 0.173 \times 10^{-8}$ Btu/(ft^2)(hr)(°R)^4. For a 1000-μ droplet falling in the furnace at a Reynolds number of 20, Nu is about 4.4. Inserting these values in equation (5.11) gives

$$\frac{h_r}{h_c} = \frac{.173 \times 10^{-8}\ 0.3(2090)^4 \left(\frac{.1}{2.54 \times 12}\right)}{.031 \times 4.4\ (2090 - 660)}$$

$$= 0.167.$$

This value of h_r/h_c is slightly lower than what is found in industrial furnaces where an average value of $h_r/h_c = 0.2$. Due to the transparency of volatile fuels in general and the hydrocarbons used in particular, the ratio h_r/h_c has to be multiplied by the absorptivity of the droplet. According to Wolfhard and Parker,[41] the absorptivity α is taken as 0.07, which gives $\alpha\ h_r/h_c = .0117$. Thus, it can be stated that in the present experiment most of the heat received by the droplet in the preheating region is by convection and conduction.

Heat Transfer to the Droplet

To simplify mathematical treatment, it is generally assumed that heat is transferred symmetrically about the center of the burning droplet when it is stationary. This is not the case when there is a relative motion between the droplet and the surrounding atmosphere. The relative velocity affects the thickness of the vapor film and the shape of the flame around the droplet. When the relative velocity is higher, the film is thinner,

the flame is nearer the droplet, and the combustion is more rapid.

The rate of combustion of a fuel droplet is governed by the amount of heat transfer to the droplet. The surrounding flame is considered the most important heat source for the vaporization of the droplet.

For an evaporating droplet falling in a certain atmosphere, the rate of heat transfer from the surrounding air is maximum at the bottom side of the droplet. The upper or the trailing portion has a lower rate of heat transfer, but this rate is higher than that on the sides of the droplet because of the eddies which occur at the wake of the droplet. These eddies increase the heat transfer coefficient.

Heat is transferred from the flame to the droplet by radiation, conduction, and convection. The heat transfer by radiation is discussed below.

Heat Transfer by Radiation from the Flame

There are two kinds of radiation from the flame to the droplet; nonluminous and luminous radiation. Carbon dioxide and water vapor are the two main compounds which contribute to nonluminous radiation, while the flame envelope is responsible for the luminous radiation. The evaluation of the amounts of these two kinds of radiation for an 800-μ n-heptane droplet is as follows:

The emission of the nonluminous gas to the droplet is given by the generally accepted equation,

$$q_{r,n} = \sigma \epsilon_g T_g^4 , \qquad (5.12)$$

where

$q_{r,n}$ = the radiated heat due to nonluminous gases, Btu/(hr)(ft^2),

σ = the Stefan-Boltzmann constant = 0.173 x 10^{-8} Btu/(ft^2)(hr)(°R)^4,

ϵ_g = the gas emissivity defined as the ratio of radiation from gas to droplet to the radiation from a black body at the same temperature, and

T_g = the temperature of the gas, °R.

For the emitting gases, ϵ_g depends on T_g, the total pressure and the partial pressure-path length product P_gL, L being the mean beam length in evaluating gas emissivity. The absorption of the gas of radiation from the surface of the droplet is $\sigma \alpha_g T_s^4$, where α_g is the absorptivity of the gas for black-body radiation from the droplet surface and T_s is the absolute temperature of the surface of the droplet. The net radiant-heat interchange per unit area is thus given by

$$\text{net } q_{r,n} = \sigma \epsilon_g T_g^4 - \sigma \alpha_g T_s^4 . \qquad (5.13)$$

If T_s is small compared to T_g, the second term in the R.H.S. of equation (5.13) can be neglected.

Analytical calculation of the flame temperature is a complex problem unless several unrealistic assumptions are made, such as spherical symmetry, fixed size of both the droplet and the flame, and radial-heat and mass transfer. A reasonable value for the flame temperature of n-heptane is 2300°K (4140°R). For this temperature, the products of combustion, taking dissociation into consideration, were determined. The details of the calculation are shown in Appendix C. The partial pressures of carbon dioxide and water vapor were found to be 0.1104 and 0.136 atmospheres, respectively.

The P_gL product for either carbon dioxide or water vapor in the flame is 0.6 D_F, where D_F is the diameter of the flame envelope. If D_F is taken as twice the droplet diameter, then

$$\text{for } CO_2 \quad P_gL = 0.1104 \times 0.6 \times \frac{0.16}{2.54 \times 12} = 3.48 \times 10^{-4} \text{ ft atm}$$

$$\text{for } H_2O, P_gL = 0.136 \times 0.6 \times \frac{0.16}{2.54 \times 12} = 4.28 \times 10^{-4} \text{ ft atm.}$$

Knowing these values of P_gL and the temperature, the emissivities of CO_2 and H_2O were found from Reference 25 to be

$$\epsilon_{CO_2} = 3.48 \times 10^{-4}$$

$$\epsilon_{H_2O} = 0.501 \times 10^{-4} .$$

When carbon dioxide and water vapor are present together, the total emissivity is less than the sum of the individual emissivities, as each gas is somewhat opaque with respect to the other. In our case, since $(PL)_{CO_2} + (PL)_{H_2O}$ is small, the correction was found to be zero and the total emissivity is 3.981×10^{-4}.

Hence,

$$q_{r,n} = (0.173 \times 10^{-8})(3.981 \times 10^{-4})(4.40)^4$$
$$= 203 \text{ Btu/hr ft}^2.$$

For the estimation of the radiated heat from the luminous flame, a reasonable value for the absorption strength of the flame KL is assumed, 0.8. According to Reference 25, the average value of L is 0.6 times the diameter of the flame. Then the average absorption strength is $0.8 \times 0.6 = 0.48$. Knowing this value of KL and the flame temperature, the flame emissivity was found to be $\epsilon_F = 0.28$, and the luminous radiation is given by

$$q_{r,l} = (0.173 \times 10^{-8})(0.28)(4140)^4$$
$$= 142500 \text{ Btu/hr ft}^2 .$$

The total radiation to the 800-μ-diameter droplet is

$$Q_r = 142703 \times \pi \left(\frac{.08}{2.54 \times 12}\right)^2 = 3.095 \text{ Btu/hr}$$
$$= 0.216 \text{ cal/sec.}$$

The above value is the total heat emitted by radiation from the flame, but a small portion is absorbed by the liquid droplet. If the absorption factor is taken to be .07 of the total radiation received (Wolfhard and Parker[41]), then

$$Q_r = 15.12 \times 10^{-3} \text{ cal/sec.}$$

For an 800-μ n-heptane droplet, $dm/d\theta$ is found as follows:

$$\frac{dm}{d\theta} = -\frac{1}{4} \pi \rho_\ell D \frac{dD^2}{d\theta} \quad . \tag{5.14}$$

From Fig. 19, $dD^2/d\theta = -.0253 \text{ cm}^2/\text{sec}$, then $dm/d\theta = 9.82 \times 10^{-4}$ g/sec. It follows that the radiation absorbed per gram of fuel evaporated is

$$\frac{Q_r}{\left(\frac{dm}{d\theta}\right)} = 15.4 \text{ cal/g} .$$

Table VII in Appendix D gives the vapor heat content at the boiling point as 111 cal/g. Thus, the contribution of radiation is only 13.88% of the total heat requirement to evaporate an 800-μ n-heptane droplet under the conditions of these experiments. The rest of the heat required by the droplet is evidently supplied by conduction and convection.

Explanation of the Combustion Curves

Examination of Figs. 10, 11, and 12 for n-heptane, isooctane, and kerosene indicates that the slope of the diameter-time curves increases as time increases. This is due to the fact that the mean slope is inversely proportional to the diameter.

The curves of Figs. 10, 11, and 12 were very near to parabolas, which gave the idea of plotting D^2 vs θ. This was also done in order to compare the data with other investigators who usually find a straight-

line relation between D^2 and θ for stationary droplets. The curves for the three fuels investigated have the same shape as shown in Figs. 13, 14, and 15.

The equation of these curves can be written as

$$D^2 = D_o^2 - C\theta , \qquad (5.15)$$

where

D = the diameter of the droplet and time θ,

D_o = the initial diameter of the droplet, and

C = the slope of the curve.

The change in the rate of combustion is thus a function of C, which is usually termed the coefficient of combustion. C depends on Nu, and in the case of small stationary droplets or droplets moving at a constant Re, the values of Nu and C are constants. C is called, in this case, the combustion constant. In this investigation, the Reynolds number of the falling droplet was continuously changing as both the velocity and the diameter of the droplet changed. The relation between the Nu and Re for low Re is shown in Fig. 2. For the range of Re_m (7 to 25) of this investigation, the mean Nu ranged from 3.4 to 4.6. This is mainly why the variation of D^2 vs θ is not a straight-line relation.

Taking as an example Fig. 14 for isooctane, it is seen that the first part of the curve is slightly convex, the middle part is fairly straight, and the last part is concave. The explanation of this curve is as follows.

As the droplet entered the furnace it was relatively cool, especially near the center. The heat transferred to the droplet is partly used in heating up the liquid and partly in evaporating it. The amount of heat necessary to heat the droplet is more important in big droplets

due to their larger mass. The convexity of the first part of the curve is very small because the droplet was heated to near its final stable temperature when the first photographing position was reached.

The middle part of the curve is nearly a straight line, meaning that the value of C is nearly constant. This is explained by the fact that the Re of the droplet did not change appreciably in this region. As the droplet reached the first photographing stage at about 87% of its terminal velocity, two factors were counteracting each other in changing its Re. The droplet was trying to attain a higher percentage of its terminal velocity, but at the same time it was reducing in size and, consequently, in velocity. The first factor was helped by the presence of the flame, which reduces the drag on the droplet. It seemed that these two factors had approximately equal effects on Re and the droplet in this region moved at a fairly constant Re. The small variation of Re for different-sized droplets in this region had no appreciable effect on Nu to change the linearity of this part of the curve. This means that Nu and C were fairly constant in that region.

The third part of the curve of Fig. 14 is concave. The Re reduces appreciably as time proceeds, because of the reduction in size and velocity of the droplet. The gain in velocity due to the flame or toward the terminal velocity is negligible as this latter is believed to be reached at this stage. The variation of Nu and C again follows the variation of Re as indicated in Fig. 2.

Due to the small variation of Nu, it was difficult to deduce quantitative information regarding the variation of C with respect to Nu. All that can be said is that the value of C increased with an increase in Nu.

The variation of C vs D for the fuels investigated is shown in Fig.

19. The values of C for kerosene were lower than the corresponding values for the pure hydrocarbons during most of the range of the droplets investigated. For n-heptane and isooctane, C varies from 0.020 to 0.0255 cm^2/sec, while for kerosene C varies from 0.021 to 0.0222 cm^2/sec.

As indicated by Figs. 12 and 15, the combustion curves of kerosene are similar to n-heptane and isooctane. The main physical properties of the fuel that affect the combustion process are the thermal conductivity, specific heat, latent heat, and heat of combustion. The values of these properties do not differ much in the fuels investigated and, consequently, the combustion curves are of the same general shape. Figures 17 and 18 show some of the burning droplets while falling in the furnace. The reduction in size was appreciable with small droplets and in some cases no pictures were obtained at the third photographing position, either because the flame around the droplet was too weak to affect the multiplier phototube or because the droplet was completely burned before reaching the third position. On the other hand, with large droplets small changes are noted. This was due to the fact that the rate of reduction of diameter was higher for small droplets than for big ones. Also, in the case of big droplets a large portion of the heat transferred to the surface of the droplet is used in internal heating.

Analytical Evaluation of the Rate of Combustion

Let us consider a fuel droplet surrounded by its diffusion flame moving in a hot atmosphere. A heat balance at the combustion surface gives

$$m_a h_a + m_f H_f = m_p h_p + dQ, \qquad (5.16)$$

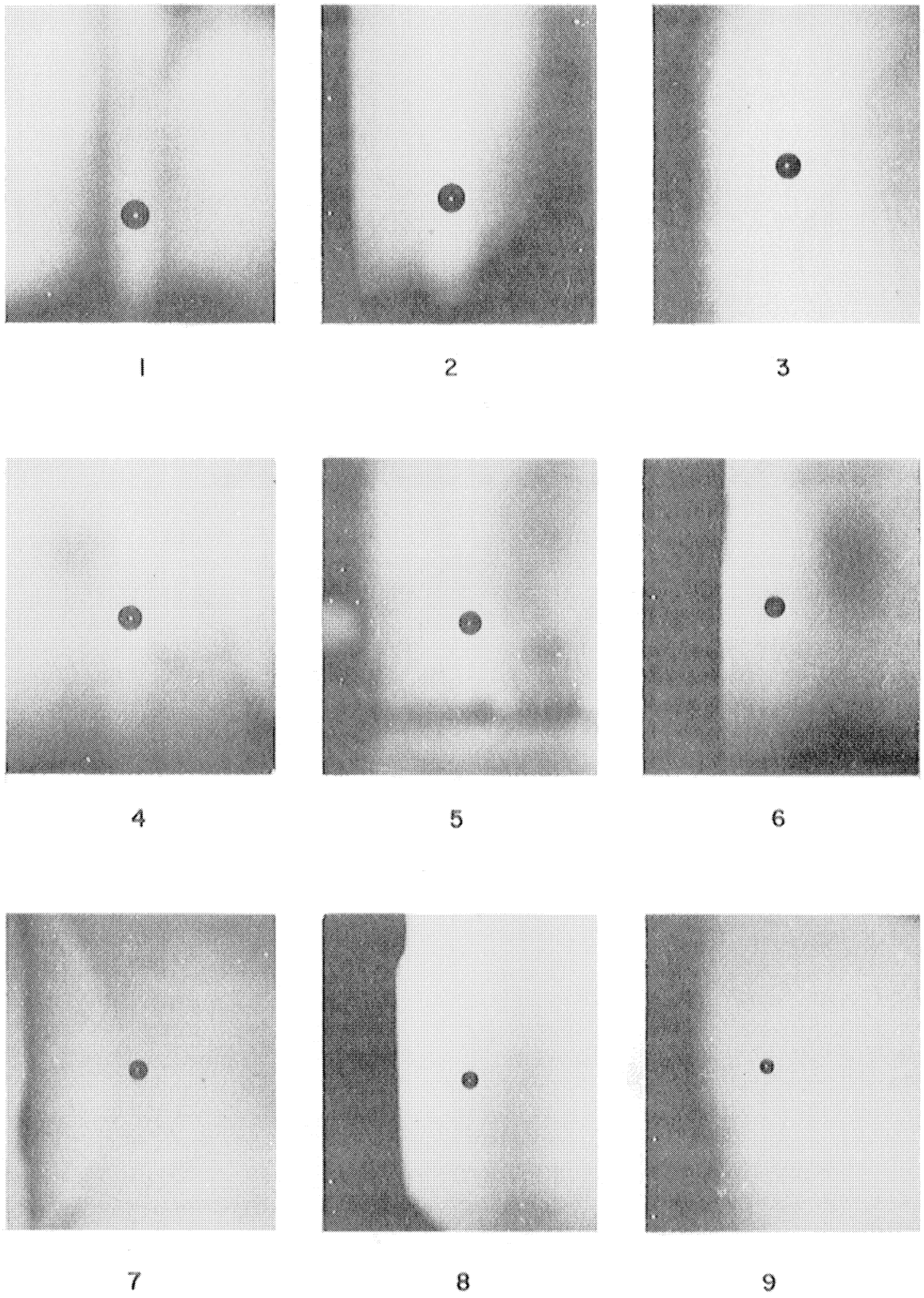

FIG. 17 PHOTOGRAPHS SHOWING
VARIOUS SIZES OF BURNING n-HEPTANE DROPLETS
(X ~ 4:1)

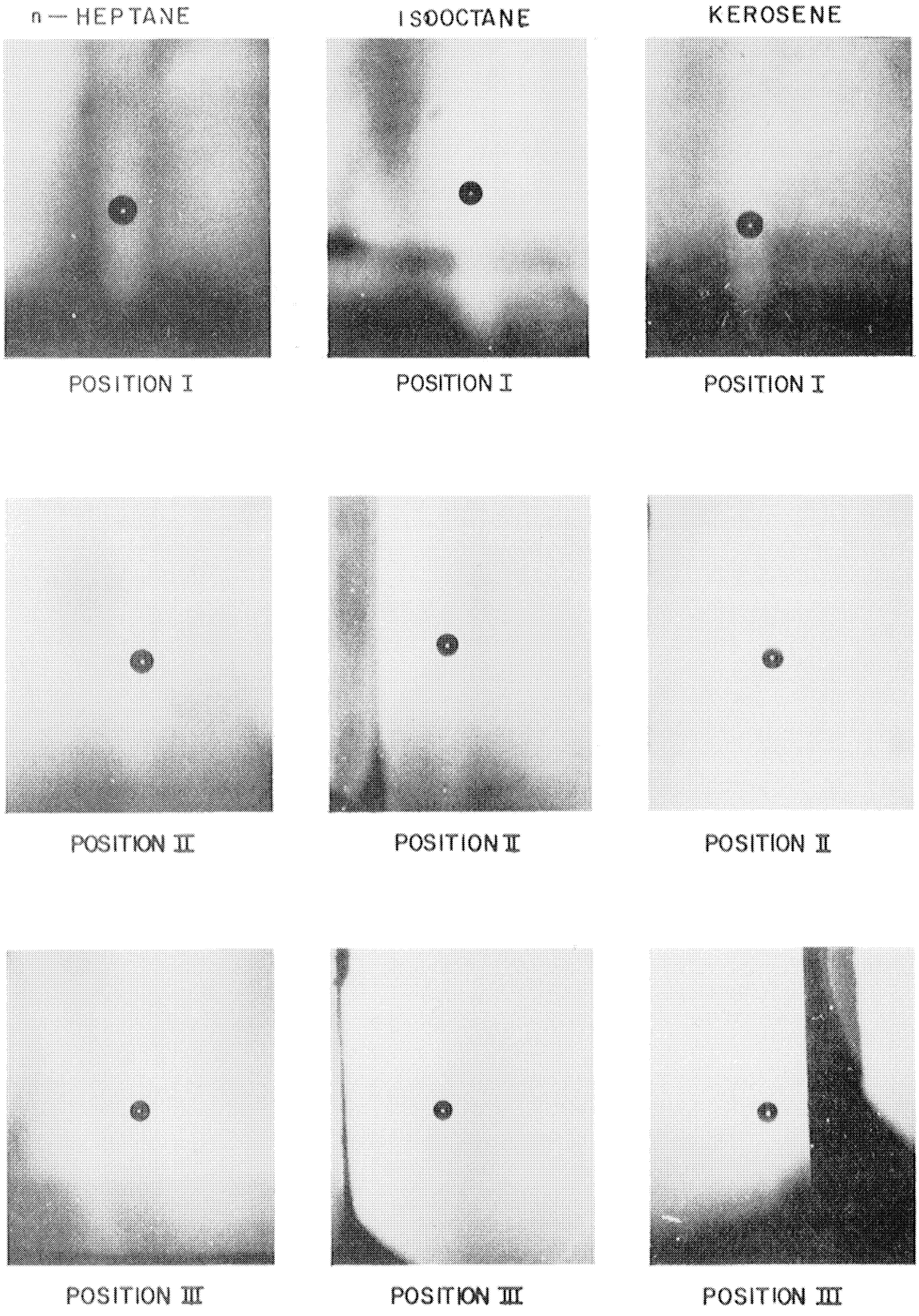

FIG. 18 SERIES OF PHOTOGRAPHS
TAKEN IN SEQUENCE OF BURNING FUEL DROPLETS
FALLING FREELY IN THE FURNACE (X ~ 4 : 1)

where

m_a = the stoichiometric weight of air used to burn the fuel,

m_f = the weight of the burned fuel,

m_p = the weight of the products of combustion,

h_a and h_p = enthalpies of air and products of combustion, respectively,

H_f = the heating value of the fuel, and

dQ = the heat exchange at the combustion surface.

Equation (5.16) can be written as

$$x\, h_a \frac{dm_f}{d\theta} + H_f \frac{dm_f}{d\theta} - (1 + x)\, h_p \frac{dm_f}{d\theta} = \frac{dQ}{d\theta} , \quad (5.17)$$

where x is the stoichiometric air-fuel ratio.

The rate of heat exchange $dQ/d\theta$ is dissipated in two opposite directions as follows:

a. Toward the droplet, supplying the sensible heat to the liquid of the droplet, the latent heat, and heating up the vapor from T_s to T_F.

b. Outward, supplying heat to the surrounding air and to the walls of the furnace.

Thus, equation (5.17) becomes

$$x\, h_a \frac{dm_f}{d\theta} + H_f \frac{dm_f}{d\theta} - (1 + x)\, h_p \frac{dm_f}{d\theta} =$$

$$\frac{dm}{d\theta}\left[c_{p_\ell}(T_s - T_\ell) + L + c_{p_v}(T_F - T_s)\right] + hA_F(T_F - T_a) + \sigma A_F(\epsilon_F T_F^4 - \alpha_w T_w^4), \quad (5.18)$$

where

c_{p_ℓ} = specific heat of the liquid of the droplet,

c_{p_v} = specific heat of the vapor,

T = the absolute temperature,

L = the latent heat of vaporization of the fuel,

h = the coefficient of heat transfer by conduction and convection,

A_F = the area of the flame,

σ = the Stefan-Boltzmann constant,

ϵ_F = the emissivity of the flame, and

α_w = the absorptivity of the furnace walls.

Subscripts s, ℓ, F, a, and w refer to surface of droplet, liquid of droplet, flame, air, and furnace wall.

Let us consider the heat balance of an 800-μ n-heptane droplet surrounded by a flame at 2300°K. The following data are used: from Fig. 2 for Re = 25, $Nu = hD/k_g = 4.7$,

$k_g = 0.052$ Btu/(hr)(ft)(°F),

$h = 46.6$ Btu/(hr)(ft^2)(°F),

$A_F = \pi(2D)^2 = 8.62 \times 10^{-5}$ ft^2,

$T_F = 4140$°R,

$T_a = 1960$°R,

$\sigma = 0.173$ Btu/(ft^2)(hr)(°R),

$\epsilon_F = 0.28$,

$\alpha_w = 0.30$,

$T_w = 2090$°R,

$x = 15.12$,

$h_a = 493.64$ Btu/lb,

$H_f = 19157$ Btu/lb,

$h_p = 21074$ Btu/lb (given in Appendix C),

$L = 136$ Btu/lb,

$c_{p_v} = 1.02$ Btu/lb-°F, and

T_s = 669 °R.

Substituting the above values in equation (5.18) gives $dm/d\theta$ = 0.00000223 lb/sec for an 800-μ droplet as compared to 0.00000218 lb/sec from the experimental results according to equation (5.14).

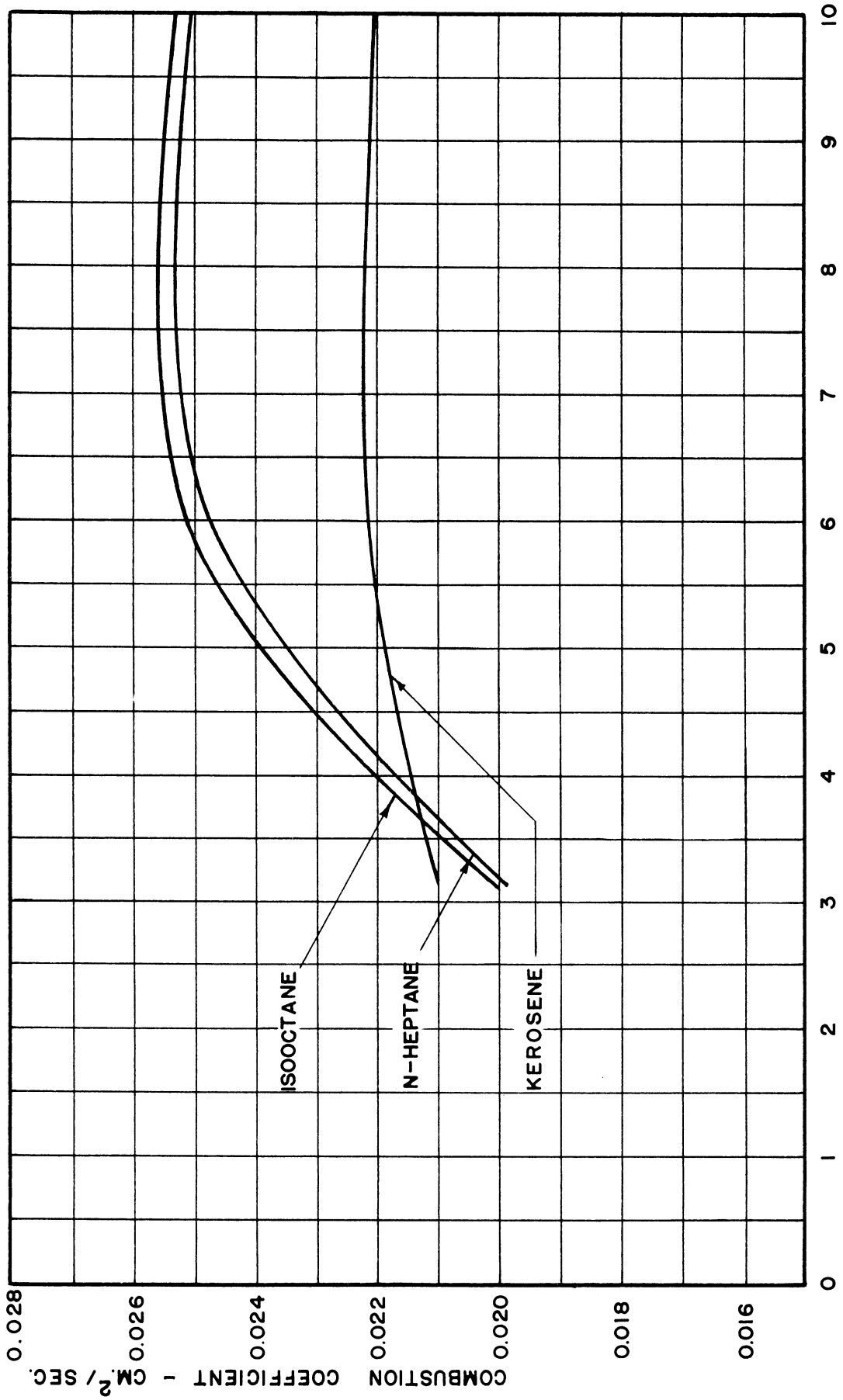

FIG. 19 VARIATION OF COMBUSTION COEFFICIENT WITH DROPLET DIAMETER.

VI. CONCLUSIONS AND RECOMMENDATIONS

Conclusions

The following conclusions could be drawn from the experimental work:

1. An appreciable decrease in the drag coefficient of the burning droplets was noted due to the presence of the flame (see page 60).

2. At the early stage of combustion the heat required to heat the interior of the droplet retarded the rate of combustion. The total heat absorbed by the droplet increased with the increase of initial droplet size.

3. Radiation from the flame was only a small portion of the heat necessary to evaporate the droplet. Most of the heat received was by conduction and convection (see page 72).

4. The rate of combustion per unit weight of the fuels investigated was controlled by the rate of heat transfer. It increased with the decrease of droplet size, other factors being unchanged.

5. The combustion depended on the nature of the fuel, droplet size, and the relative velocity between the falling droplets and the atmosphere, other factors being unchanged.

6. The change of droplet size of n-heptane, isooctane, and kerosene due to evaporation during combustion, can be represented by the equation

$$D^2 = D_o^2 - C\theta .$$

The combustion coefficient C depended on the type of fuel, the diameter of the droplet, and the relative velocity between the falling droplet and the surrounding atmosphere.

7. A theoretical approach to the study of a burning droplet under

forced convection is a very difficult problem, as both the temperature and the composition vary continuously in the region surrounding the droplet.

Recommendations

The effect of the relative velocity of the falling droplet on the heat transfer from the flame to the droplet is an important factor in studying the rate of combustion. The relative velocity must be accurately known and it is preferable to have a complete knowledge of the variation of Reynolds number during the combustion process.

The mean velocity of the falling droplet has been determined by measuring the distance of fall and the time interval between the photographing positions. To obtain a complete history of the velocity along the path, two methods are recommended; by taking two pictures of the droplet in quick succession while passing in front of the camera, or by replacing the cameras by movie cameras.

A new design of the fuel dropper will permit extension of the data to small-sized droplets.

If it is desired to study the nature of burning, then combustion from fixed surfaces is recommended. This has the advantage that the dimensions of the flame remain unchanged and the volume bounded by the flame, excluding the droplet, remains constant with time. The energy equation could be easily applied to this fixed control volume and an estimate of the combustion temperature could be calculated.

VII. APPENDICES

APPENDIX A

DETAILS OF THE CONSTRUCTION AND PERFORMANCE OF THE EXPERIMENTAL EQUIPMENT

The experimental equipment consisted of four units: the furnace and the dropper, the photographing equipment, the detection equipment, and the timing equipment. The details of the construction and operation of these units are described below.

The Furnace

The furnace as shown in Figs. 3 and 4 consisted of two heating elements embedded in two 4 x 1-1/4 x 45 inch alundum pieces placed opposite to each other with a 1-inch space between them. The two alundum pieces were cast in two stainless-steel channels, thus forming the two side-wall heating surfaces of the furnace. The space between the alundum pieces (1 x 4 x 45 inches) is the test section or the hot atmosphere through which the droplets fell. When the alundum pieces were cast, they were left for two days to dry, then they were baked in an oven heated to temperatures of 600°, 800°, and 1000°F, respectively, for a period of four hours at each temperature.

The resistance of each element was 28.5 ohms, divided into three sections of 9.5 ohms each. The resistance wire was 16-gage Chromel A (0.252 ohms per foot); it was made into a 3/8-inch-outside-diameter helix before being cast in the alundum. Two hundred and twenty volts were applied to every two sections of the resistance wire (19 ohms), giving a current of 11.58 amperes and a total power of 7.64 kw. Every heating element had two taps to control the temperature of the furnace.

The outside dimensions of the furnace were 4 x 17-1/2 x 45 inches. The insulation was made up of two layers of different materials: 2-1/2 inches of firebrick and 5 inches of vermiculite. The whole insulation was contained within a steel shell made of 1/16-inch steel sheet. The lid and bottom pieces, which were removable, were clamped by sheet-metal screws.

The outside of the furnace was covered by an asbestos sheet 1/16 inch thick. It was held in place by means of aluminum straps 3/4 inch wide.

The entire furnace length was provided with two opposite continuous glass windows which allowed the droplet to be photographed at any position in the furnace, and the entire burning process within the furnace could be observed. The glass windows were made of pieces of high-temperature Pyrex glass bought from the Corning Glass Company. Each piece had the dimensions of 3 x 1-1/4 x 1/8 inches. A considerable amount of heat was lost through the glass windows, but some sacrifice was necessary for visual observation.

Three iron-constantan thermocouples were used to determine the temperature within the furnace, their tips being shielded by platinum foil (0.01 inch thick). The thermocouple wire was passed through a 1/8-inch, twin-bore ceramic tubing which in turn was inserted in a stainless-steel tube and clamped to it by a set screw. By means of this screw the thermocouple could be moved inwards and outwards, and thus temperature traverses could be made in the furnace. The thermocouple wires led to the terminals at the selector switch and a potentiometer. A Leeds and Northrup potentiometer was used to read the temperature. The wiring of the furnace and the thermocouple is shown in Fig. 20. The operating temperature of the furnace was 1500°F, and the maximum temperature reached was 1700°F. Operation at higher temperatures would necessitate the use of a larger size of resistance wire

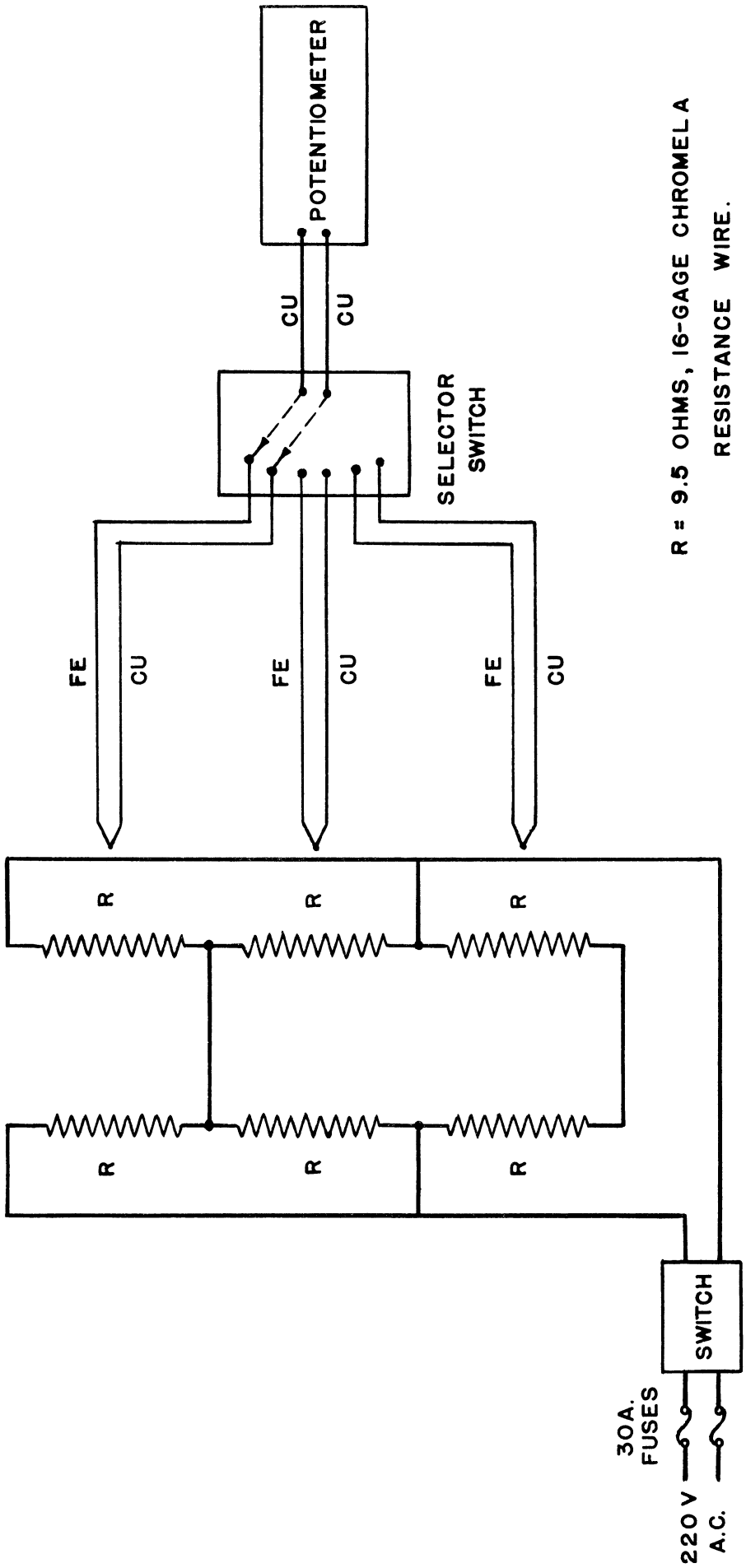

FIG.20 WIRING DIAGRAM OF THE FURNACE AND THERMOCOUPLES.

or a different kind of heating unit.

The furnace was mounted on a platform made of 2-inch angle iron so that the bottom of the furnace was 2 feet above the floor. An angle-iron frame was attached to this platform to provide a stand for mounting other pieces of equipment.

The furnace test section was completely closed, except for a 1/4-inch hole at the top of the furnace for the entrance of the fuel droplets. Sufficient air was admitted into the furnace, normally after the fall of every five droplets, by removing a plug at the bottom of the test section and allowing the furnace to purge itself.

Fuel Dropper

A hypodermic needle of 0.0185-inch outside diameter was soldered to a 1/4-inch-outside-diameter copper tube to form the fuel supply line. The tip of the needle was cut square and carefully ground by a fine grinding stone. The copper tube was centered into a 4-1/2-inch-long, 1/2-inch-outside-diameter brass tube which served as the air jacket. The tip of the needle passed through a small hole drilled at the center of a circular brass plate placed at the end of the brass tube. The nozzle plate was held against one end of the brass tube by a cap cut. The fuel line extended through the other end. The air nozzle was made detachable so that nozzles of various sizes and shapes could be used if it was deemed necessary for proper drop formation. An opening in the side of the brass tube was provided to admit air into the tube, which then flowed out through the nozzle. The centering of the needle in the small hole was done by two sets of centering screws which also hold the needle in position. The smaller the air outlet around the hypodermic needle, the better was the operation of the dropper.

The droplet had to fall through a small entrance hole at the top of the furnace, which made it necessary that the path of the droplets be as close as possible to the vertical. Droplets leaving the tip of the dropper fell through a Pyrex glass tube 1/2 inch in diameter before entering the furnace. The function of the Pyrex tube was to eliminate any air currents in the room that might deviate the falling droplets from the vertical path. Compressed air from the laboratory supply line was introduced at the side of the brass tube, and it was controlled by a needle valve. The velocity of the concentric air jet was kept low, otherwise violent turbulence occurred, causing the droplets to deviate from the vertical path. The head of the fuel was about 6 inches above the needle tip. The number of droplets produced in a unit time was controlled by the fuel head at the nozzle. The size of the droplets was regulated by the air velocity from the orifice surrounding the needle and the outside diameter of the hypodermic needle.

No quantitative measurements of the size of the droplets were made, but with small needles and high air pressure, the droplets were so small that it was difficult to see them when they left the needle tip.

Photographic Equipment

Pictures of falling droplets were taken at several positions (10-1/4 inches apart) along the furnace and the time was recorded at each position. In the design of the photographic equipment, a small lens-to-object distance was desirable. This had the advantage of short focal-length lenses and camera bodies. Each photographing position had an Argus C-3 camera box with an extension tube 4 inches long attached. The inside of the extension tube was painted dull black to cut down light reflections from the tube

wall. On the other end of the tube, a Schneider Coponar lens with a focusing mount was attached by two set screws. The lenses were made by Bausch and Lomb Company. They had a speed of f/4.5 and a focal length of 75 mm. The magnification ratio was about 1:1 and was determined by photographing an accurately measured wire. The cameras were mounted in such a way that they could be moved upward or downward along the furnace and also could be moved inward or outward from the furnace. In front of every lens a circular piece of heat-absorbing glass was placed to reduce the radiant heat passing to the lens from the furnace. An asbestos sheet 36 x 6 x 1/4 inches was placed in front of the lenses for further protection from the heat. The sheet was removed only while taking pictures.

Opposite to each lens, on the other side of the furnace, a high-speed General Electric photolight was used as a rapid light source. The photolight provided a flash of light of an extremely short duration (approximately one microsecond), which permitted the use of the open-shutter technique so that the shutters of the cameras were kept open during the entire time of fall of the droplet. The length of exposure was determined by the duration of the illumination. The photolight combined a short-gap, high-pressure, inert-gas-filled flash tube with an energy-storage capacitor, a high-voltage transformer, a rectifier, and a trigger circuit which released the energy from the capacitor into the flash tube at the proper time. Once the unit had released a flash, it automatically reset and was ready for the next flash after a period of approximately five seconds. The five-second delay was necessary to allow the capacitor to become fully charged. The flashing of the photolight was done by triggering a thyratron tube in the detection circuit. This is explained in detail in describing the detection equipment. The peak flash intensity occurred from 2 to 5 microseconds after the

triggering of the thyratron tube. The photolights were placed on a wooden stand so that the axis of each light coincided with the axis of the corresponding camera. Ground glass placed in front of the photolights served as a light diffuser. Thirty-five-mm Kodak plus-X film was used in photographing the falling droplets.

Detection Equipment

At each photographing position, and on an inclined axis, a multiplier phototube was used for the detection of the falling droplet. The multiplier phototube was totally enclosed, except for a small horizontal slit of dimensions 1/16 x 1-1/4 inches, as shown in Fig. 9. The actual function of the multiplier phototubes and the triggering circuit was to flash the General Electric photolight at the instant when the droplet was in the field of view of the camera. A 5-inch-focal-length lens was used to collect the light from the burning droplet and focus it on the multiplier phototube. To protect these lenses and the multiplier phototubes from the heat of the furnace, a circular piece of heat-absorbing glass was mounted in front of each lens. A 1/32-inch horizontal slit was placed in front of the phototube box. This slit served as a knife edge so that the light from the burning droplet had to pass through the two slits in order to reach the multiplier phototube.

Figure 6 shows the detection-circuit diagram of one of the four identical stages. The photomultiplier tube was type 931-A, manufactured by RCA; it had 9 stages and was capable of multiplying feeble photoelectric currents at the cathode by an average value of 1,000,000 times when operated at 100 volts per stage. The output current was a linear function of the exciting illumination under normal operating conditions. The manner in

which this tube operated was as follows.

The incident light from the burning droplet passed through a grid to fall on the photocathode, and then the emitted photoelectrons were guided by the electrostatic field to fall on the dynode or the secondary emitting cathode 1, from which, after amplification, the secondary electrons passed to dynode 2 and so on around the tube, until all secondary electrons were collected by anode 10.

The applied potential across the multiplier phototubes was 1080 volts d.c. from twelve 90-volt dry cells. The triggering coil of the photolight was connected to the plate of the thyratron tube and the photolight flashed when the thyratron triggered. The total delay between the detection of the falling droplet and the flashing of the photolight was in the micro-seconds range.

Timing Equipment

The elapsed time between the pictures had to be accurately established to permit the determination of the rate of burning. This was accomplished by recording the instant when the photolights flashed in the manner described below.

The plate of each thyratron tube was connected to the input of a Tektronix cathode-ray oscilloscope. The sweep of the scope was made to run when triggered by the first thyratron tube and each sweep was started independently of the preceding sweep. When the first thyratron tube triggered, the beam moved linearly to the right at a rate determined by the sweep generator, and the triggering of the remaining thyratrons gave pips or pulses on the screen. At the end of the sweep, the beam returned to the left side again to await another trigger. The sweep rate of the

scope ranged from 0.3 sec/cm to 3 microseconds/cm.

The output of a square-wave generator, manufactured by Hewlett Packard Company, was fed to the scope. The function of the generator was to give pulses on the screen at exactly equal intervals. These pulses were used to check the sweep rate. To reduce the square wave into a pulse, a differentiating circuit, consisting of a capacitor and a resistance of values 0.05 microfarad and 1000 ohms, was introduced in the circuit as shown in Fig. 8. After setting the sweep rate at the required value, the pulses of the square-wave generator were too close to each other and, to overcome this difficulty, a crystal diode was connected to the output of the generator before it was fed to the scope. The crystal diode acted as a rectifier, eliminating every other pulse. Looking at the screen, the square-wave generator gave upward pulses only, spaced at equal intervals of 1/60 of a second. The triggering of the thyratron tubes gave downward pulses, and thus it was easy to differentiate between the different pulses. A Polaroid camera, mounted on the screen, was used to photograph the timing pips. A sequence of exposures per frame could be obtained by the sliding camera-back mechanism of this camera. The camera back could be positioned for any desired number of oscillograms per frame, up to a maximum of nine. In this investigation only five oscillograms per frame were photographed. A typical photograph of the timing pulses is shown in Fig. 7.

APPENDIX B

TERMINAL VELOCITY AND ELEVATION OF THE FUEL DROPPER

Fuel droplets fell under gravity, buoyancy, and drag forces in the vertical furnace. The equation of a falling droplet is

$$\frac{\pi D^3 \rho}{6} \frac{dV}{dt} = \frac{\pi D^3 \rho g}{6} - \frac{\pi D^3 \rho' g}{6} - \frac{1}{8} C_D \rho' \pi D^2 V^2 ,$$

where

D = the diameter of the droplet,

ρ = the density of the liquid of the droplet,

ρ' = the density of the medium into which the droplet falls,

V = the velocity of the droplet,

g = the acceleration due to gravity, and

C_D = the coefficient of drag.

The above equation can be written as

$$\frac{dV}{dt} = g\left(1 - \frac{\rho'}{\rho}\right) - \frac{3}{4} C_D \frac{\rho'}{\rho} \frac{V^2}{D} . \qquad \text{(B1)}$$

The condition for reaching the maximum or terminal velocity is attained when $dV/dt = 0$; substituting this condition in the above equation we have

$$V^2 = \frac{4D\, g(\rho - \rho')}{3 C_D \rho'} \qquad \text{(B2)}$$

and

$$C_D = \frac{4D\, g(\rho - \rho')}{3V^2 \rho'} . \qquad \text{(B3)}$$

If the droplet is small, the flow of the air around it is likely to be laminar, and the viscosity of the air is an important factor in determining the resistance. If the droplet is large, the flow is likely to be turbulent and is accompanied by eddies behind the droplet.

To determine terminal velocities of various sizes of droplets, the method indicated in Reference 4 is used. From equation (B3), we have

$$\log C_D = \log \frac{4g(\rho - \rho')D}{3\rho'} - 2 \log V, \qquad \text{(B4)}$$

and from Reynolds number

$$\log Re = \log \frac{D\rho'}{\mu'} + \log V \quad . \qquad \text{(B5)}$$

Eliminating V between these two equations gives

$$\log C_D = -2 \log Re + \log \left[\frac{4g(\rho - \rho')D^3\rho'}{3\mu'^2} \right] , \qquad \text{(B6)}$$

which is an equation of a straight line between log C_D and log Re with a slope of -2 passing through the points:

$$C_D = \frac{4g(\rho - \rho')D^3\rho'}{3\mu'^2} , \quad Re = 1$$

and

$$C_D = 1, \quad Re = \sqrt{\frac{4g(\rho - \rho')D^3\rho'}{3\mu'^2}} \quad .$$

The intersection of this line with the Goldstein curve gives the desired value of Re incorporating the value of V.

To evaluate the terminal velocity of an n-heptane droplet of a 1000-micron diameter, with the assumption that no evaporation occurs, we have,

ρ of n-heptane at 60°F = 42.8 lb/ft^3,

ρ' of air at 60°F = 0.0737 lb/ft^3,

$g = 32.2$ ft/sec^2,

drop diameter $D = 0.1/2.54 \times 12$ ft,

μ' of air at 60°F $= 0.0000121$ lb/sec ft,

$Re = 1$,

$$C_D = \frac{4 \times 32.2(42.8 - .0737)\left(\frac{.1}{2.54 \times 12}\right)^3 \times .0737}{3(.0000121)^2} = 32600,$$

and

$C_D = 1$,

$$Re = \sqrt{\frac{4 \times 32.2(42.8 - .0737)\left(\frac{.1}{2.54 \times 12}\right)^3 \times .0737}{3(.0000121)^2}} = 180.7 .$$

The straight line through the point $C_D = 1$ and $Re = 180.7$ with a slope of -2 intersecting the Goldstein curve at $Re = 225$, as shown in Fig. 21.

$$Re = 225 = \frac{\rho' VD}{\mu'} = \frac{0.0737V \times \frac{1}{2.54 \times 12}}{0.0000121}$$

$$V = 11.25 \text{ ft/sec} .$$

Using the same procedure, Table I was computed, giving terminal velocities for n-heptane droplets of different diameters. This relation is shown in Fig. 22.

For comparison, the terminal velocities of n-heptane droplets falling in heated air at 1500°F were computed. No evaporation or combustion was assumed to take place, as if the air were an inert gas. The temperature of the droplet surface was assumed to be the boiling temperature of the liquid. The density of n-heptane was calculated from the following formula given in Reference 8:

$$\frac{d\rho}{dt} = - 0.0008411(1 + 0.0009019t) \text{ per °C.}$$

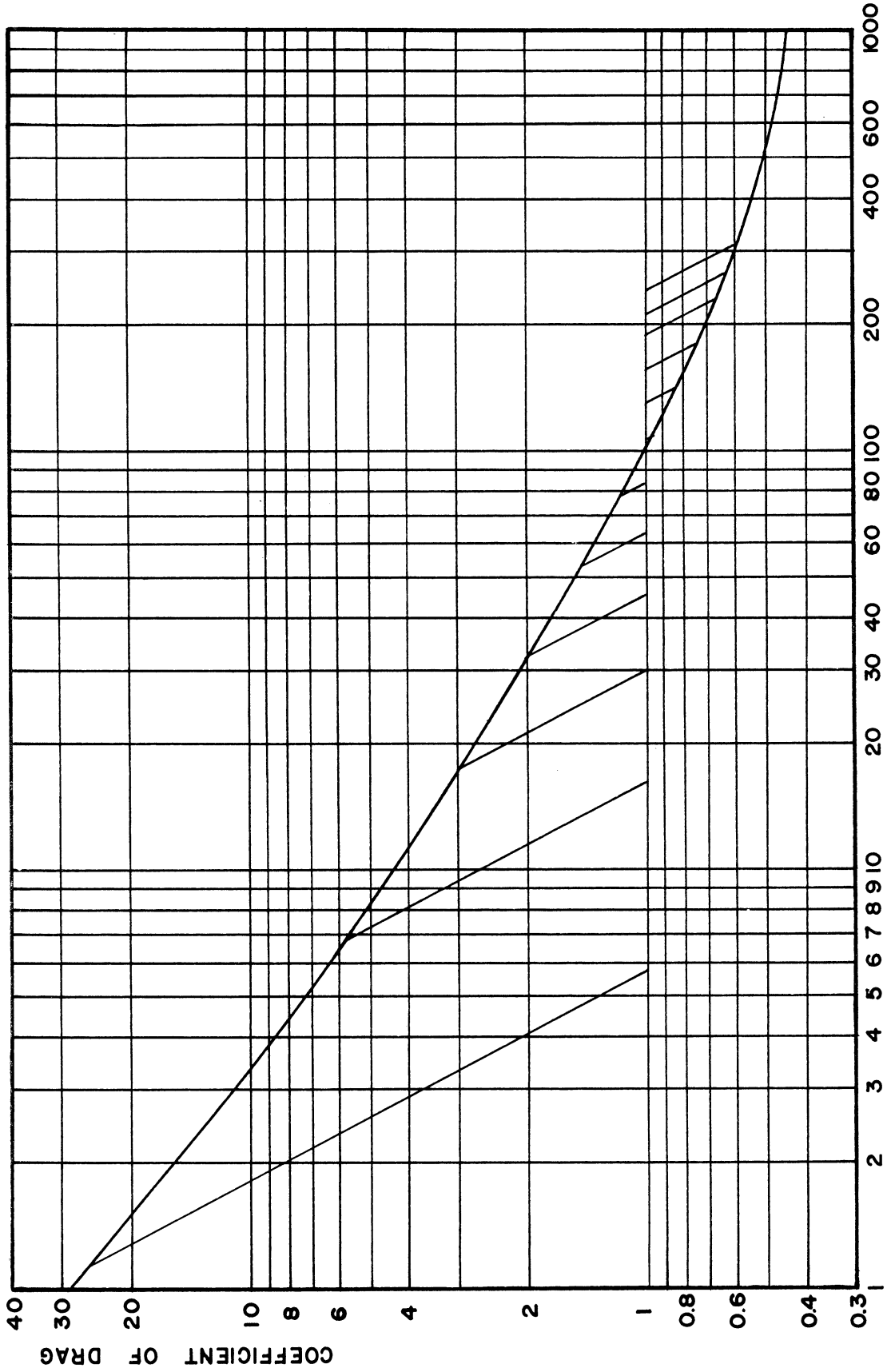

FIG. 21 RELATION OF REYNOLDS NUMBER AND COEFFICIENT OF DRAG.

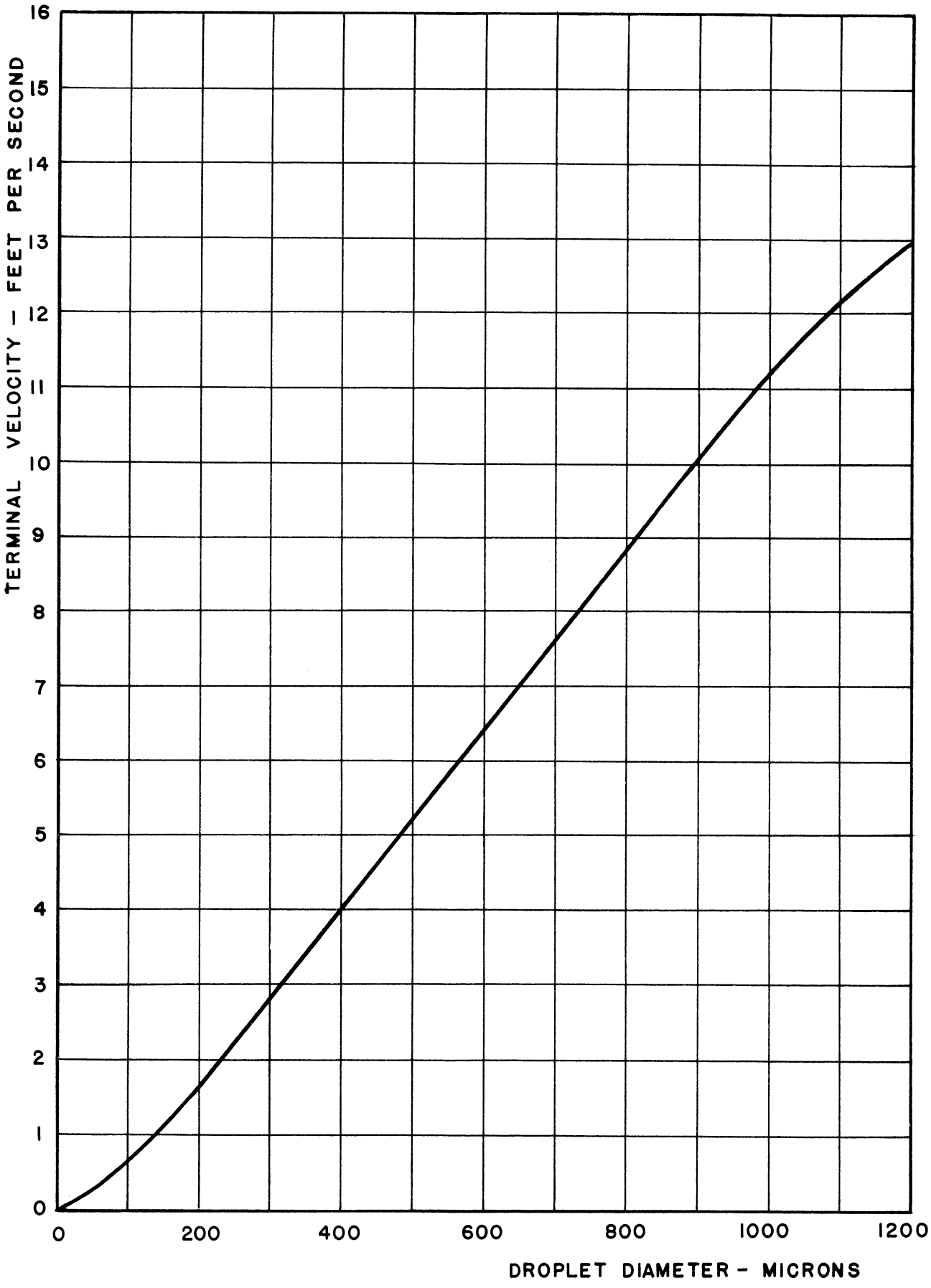

FIG. 22 TERMINAL VELOCITY OF N-HEPTANE DROPLETS IN AIR AT 60 °F

TABLE I

TERMINAL VELOCITY OF n-HEPTANE DROPLETS IN AIR AT 60°F

Droplet Diameter in Microns	Re	Terminal Velocity in ft/sec
1200	313	13.05
1100	265	12.05
1000	225	11.25
900	182	10.10
800	142	8.87
700	108	7.72
600	79	6.58
500	54	5.40
400	32	4.00
300	17	2.83
200	6.8	1.70
100	1.13	0.565
0	0	0

Integrating $d\rho$ between the limits $\rho_{15.6}$ and $\rho_{98.3}$ and dt between the limits 15.6°C and 98.3°C, we have

$$\int_{\rho_{15.6}}^{\rho_{98.3}} d\rho = - \int_{15.6}^{98.3} 0.0008411(1 + 0.0009019t)\, dt$$

$$\therefore \quad \rho_{98.3} - 0.689 = - \left[0.0008411\, t(1 + 0.00045095t) \right]_{15.6}^{98.3}$$

$$= - 0.0695$$

Hence,

$$\rho_{98.3} = 0.6185,$$

and the density of n-heptane at its boiling point is $0.6185 \times 62.43 = 38.6$ lb/ft^3.

μ' of air at 1500°F = 0.00002955 lb/sec ft

ρ' of air at 1500°F = 0.0201 lb/ft^3

$C_D = 1$,

$$R_e = \sqrt{\frac{4 \times 32.2(38.6 - 0.0201)\left(\frac{D}{2.54 \times 12}\right)^3 \times 0.0201}{3 \times (0.00002955)^2}},$$

$$Re = \sqrt{38.2 \times 10^9 \left(\frac{D}{2.54 \times 12}\right)^3} \quad .$$

Also,

$$V = \frac{\mu' Re'}{\rho' D} \quad .$$

Using different values of droplet diameter, Re' is determined by the point of intersection of the straight line of slope -2 with the Goldstein curve. Table II was computed and the results are shown in Fig. 23.

TABLE II

TERMINAL VELOCITY OF n-HEPTANE DROPLETS IN AIR AT 1500°F

Drop Diameter in Microns	Re	Terminal Velocity in ft/sec
1200	35.5	13.25
1100	29.2	11.90
1000	23.5	10.52
900	18.7	9.31
800	14.0	7.86
700	10.7	6.85
600	7.3	5.45
500	4.9	4.40
400	2.7	3.03
300	1.3	1.945
200	0.46	1.03
100	----	----
0	0	0

Comparing Figs. 22 and 23, it can be seen that the terminal velocity is less in hot air for the above range of droplet sizes, other factors being the same. This is due to the fact that the increase in the air viscosity, which accompanies an increase in temperature, increases the friction forces with a resulting decrease of the droplet velocity. The ratio of Re of Tables I and II varies from 9 to 15 for the corresponding size of droplets. The lower and higher figures are for large and small droplets, respectively.

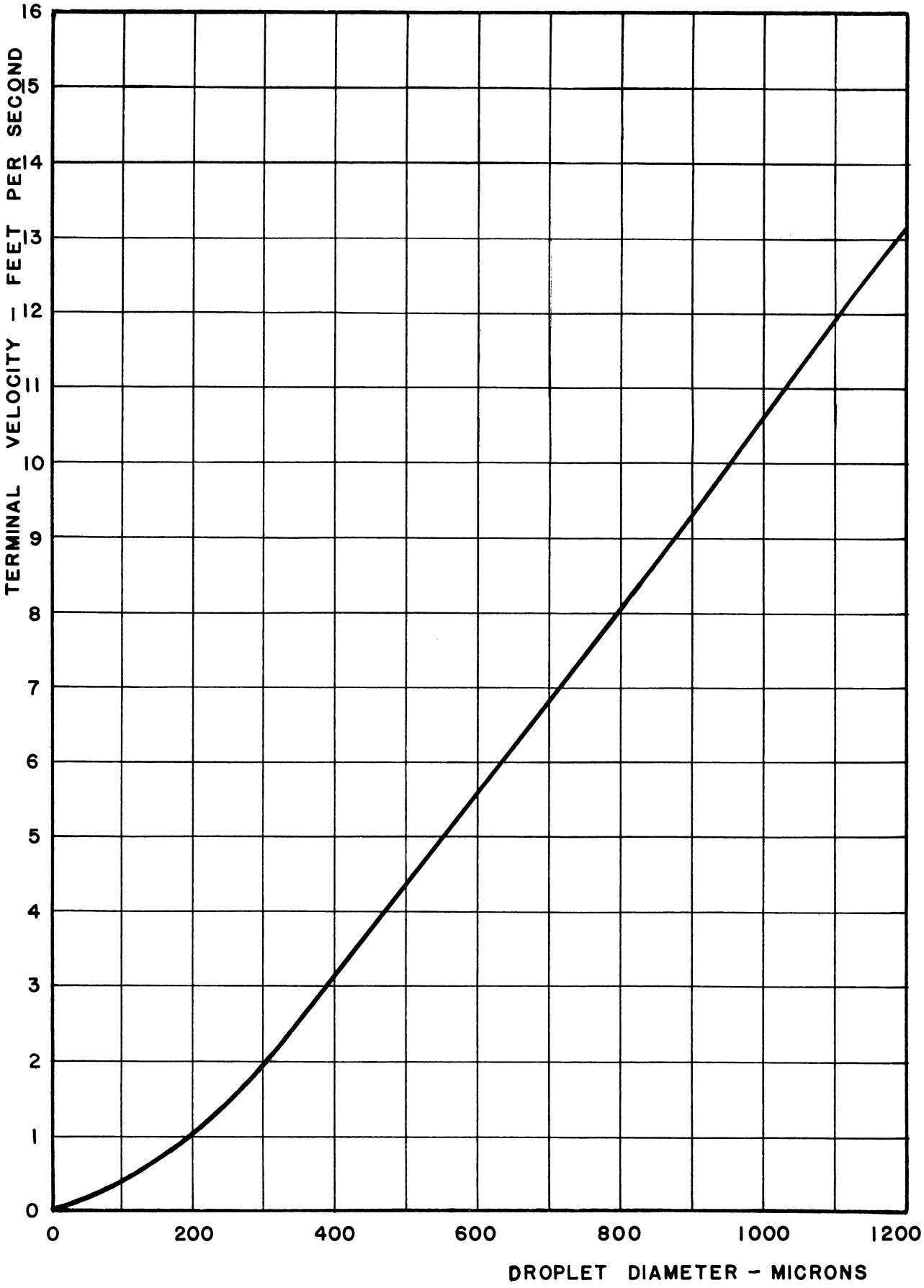

FIG. 23 TERMINAL VELOCITY OF N-HEPTANE DROPLETS IN AIR AT 1500 °F

Determination of the Elevation of the Fuel Dropper

The equation of a freely falling droplet is

$$\frac{dV}{dt} = g\left(1 - \frac{\rho'}{\rho}\right) - \frac{3}{4} C_D \frac{\rho'}{\rho} \frac{V^2}{D} \quad . \tag{B1}$$

At steady state,

$$\frac{dV}{dt} = 0 \ .$$

Hence,

$$V_{max} = \sqrt{\frac{4D\ g(\rho - \rho')}{3\ C_D\ \rho'}} \quad \text{and} \quad C_D = \frac{4D\ g(\rho - \rho')}{3\ C_D \rho'} \quad .$$

Integrating equation (B1), we have

$$t = \int_0^t dt = \int_{V_o}^{V} \frac{dV}{\left[g\left(1 - \frac{\rho'}{\rho}\right) - \frac{3}{4} C_D \frac{\rho'}{\rho} \frac{V^2}{D}\right]} \quad .$$

Multiplying numerator and denominator by $4D^3\rho\rho'/3\ \mu'^2$, we have

$$t = \frac{4D^3\ \rho\rho'}{3\ \mu'^2} \int_{V_o}^{V} \frac{dV}{\left[g\left(1 - \frac{\rho'}{\rho}\right) \cdot \frac{4D^3\rho\rho'}{3\ \mu'^2} - \frac{3}{4} C_D \frac{\rho'}{\rho} \frac{V^2}{D} \cdot \frac{4D^3\rho\rho'}{3\ \mu'^2}\right]}$$

$$t = \frac{4D^3\rho\rho'}{\mu'^2} \int_{V_o}^{V} \frac{dV}{\frac{4g(\rho - \rho')D^3\rho'}{3\ \mu'^2} - \frac{\rho'^2 V^2 D^2}{\mu'^2} C_D} \quad . \tag{B7}$$

But

$$V^2_{max} = \frac{4D\ g(\rho - \rho')}{3\ C_D\ \rho'} \ ,$$

where C_D corresponds to V_{max} or Re_{max}. Multiplying both sides of this equation by $\frac{\rho'^2 D^2}{\mu'^2} C_D$, we get

$$\frac{\rho'^2\ V^2_{max}\ D^2}{\mu'^2} C_D = \frac{4}{3} \frac{D^3 g(\rho - \rho')\rho'}{\mu'^2} \quad .$$

Substituting the above value for the first term in the denominator of equation (B7) and putting $dRe = \frac{\rho' D}{\mu'} dV$, equation (B7) reduces to

$$t = \frac{4}{3} \frac{D^2 \rho}{\mu'} \int_{V_o}^{V} \frac{dRe}{(C_D\ Re^2_{max}) - (C_D\ Re^2)} \quad . \qquad (B8)$$

Equation (B8) gives a relation between the value of Re and the elapsed time.

The integral is best evaluated by graphical integration where

$$\frac{1}{(C_D\ Re^2_{max}) - (C_D\ Re^2)}$$

is plotted vs Re, as shown in Fig. 24.

The terminal velocity of a 1000-micron n-heptane drop, falling in air at 60°F and atmospheric pressure, was found before to be 11.25 ft/sec. Taking values of velocities below this terminal velocity, Table III was computed, using the Goldstein curve for the determination of C_D for the different droplet velocities.

TABLE III

THE FACTOR $\frac{1}{(C_D\ Re^2_{max}) - (C_D\ Re^2)}$ FOR DIFFERENT VALUES OF VELOCITIES OF A 1000-MICRON n-HEPTANE DROPLET FALLING IN AIR AT 60°F

Velocity in ft/sec	Re	C_D	$C_D\ Re^2$	$\frac{1}{(C_D\ Re^2_{max}) - (C_D\ Re^2)}$
11.25	225 = Re_{max}	0.67	33900 = $(C_D\ Re^2_{max})$	∞
10	199	0.71	28100	1.725×10^{-4}
9.7	193	0.72	27000	1.450×10^{-4}
9	179.3	0.75	24100	1.020×10^{-4}
8	159.3	0.78	19750	0.707×10^{-4}
5	99.5	1.00	9900	0.417×10^{-4}
2	39.8	1.72	2720	0.321×10^{-4}
0	0	--	0	0.295×10^{-4}

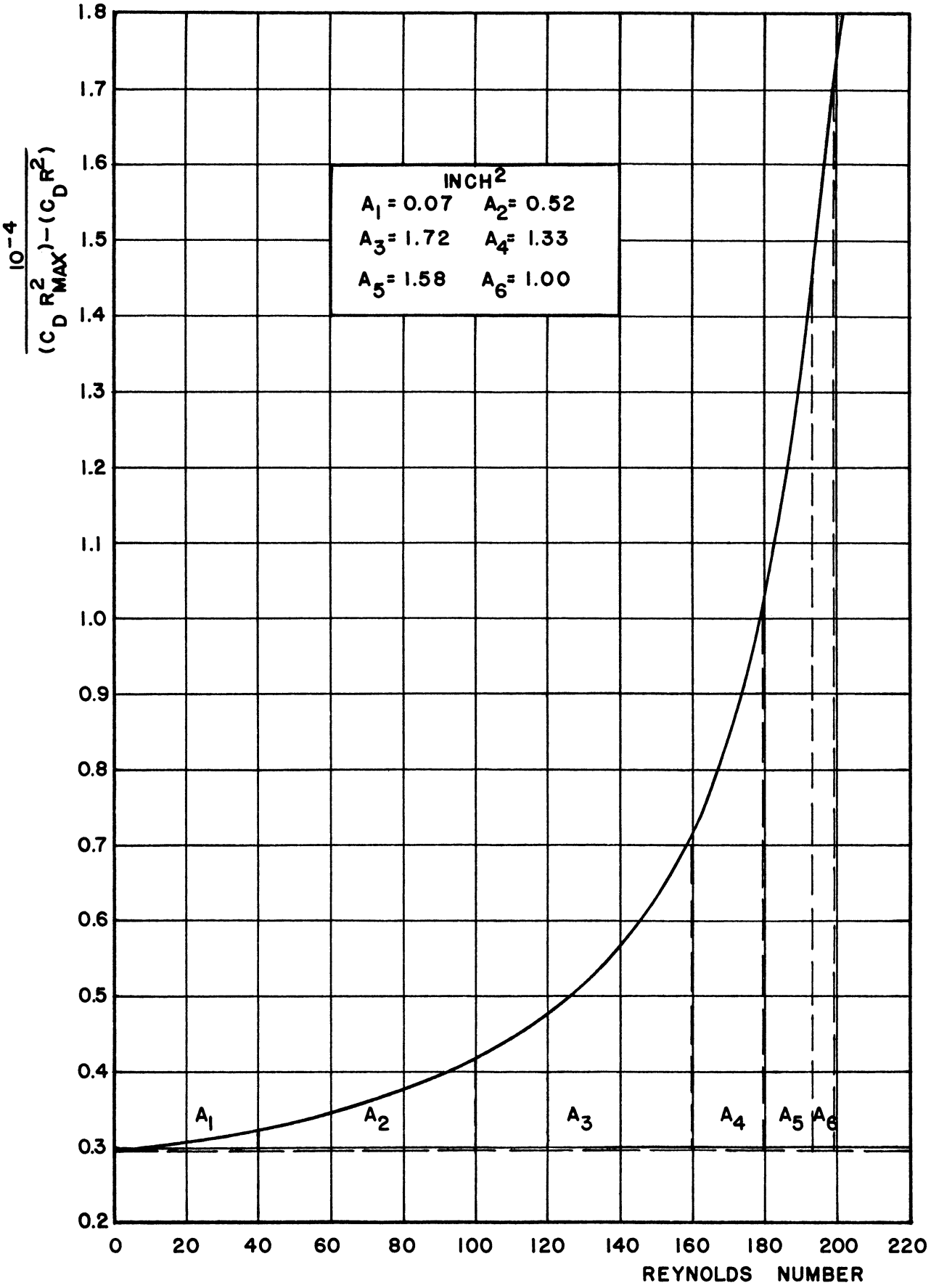

FIG. 24 VARIATION OF $\frac{1}{(C_D Re^2_{MAX}) - (C_D Re^2)}$ WITH REYNOLDS NUMBER

The area under the curve of Fig. 24 was divided by vertical straight lines at the velocities indicated in Table III. Each area was measured by a planimeter and multiplied by the scale of the drawing. By using equation (B8), the elapsed intervals of time to reach the above-indicated velocities were calculated. As an example, the time required for a 1000-micron n-heptane droplet to reach 8 ft/sec was calculated as follows:

$$t = \frac{4D^2\rho}{3\mu'} \int_0^V \frac{dRe}{(C_D Re^2_{max}) - (C_D Re^2)}$$

$$= \frac{4\left(\frac{.1}{2.54 \times 12}\right)^2 \times 42.8}{3 \times 0.0000121} \int_0^V \frac{dRe}{(C_D Re^2_{max}) - (C_D Re^2)}$$

or

$$t = 50.7 \text{ (area under the curve)} .$$

The area under the curve of Fig. 24, till a velocity of 8 ft/sec was reached, was 2.31 square inches, which, when multiplied by the horizontal and vertical scales, gives

$$2.31 \ (.2 \times 10^{-4})(40) = 0.00185 .$$

Hence,

$$t = 50.7 \times 0.00185 = 0.0938 \text{ sec} .$$

Table IV was thus computed for different velocities.

TABLE IV

TIME TO ATTAIN A CERTAIN VELOCITY FOR A 1000-MICRON n-HEPTANE DROPLET FALLING IN AIR AT 60°F

Velocity in ft/sec	Area Under Curve Divided by the Scale of the Drawing in Square Inches	Elapsed Time to Attain the Velocity in Seconds
11.25	∞	∞
10	6.22	0.2525
9.7	5.22	0.212
9	3.64	0.1476
8	2.31	0.0938
5	0.59	0.0239
2	0.07	0.00284
0	0.00	0

The above values of velocity were plotted against time as shown in Fig. 25. The area under this curve, measured by a planimeter and multiplied by the scale of the drawing, gave the distance of fall.

$$\text{Distance of fall } s = \int_0^t V dt \,. \qquad (B9)$$

The distance travelled by a 1000-micron n-heptane droplet to reach 87% of its terminal velocity was found to be s = 1.718 ft. An appreciable increase over this distance will increase the velocity only slightly. The dropper was thus placed 21 inches above the first photographing position.

It should be remembered that to reach the terminal velocity, an infinite time is necessary, as the curve of velocity vs time is asymptotic to the terminal-velocity line and intersects at infinity. Another important point to note from the same curve is the high initial acceleration of the droplet when it leaves the dropper. The acceleration is lower as the droplet gains speed toward its terminal velocity, which it theoretically attains after infinite time.

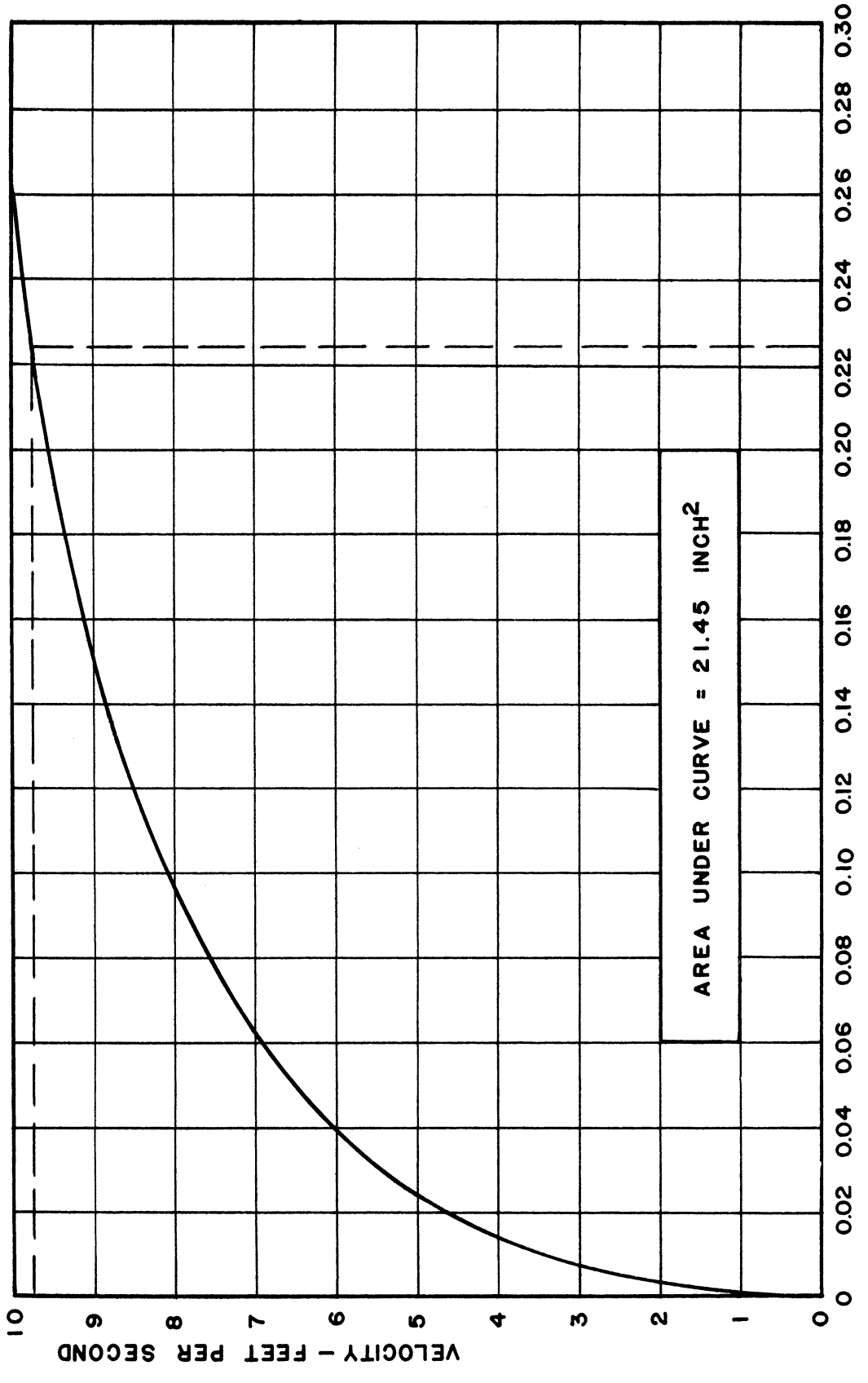

FIG. 25 VELOCITY-TIME RELATION OF A 1000 MICRON N-HEPTANE DROPLET FALLING IN AIR AT 60 °F.

APPENDIX C

COMBUSTION OF n-HEPTANE AT 2300°K

As indicated in Reference 11, the dissociation equilibria are

$$CO_2 \rightleftharpoons CO + \frac{1}{2} O_2 \tag{C1}$$

$$H_2O \rightleftharpoons H_2 + \frac{1}{2} O_2 \tag{C2}$$

$$H_2O \rightleftharpoons \frac{1}{2} H_2 + OH \tag{C3}$$

$$\frac{1}{2} H_2 \rightleftharpoons H \tag{C4}$$

$$\frac{1}{2} O_2 \rightleftharpoons O \tag{C5}$$

$$\frac{1}{2} N_2 + \frac{1}{2} O_2 \rightleftharpoons NO \ . \tag{C6}$$

In chemical equilibrium, the following equations must be obeyed:

$$K_1 = \frac{P_{CO} \cdot \sqrt{P_{O_2}}}{P_{CO_2}} \tag{C7}$$

$$K_2 = \frac{P_{H_2} \cdot \sqrt{P_{O_2}}}{P_{H_2O}} \tag{C8}$$

$$K_3 = \frac{P_{OH} \cdot \sqrt{P_{H_2}}}{P_{H_2O}} \tag{C9}$$

$$K_4 = \frac{P_H}{\sqrt{P_{H_2}}} \tag{C10}$$

$$K_5 = \frac{P_O}{\sqrt{P_{O_2}}} \tag{C11}$$

$$K_6 = \frac{P_{NO}}{\sqrt{P_{N_2} \cdot P_{O_2}}} \quad , \tag{C12}$$

where P_{CO}, P_{O_2} ..., etc., are the partial pressures of CO, O_2, etc., in atmospheres and K_1 to K_5 are the equilibrium constants. Values of these constants are available in tables of chemical data. The initial mixture is

$$C_7H_{16} + 11\ O_2 + 3.76 \times 11\ N_2 \ .$$

The number of gram atoms of carbon to hydrogen is

$$\frac{n_C}{n_H} = \frac{7}{16} = 0.4375 \ , \tag{C13}$$

and

$$\frac{n_O}{n_H} = \frac{22}{16} = 1.375 \tag{C14}$$

$$\frac{n_N}{n_H} = \frac{3.76 \times 22}{16} = 5.16 \ . \tag{C15}$$

Also, the following equations have to be satisfied:

$$n_C = P_{CO_2} + P_{CO} \tag{C16}$$

$$n_H = 2P_{H_2O} + 2P_{H_2} + P_H + P_{OH} \tag{C17}$$

$$n_O = 2P_{CO_2} + P_{CO} + P_{H_2O} + 2P_{O_2} + P_{OH} + P_O + P_{NO} \tag{C18}$$

$$n_N = 2P_{N_2} + P_{NO} \ . \tag{C19}$$

The total pressure is atmospheric, thus

$$P = P_{CO_2} + P_{CO} + P_{H_2O} + P_{O_2} + P_{H_2} + P_{OH} + P_H + P_O + P_{N_2} + P_{NO} = 1. \tag{C20}$$

We have ten unknown partial pressures and ten equations; six of equilibrium constants, three of ratios of atoms, and the total-pressure equation.

The values of the equilibrium constants for a combustion temperature of 2300°K are

$$K_1 = 1 \times 10^{-2} \qquad K_4 = 9.66 \times 10^{-3}$$

$$K_2 = 2.04 \times 10^{-3} \qquad K_5 = 5.4 \times 10^{-3}$$

$$K_3 = 1.56 \times 10^{-3} \qquad K_6 = 4 \times 10^{-2}$$

Also,

$$\frac{n_C}{n_H} = 0.4375 \qquad \frac{n_O}{n_H} = 1.375 \qquad \frac{n_O}{n_H} = 5.16$$

$$P = P_{CO_2} + P_{CO} + P_{H_2O} + P_{H_2} + P_{OH} + P_H + P_O + P_{N_2} + P_{NO} = 1 .$$

We assume a value for P_{CO_2}/P_{CO} and P_{H_2O}, then calculate n_O/n_H and P to see if they correspond to the values given above. Some of the trials are shown in Table V. Column 6 in the table gives $n_O/n_H = 1.374$ and P = 1.004609, which are close to the required values. Thus, column 6 of the table gives the correct composition of the burnt gases at a temperature of 2300°K.

Number of mols of products of combustion after

dissociation = 7/0.1236 = 56.6 mols of products/mol of fuel.

Table VI gives the enthalpy or heat content of the products of combustion of n-heptane at 2300°K.

$$h_p = 21074.35 \text{ Btu/lb of fuel.}$$

TABLE V

CALCULATION OF COMPOSITION OF n-HEPTANE FLAME
ASSUMING T_F = 2300°K

Trial No.	1	2	3	4	5	6
P_{CO_2}/P_{CO}	15	10	8	9	8	8.5
P_{H_2O}	0.13	0.135	0.135	0.135	0.136	0.136
PO_2	0.0225	0.01	0.0064	0.0081	0.0064	0.00722
P_O	0.00081	0.00054	0.000432	0.000486	0.000432	0.000458
P_{H_2}	0.00177	0.002755	0.00344	0.003055	0.003465	0.00326
P_H	0.000406	0.000507	0.000566	0.000534	0.000568	0.000551
P_{OH}	0.00482	0.00401	0.00359	0.00381	0.00361	0.00372
n_C	0.1171	0.1225	0.1230	0.1226	0.1238	0.1236
n_H	0.2676	0.2800	0.2811	0.28044	0.2831	0.28259
P_{CO}	0.00732	0.01115	0.01366	0.01226	0.01375	0.0130
P_{CO_2}	0.1097	0.1115	0.1092	0.1103	0.1100	0.1104
n_O	0.40734	0.39370	0.38382	0.388356	0.386592	0.388418
P_{N_2}	0.690	0.7225	0.725	0.723	0.731	0.730
P_{NO}	small	---	---	---	---	---
n_N	0.138	0.1445	0.145	0.1446	0.1462	0.1460
n_O/n_H	1.52	1.405	1.368	1.385	1.366	1.374
P	0.967326	0.997962	0.997288	0.996545	1.005225	1.004609

TABLE VI

CALCULATION OF ENTHALPY OF PRODUCTS
OF COMBUSTION OF n-HEPTANE AT 2300°K

Constituent	mol Fraction per mol of Products	Weight of Constituent per mol of Products	Weight of Constituent per lb of Fuel	Enthalpy Btu/mol	Enthalpy per lb of Fuel
CO_2	0.1104	4.85	2.745	51300	3200
H_2O	0.136	2.445	1.385	42300	3260
O_2	0.00722	0.231	0.131	34100	139.5
CO	0.013	0.364	0.206	32800	241
OH	0.00372	0.633	0.359	31450	665
H_2	0.00326	0.00652	0.0037	30850	57
O	0.000458	0.00733	0.00415	20950	5.43
H	0.000551	0.000551	0.000312	20600	6.42
N_2	0.73	20.45	11.60	32550	13500
NO	--	--	--	33600	--

Enthalpy of products h_p = 21074.35 Btu/lb of fuel.

APPENDIX D

PROPERTIES OF THE FUELS

The heat of combustion, latent heat of vaporization, and the specific heat of the vapor are the main properties of the fuel which affect the rate of combustion. High combustion temperature and low latent heat give a high combustion rate.

The surface properties of the liquid fuel are the most important ones to predict the degree of atomization of the fuel into fine particles. The density, surface tension, and viscosity of the fuel are the main physical properties of a fuel which affect the droplet size. The viscosity is the most important factor and, for liquid fuels, it may vary from 0.6 to 1200 centistokes. The mean volatility of a fuel is of importance since this determines the amount of preheating. The amount of preheating governs the use which may be made of the latent heat of the liquid fuel.

Two pure hydrocarbon fuels and kerosene were tested in this investigation. The pure hydrocarbons used were n-heptane and 2, 2, 4-trimethylpentane (isooctane). They were bought from the Phillips Petroleum Company. The properties of these fuels are given in Tables VII, VIII, and IX.

Odorless kerosene bought from the Fisher Scientific Company had the following properties:

Specific gravity of liquid at 60/60°F	0.793
API gravity at 60°F	47.0
Color, Saybolt	30
Flash-point, tag close cup	155°F
Corrosion, copper strip at 212°F	negative

Unsulfonated residue	99% of volume
Liquid thermal conductivity at 86°F Btu/ft hr°F	0.086
Heat of combustion, Btu/lb	19,800
Distillation:	
Initial boiling point	387°F
10% recovered	406°F
50% recovered	419°F
90% recovered	450°F
95% recovered	470°F
Dry point	490°F

TABLE VII

PROPERTIES OF HYDROCARBON FUELS

Fuel	n-Heptane	Isooctane
Formula	C_7H_{16}	C_8H_{18}
Molecular weight	100.198	114.224
Ratio of combustible hydrogen to carbon	2.28	2.25
Specific gravity, 60/60°F	0.689	0.696
Freezing point, °F	-131.3	-161.0
Boiling point, °F	209.1	210.6
Critical temperature, °F	512.5	515.
Critical pressure, atmospheres	26.8	27.
Surface tension at 20°C dynes/cm	20.30	21.14
Specific heat (liquid) (ratio to that of water)	$0.525^{65°F}$	$0.489^{72°F}$
Liquid thermal conductivity at 86°F Btu/ft hr°F	0.081	0.083
Heat of vaporization at normal boiling point, Btu/lb	136.0	116.8
Heat of combustion, Btu/lb,	20668	20556
Vapor heat content at boiling point (reference temperature 0°K) cal/g,	111.0	99.0
Btu/lb	199.6	178.1

TABLE VIII

PROPERTIES OF NORMAL HEPTANE C_7H_{16}

Specification: Pure grade containing not less than 99 mol per cent normal heptane.

Impurities: Small amounts of cis-1, 2-dimethylcyclopentane and 3-ethylpentane are usually present.

Typical properties:

Property	Value	Test Method
Freezing point, °F	-131.3	ASTMD1015 - 49T
Boiling point, °F	209.1	Modified Cottrell
Specific gravity of liquid at 60/60°F	0.689	ASTMD287 - 52
API gravity at 60°F	74.0	ASTMD287 - 52
Density of liquid at 60°F, lb/gal	5.73	Calculated
Vapor pressure at 100°F, psia	1.62	ASTMD323 - 52
Refractive index at 20°C	1.388	----
Flash point, approximate, °F	42	Tag open cup
Color, Saybolt	+30	ASTMD156 - 53T
Acidity, distillation residue	Not acid	ASTMD235 - 39
Aniline point, °F	156.9	ASTMD611 - 53T
Nonvolatile matter	None	ASTMD268 - 49

TABLE IX

PROPERTIES OF 2, 2, 4-TRIMETHYLPENTANE (ISOOCTANE) C_8H_{18}

Specifications: Pure grade containing not less than 99 mol per cent isooctane.

Impurities: Small amounts of other C_8 isoparaffins are usually present. Traces of olefins and organic fluorides may also be present in pure grade.

Typical properties:

Property	Value	Test Method
Freezing point, °F	-161.0	ASTMD1015 - 49T
Boiling point, °F	210.6	Modified Cottrell
Specific gravity of liquid at 60/60°F	0.696	ASTMD287 - 52
at 20/4°C	0.692	Westphal Balance
API gravity at 60°F	71.8	ASTMD287 - 52
Density of liquid at 60°F lb/gal	5.79	Calculated
Vapour pressure at 70°F, psia	0.8	Calculated
at 100°F, psia	1.7	ASTMD323 - 52
at 130°F, psia	3.3	Calculated
Refractive index at 20°C	1.392	
Flash point, approximate, °F	40	Tag open cup
Color, Saybolt	+30	ASTMD156 - 53T
Sulfur content, weight %	< 0.01	ASTMD1266 - 53T
Acidity, distillation residue	Not acid	ASTMD235 - 39
Nonvolatile matter	None	ASTMD268 - 49

APPENDIX E

EXPERIMENTAL DATA

The experimental data for n-heptane, isooctane, and kerosene are given in Tables X, XII, and XIV. The diameters of the droplet at the first, second, and third photographing positions are indicated by D_1, D_2, and D_3. The first and second intervals of time are indicated by Θ_1 and Θ_2. D_{m_1} and D_{m_2} are the arithmetic mean diameters during the intervals Θ_1 and Θ_2. The values of the diameters are in microns and the time intervals in seconds.

In Tables XI, XIII, and XV, the D^2 is in square millimeters. The mean velocities V_{m_1} and V_{m_2} are in feet per second and are calculated by knowing the distance between the photographing positions and the time between successive flashes. Re_m is the mean Reynolds number and equal to $\rho' V_m D_m / \mu'$.

TABLE X

COMBUSTION OF n-HEPTANE IN AIR
(Measured Values)

Average furnace temperature: 1500°F

Magnification of film: 19.45

D_1 microns	D_{m_1} microns	D_2 microns	D_{m_2} microns	D_3 microns	θ_1 seconds	θ_2 seconds	θ_{total} seconds
1160	1101	1042	983	923	0.103	0.0888	0.1918
863	748	632	--	--	0.1333	--	0.1333
667	521	375	--	--	0.1408	--	0.1408
1145	1086	1026	988	950	0.0963	0.0822	0.1785
934	882	830	703	575	0.0992	0.0917	0.1909
1105	1074	1042	957	872	0.0935	0.0904	0.1839
1125	1084	1042	983	923	0.0925	0.0836	0.1761
1027	956	882	--	--	0.101	--	0.101
846	762	677	--	--	0.1250	--	0.1250
778	645	512	--	--	0.1335	--	0.1335
862	759	656	--	--	0.1268	--	0.1268
810	674	538	--	--	0.1218	--	0.1218
922	838	753	--	--	0.1230	--	0.1230
973	909	845	756	667	0.12	0.1	0.22
835	725	615	487	359	0.1258	0.118	0.2438
1026	--	--	--	718	0.0978	0.0876	0.1854
1078	--	--	--	867	--	--	0.1775
1130	1065	1000	931	862	0.095	0.0842	0.1792
1047	999	950	873	796	0.0977	0.0888	0.1865
1104	1052	1000	952	903	0.095	0.0842	0.1792

TABLE XI

COMBUSTION OF n-HEPTANE IN AIR
(Calculated Values)

D_1^2 (mm^2)	D_2^2 (mm^2)	D_3^2 (mm^2)	V_{m_1} (ft/sec)	V_{m_2} (ft/sec)	$R_{e_{m_1}}$	$R_{e_{m_2}}$
1.348	1.09	0.853	8.28	9.60	20.40	21.03
0.745	0.400	--	6.40	--	10.68	--
0.445	0.141	--	6.05	--	7.04	--
1.315	1.055	0.910	8.87	10.38	21.50	25.06
0.873	0.690	0.331	8.60	9.30	16.93	14.58
1.225	1.09	0.760	9.12	9.45	21.85	20.15
1.270	1.09	0.853	9.22	10.20	22.3	22.35
1.055	0.779	--	8.45	--	18.02	--
0.717	0.460	--	6.82	--	11.60	--
0.605	0.263	--	6.38	--	9.17	--
0.742	0.430	--	6.72	--	11.40	--
0.657	0.290	--	7.00	--	10.52	--
0.852	0.568	--	6.93	--	12.96	--
0.950	0.715	0.445	7.1	8.53	14.40	14.40
0.700	0.378	0.129	6.78	7.22	10.97	7.83
1.055	--	0.516	8.72	9.73	--	--
1.165	--	0.752	--	--	--	--
1.280	1.000	0.745	8.97	10.14	21.30	21.10
1.100	0.903	0.635	8.72	9.60	19.44	18.70
1.224	1.000	0.816	8.97	10.14	20.90	21.35

TABLE XII

COMBUSTION OF ISOOCTANE IN AIR
(Measured Values)

Average furnace temperature: 1500°F

Magnification of film: 19.45

D_1, microns	D_{m_1}, microns	D_2, microns	D_{m_2}, microns	D_3, microns	θ_1, sec	θ_2, sec	θ_{total}, sec
1182	1144	1105	1074	1043	0.0925	0.0814	0.1739
1028	964	900	846	796	0.1052	0.0866	0.1918
1182	--	--	--	1006	--	--	0.1790
802	697	592	--	--	0.111	--	0.111
977	902	827	--	--	0.1035	--	0.1035
1173	--	--	--	1038	--	--	0.1742
1163	1122	1080	1040	1000	0.0948	0.0822	0.1770
1002	938	873	827	781	0.0947	0.0784	0.1731
1130	--	--	--	848	0.1050	0.0858	0.1908
1140	1071	1002	964	925	0.1036	0.0865	0.1901
1182	1144	1105	1041	976	0.0862	0.0788	0.1650
--	--	1028	982	935	--	0.0788	0.0788
1232	1140	1048	1002	955	0.0938	0.0825	0.1763
1088	1032	976	925	873	0.106	0.0735	0.1794
1182	1136	1090	--	--	0.0968	0.0833	0.1801
1182	1136	1090	--	--	0.0938	0.081	0.1748
1038	969	900	835	770	0.0975	0.0862	0.1837
--	--	914	842	770	0.0975	0.0900	0.1875
745	604	462	--	--	0.154	--	0.1540
884	781	678	596	514	0.1153	0.0977	0.2130
823	707	591	--	--	0.1348	--	0.1348
772	638	503	--	--	0.1443	--	0.1443
873	771	668	--	--	0.1303	--	0.1303
873	771	668	--	--	0.1318	--	0.1318
925	835	745	--	--	0.1272	--	0.1272

TABLE XIII

COMBUSTION OF ISOOCTANE IN AIR
(Calculated Values)

D_1 (mm^2)	D_2 (mm^2)	D_{32} (mm^2)	V_{m_1} (ft/sec)	V_{m_2} (ft/sec)	$R_{e_{m_1}}$	$R_{e_{m_2}}$
1.400	1.222	1.090	9.23	10.50	23.50	25.20
1.060	0.810	0.635	8.12	9.86	17.45	18.60
1.400	--	1.015	--	--	--	--
0.644	0.351	--	7.70	--	11.95	--
0.957	0.684	--	8.25	--	16.60	--
1.380	--	1.080	--	--	--	--
1.355	1.170	1.000	9.00	10.40	22.50	24.10
1.004	0.762	0.610	9.02	10.90	18.86	20.10
1.280	--	0.720	8.13	9.95	--	--
1.300	1.004	0.856	8.25	9.87	19.72	21.25
1.400	1.222	0.953	9.92	10.82	25.28	25.15
--	1.060	0.873	--	10.82	--	23.68
1.520	1.100	0.912	9.10	10.35	23.10	23.55
1.185	0.952	0.762	8.06	11.61	18.58	23.95
1.400	1.190	--	8.82	10.25	22.35	--
1.400	1.190	--	9.10	10.55	23.05	--
1.080	0.810	0.595	8.77	9.92	18.95	18.46
--	0.835	0.595	8.77	9.5	--	17.85
0.555	0.214	--	5.55	--	7.48	--
0.780	0.460	0.264	7.41	8.75	12.94	11.65
0.678	0.350	--	6.33	--	10.00	--
0.597	0.254	--	5.92	--	8.42	--
0.762	0.446	--	6.55	--	11.26	--
0.762	0.446	--	6.48	--	11.15	--
0.855	0.555	--	6.72	--	12.52	--

TABLE XIV

COMBUSTION OF KEROSENE IN AIR
(Measure Values)

Average furnace temperature: 1500°F

Magnification of film: 19.45

D_1 microns	D_{m_1} microns	D_2 microns	D_{m_2} microns	D_3 microns	θ_1 sec	θ_2 sec	θ_{total} sec
1132	1086	1040	993	946	0.0984	0.0888	0.1872
1028	964	900	841	782	0.1036	0.0925	0.1961
745	655	565	--	--	0.1183	--	0.1183
1055	995	935	884	832	0.1000	0.0888	0.1888
1080	1024	977	939	900	0.0977	0.0814	0.1791
1152	1104	1055	1011	967	0.0963	0.0814	0.1777
1142	1085	1028	977	925	0.0977	0.0888	0.1865
848	707	565	--	--	0.1280	0.1035	0.2315
1028	977	925	874	822	0.1080	0.0888	0.1968
822	707	591	--	--	0.1182	--	0.1182
822	681	540	425	309	0.1330	0.1168	0.2498
1095	--	--	--	898	0.1082	0.0925	0.2007
1105	1057	1008	967	925	0.1036	0.0888	0.1924
976	925	873	770	667	0.1020	0.0888	0.1908
1016	945	873	797	720	0.0925	0.0852	0.1778
--	--	565	463	360	0.1332	0.1146	0.2478
720	586	452	--	--	0.1480	--	0.1480
900	810	720	--	--	0.1316	--	0.1316
694	578	462	--	--	0.1405	--	0.1405
694	537	380	--	--	0.1442	--	0.1442
863	761	658	--	--	0.1302	--	0.1302
668	527	385	--	--	0.1568	--	0.1568

TABLE XV

COMBUSTION OF KEROSENE IN AIR
(Calculated Values)

D_1^2 (mm^2)	D_2^2 (mm^2)	D_3^2 (mm^2)	V_{m_1} (ft/sec)	V_{m_2} (ft/sec)	Re_{m_1}	Re_{m_2}
1.280	1.082	0.895	8.68	9.63	21.00	21.30
1.060	0.810	0.612	8.24	9.23	17.70	17.30
0.555	0.319	--	7.22	--	10.55	--
1.115	0.873	0.692	8.55	9.63	18.98	19.00
1.170	0.953	0.810	8.75	10.50	20.00	21.95
1.330	1.115	0.934	8.87	10.50	21.85	23.65
1.305	1.060	0.854	8.75	9.63	21.15	20.95
0.720	0.319	--	6.68	8.26	10.53	--
1.060	0.854	0.677	7.90	9.63	17.25	18.78
0.677	0.349	--	7.22	--	11.40	--
0.677	0.291	0.0955	6.42	7.31	11.10	6.92
1.200	--	0.806	7.90	9.23	--	--
1.220	1.015	0.854	8.25	9.63	19.46	20.80
0.953	0.762	0.445	8.38	9.63	17.30	16.56
1.035	0.762	0.518	9.23	10.02	19.43	18.15
--	0.319	0.130	6.41	7.45	--	7.70
0.518	0.205	--	5.78	--	7.57	--
0.810	0.518	--	6.50	--	11.75	--
0.482	0.214	--	6.08	--	7.85	--
0.482	0.144	--	5.92	--	7.08	--
0.745	0.433	--	6.56	--	11.14	--
0.446	0.149	--	5.46	--	6.41	--

BIBLIOGRAPHY

1. Bolt, J. A., et al. "The Combustion of Liquid Fuel Drops in Free Flight," Univ. of Mich., Eng. Res. Inst. Project M988, ATI No. 17922, August, 1952.

2. Bolt, J. A., et al. "The Generation and Burning of Uniform-Size Liquid Fuel Drops," Univ. of Mich., Eng. Res. Inst. Project 1988, May, 1953.

3. Bolt, J. A., and Saad, M. A. "Burning of Individual Fuel Drops in a Furnace," Univ. of Mich., Eng. Res. Inst. Project 2253-3, July, 1955.

4. Brown, G. G., et al. Unit Operations. New York: John Wiley and Sons, Inc., 1950.

5. Chang, T. Y. "Combustion of Heavy Fuel Oil," Sc.D. Dissertation, Chem. Eng. Dept., M.I.T., 1941.

6. Diederichsen, J., and Hall, A. R. The Burning of Single Drops of Fuel in Air at Pressures up to Twenty Atmospheres. RAE Technical Note RPD 50.

7. Doss, M. P. Physical Constants of the Principal Hydrocarbons. 4th edition. New York: Technical and Research Div. of the Texas Co., 1943.

8. Egloff, G. Physical Constants of Hydrocarbons, Vol. I. New York: Reinhold Publ. Corp., 1939.

9. El-Wakil, M. M., et al. A Theoretical Investigation of the Heating-Up Period of Injected Fuel Droplets Vaporizing in Air. NACA TN-3179 (1954).

10. Fledderman, R. G., and Hanson, A. R. The Effects of Turbulence and Wind Speed on the Rate of Evaporation of a Fuel Spray. U.S. Navy, Bureau of Ordnance, Report CM667.

11. Gayden, A. G., and Wolfhard, H. G. Flames. London: Chapman and Hall, Ltd., 1953.

12. Giffen, E., and Muraszew, A. The Atomization of Liquid Fuels. London: Chapman and Hall, Ltd., 1953.

13. Godsave, G. A. E. The Combustion of Drops in a Fuel Spray. NTGE (England), Memorandum M95, 1950.

BIBLIOGRAPHY (Cont.)

14. Godsave, G. A. E. The Burning of Single Drops of Fuel. NGTE (England): Part I, "The Temperature Distribution and Heat Transfer in the Pre-Flame Region," Report R66 (1950); Part II, "Experimental Results," Report R87 (1951); Part III, "Comparison of Experimental and Theoretical Burning Rates and Discussion of the Mechanism of Combustion Process," Report R88 (1952); Part IV, "The Flow of Heat and Carbon Residue Formation in Drops of Fuel," Report R125 (1952).

15. Godsave, G. A. E. "Studies of the Combustion of Drops in a Fuel Spray-The Burning of Single Drops of Fuel," Fourth International Symposium on Combustion, 1952.

16. Gohrbrandt, W. The Evaporation of Spheres in a Hot Air Stream. NGTE (England), Memorandum M110 (1951).

17. Gunn, R., and Kinzer, G. D. "The Terminal Velocity of Fall for Water Droplets in Stagnant Air," J. Meteor., 6:243 (1949).

18. Hodgman, C. D. Handbook of Chemistry and Physics. 26th edition. Cleveland: Chemical Rubber Publ. Co., 1955.

19. Hughes, H. H. and Gilliland, E. R. "The Mechanics of Drops," Chem. Eng. Prog., 48:497 (1952).

20. Ingebo, R. D. Vaporization Rates and Heat Transfer Coefficients for Pure Liquid Drops. NACA TN-2368 (1951).

21. Ingebo, R. D. Study of Pressure Effects on Vaporization Rate of Drops in Gas Streams. NACA TN-2850 (1953).

22. Jakob, M. Heat Transfer. Vol. I. 1st edition. New York: John Wiley and Sons, Inc., 1949.

23. Kobayasi, K. "Evaporation Velocity of Single Droplets of Liquids," Tokyo Univ. Technology Reports, 18:209-222 (1954).

24. Maxwell, J. B. Data Book on Hydrocarbons. New York: D. Van Nostrand Co., Inc., 1950.

25. McAdams, W. H. Heat Transmission. 2nd edition. New York: McGraw-Hill Book Co., Inc., 1942.

26. Perry, J. H. Chemical Engineers' Handbook. 3rd edition. New York: McGraw-Hill Book Co., Inc., 1950.

27. Ranz, W. E. and Marshall, W. R. "Evaporation from Drops," Chem. Eng. Prog., Part I, 48:141 (1952).

28. Rodda, S. Photo-Electric Multipliers. London: MacDonald and Co., Ltd., 1953.

BIBLIOGRAPHY (Concl.)

29. Rossini, F. D., et. al. Selected Values of Properties of Hydrocarbons. Washington, D. C.: U.S. Dept. of Commerce, Natl. Bureau of Standards, 1947.

30. Sherwood, T. K. Absorption and Extraction. 1st edition. New York: McGraw-Hill Book Co., Inc., 1937.

31. Simpson, H. C. "Combustion of Droplets of Heavy Liquid Fuels," Sc.D. Dissertation, Chem. Eng. Dept., M.I.T., 1954.

32. Spalding, D. B. "Combustion of Liquid Fuel in a Gas Stream, Part I," Fuel, 29:2 (1950); Part II, ibid., p. 25.

33. Spalding, D. B. "Combustion of Fuel Particles," Fuel, 30:121 (1951).

34. Spalding, D. B. "Experiments on the Burning and Extinction of Liquid Fuel Spheres," Fuel, 32:169 (1953).

35. Spalding, D. B. "Heterogeneous Combustion in Laminar Flow," Aeronautical Res. Council (Combustion of Fuels Sub-committee), 13, 711, C. F. 159 (1951).

36. Spalding, D. B. "Some Fundamentals on Combustion," Gas Turbine Series, Vol. II. New York: Academic Press, Inc., 1955.

37. Spalding, D. B. "The Combustion of Liquid Fuels," Fourth International Symposium on Combustion, 1952.

38. Topps, J. E. C. An Experimental Study of the Evaporation and Combustion of Falling Droplets. NGTE (England), Memorandum M105 (1951).

39. Walton, W. H., and Prewett, W. C. "Production of Sprays and Mists of Uniform Drop Size by Means of Spinning Disc Type Sprayers," Proc. Phys. Soc., 62, Part 6, Section B, June, 1949.

40. Weinberg, S. "Heat Transfer to Low Pressure Sprays of Water in a Steam Atmosphere," Inst. of Mech. Engineers, Proc. (B), vol. 1B, No. 6(1952).

41. Wolfhard, H. G., and Parker, W. G. "Evaporation Processes in a Burning Kerosene Spray," J. Inst. Pet., 35:118 (1949).